DIAGENETIC PRESSURE SEAL ANALYSIS USING FLUID INCLUSIONS AND STABLE ISOTOPES, THE SIMPSON GROUP (MIDDLE ORDOVICIAN), ANADARKO BASIN, OKLAHOMA

By
DAVID BRIAN MITCHELTREE

Submitted to the Faculty of the Graduate College of
New Mexico Institute of Mining and Technology
in partial fulfillment of the requirements
for the Degree of
MASTER OF SCIENCE
March, 1991

Acknowledgments

I would like to thank and express my gratitude to everyone who contributed to this research project. Principally, Dr. David I. Norman, who contributed a fair amount of time and an array of ideas and discussion to this project.

Further thanks are extended to Dr. David E. Powley for his interest in being a committee member, for presenting his ideas and concepts at Tech and suggesting the Weaver core for this study. I also appreciated the discussions on isotopes with Dr. Andrew R. Campbell, and his consenting to be a committee member. Dr. Peter Mozley provided literature, enlightening discussion on isotopes and the program Mastercarb 1.0. All of which greatly helped in understanding the isotopic results.

Funding for this project came from two sources. Dr. Zuhair Al-Shaieb at Oklahoma State University provided funding in addition to his interest in the project, a sincere thanks. Further funding came from the efforts of Dr. Norman in securing monies for new research from New Mexico Tech. Much thanks is extended to the Chemistry Dept. for employing me as an instructor, and the New Mexico Bureau of Mines for further employment as a grad.

A personal thanks is in order for Vanessa A. Tigert for freely giving and discussing information, and doing prior research integral to this project. Dr. Al-Shaieb also provided valuable information and discussion that was extremely useful in completion of this work. I'm indebted to the assistance and conversational value of Walter at the Oklahoma Core Library in helping me unload and reload a record amount of core boxes in a very limited amount of time. Thanks also to Eldon Cox for allowing unbridled access to the Weaver core and data at the Core Library. Chevron USA Inc. (Houston) provided additional data on the Weaver from it's current well file. Thanks also to Martha Cather at PRRC for allowing me to use the scope and camera equipment. Larry Kerns, of petroleum engineering dept. fame provided some interesting discussions, thanks. I would also like to thank Dr. Bill McIntosh and Jake Turin for laser printer usage. Brian Vaughn provided computer program assistance.

A special salute to DH and Lucho, how we made it is truly amazing in retrospect isn't it !?. General thanks to the rest of the grads and undergrads for friendship, assorted help and stimulating the old synapses occasionally.

Of course my parents, sister and road-tripping brothers deserve a note of thanks for their life long love and support over varying distances.

Stable isotope analysis was completed with the help of

Laurie D. Benton, but more importantly her love, conversation and support during the thesis has made my life far richer, I'm forever indebt.

TABLE OF CONTENTS

LIST OF FIGURES

FIGURE PAGE

LIST OF PLATES

ABSTRACT

DIAGENETIC PRESSURE SEAL ANALYSIS USING FLUID INCLUSIONS AND STABLE ISOTOPES, THE SIMPSON GROUP (MIDDLE ORDOVICIAN), ANADARKO BASIN, OKLAHOMA

Multi-layered diagenetic quartz, calcite and dolomite mineralization in the Simpson Group (Middle Ordovician) have formed a pressure seal at depth in the Anadarko Basin, Oklahoma, USA. Drill core from the Weaver Unit No. 1 well was selectively sampled from the depths of 11,014 to 12,067 ft. (3357 to 3657 m). Fluid and hydrocarbon inclusions were microthermometrically analyzed in a variety of diagenetic features (cements, fractures, void-fill, vug and stylolitic) for each type of mineralization. $\delta^{18}O$ and $\delta^{13}C$ stable isotope values were determined for some of the diagenetic carbonate mineralization. The $\delta^{18}O$ water (SMOW) values were constrained by fluid inclusion temperatures of homogenization (Th).

Fluid and hydrocarbon inclusion Th values indicate that diagenetic mineralization occurred with a thermal gradient at or greater than that currently present. But, less than the maximum paleo-thermal gradient for the Anadarko Basin indicated by vitrinite reflectance data. The diagenetic mineralization occurred at depth, over a broad temperature range, from fluids of highly variable density and lower salinity than that of current formation waters. Mineral oxygen and carbon values (PBD) for carbonates are light, indicating higher temperatures of mineral precipitation than expected for a purely marine water source. The $\delta^{18}O$ water values (SMOW) straddle that of standard mean ocean water with later diagenetic mineralization apparently becoming lighter (more) negative. The occurrence of potentially mobile hydrocarbon phases (gas and condensates) was late in the diagenetic time frame for quartz, calcite and dolomite.

Investigation

A fluid inclusion and limited stable isotope analysis of the Simpson Group interval drill core from the Gulf Oil Co. Weaver Unit No. 1, McClain County, Oklahoma (Fig. 1) is presented here. Pressure data analyzed by Tigert (1989) indicates that this cored interval is part of a pressure seal, apparently positioned between an upper underpressured compartment and a lower overpressured compartment (Fig. 2 and 3). The Simpson Group core had been studied with respect to petrography, depositional environments, geologic history and diagenesis (Tigert, 1989). The geochemistry of diagenetic mineralization is presented here in an attempt to understand pressure seal genesis as proposed in current theory.

Introduction

Abnormally pressured compartments and their pressure seals were recognized in some 180 deep sedimentary basins worldwide (Powley, 1987). Compartments, generally in sedimentary rocks, have an internal volume which exhibits hydraulic continuity. Commonly they are encountered during drilling at an average depth of 10,000 ft. (3,048 m) in basins undergoing subsidence (Hunt, 1990). Abnormally

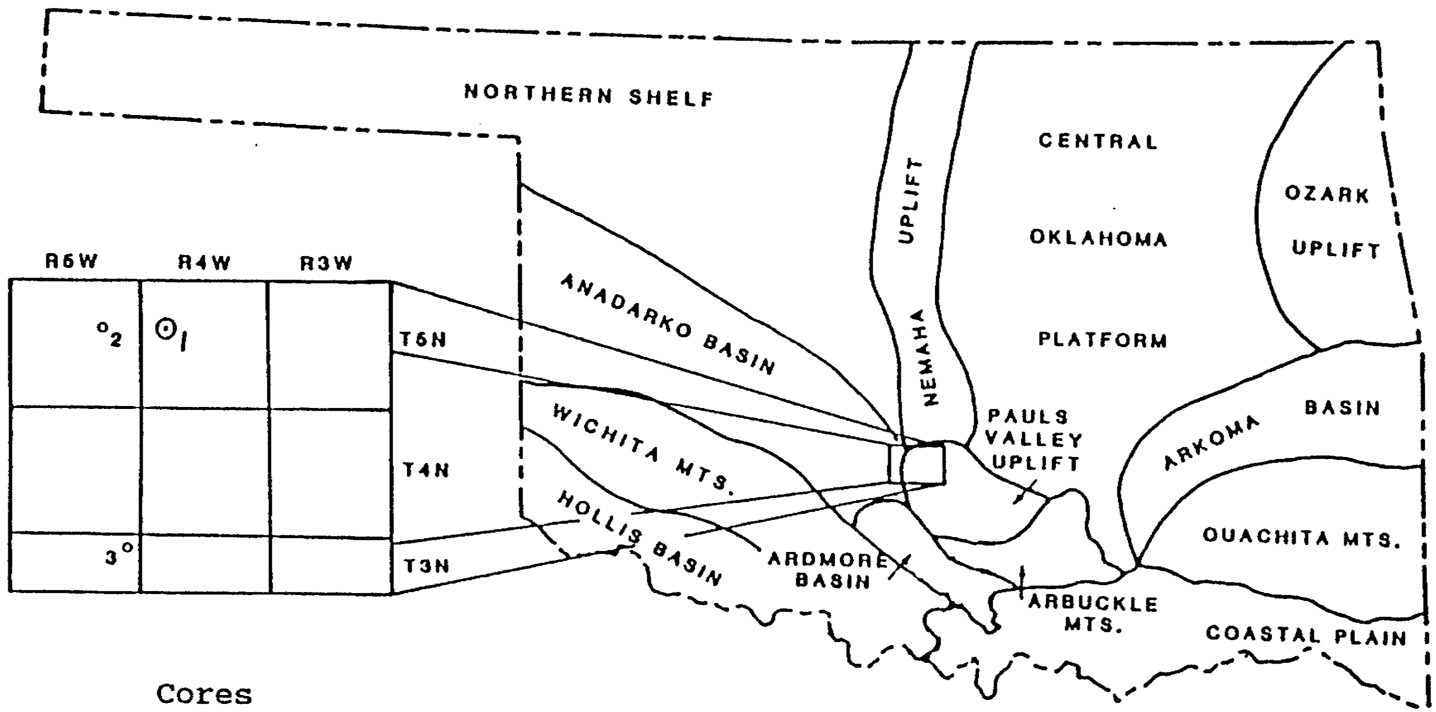

Cores

1. Weaver Unit No. 1, Gulf Oil Corp.
2. Costello No. 1, Gulf Oil Corp.
3. Sunray DX Parker, Mazur No. 1

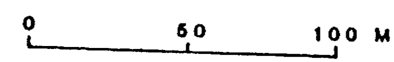

Figure 1. Core locations and tectonic features of Oklahoma (modified after Weber, 1978).

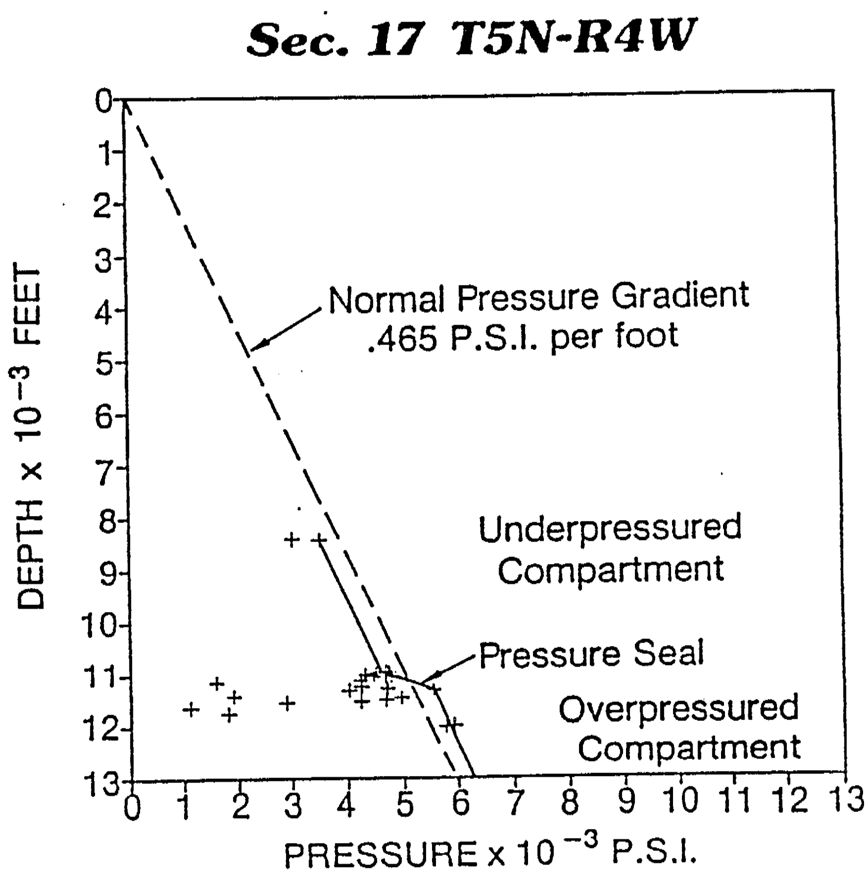

Figure 2. Pressure-depth profile identifying abnormal pressures in the southwestern corner of McClain Co., Okla. Abnormal pressures exhibit a higher or lower gradient than the normal gradient of 0.465 psi/ft. (from Tigert, 1989).

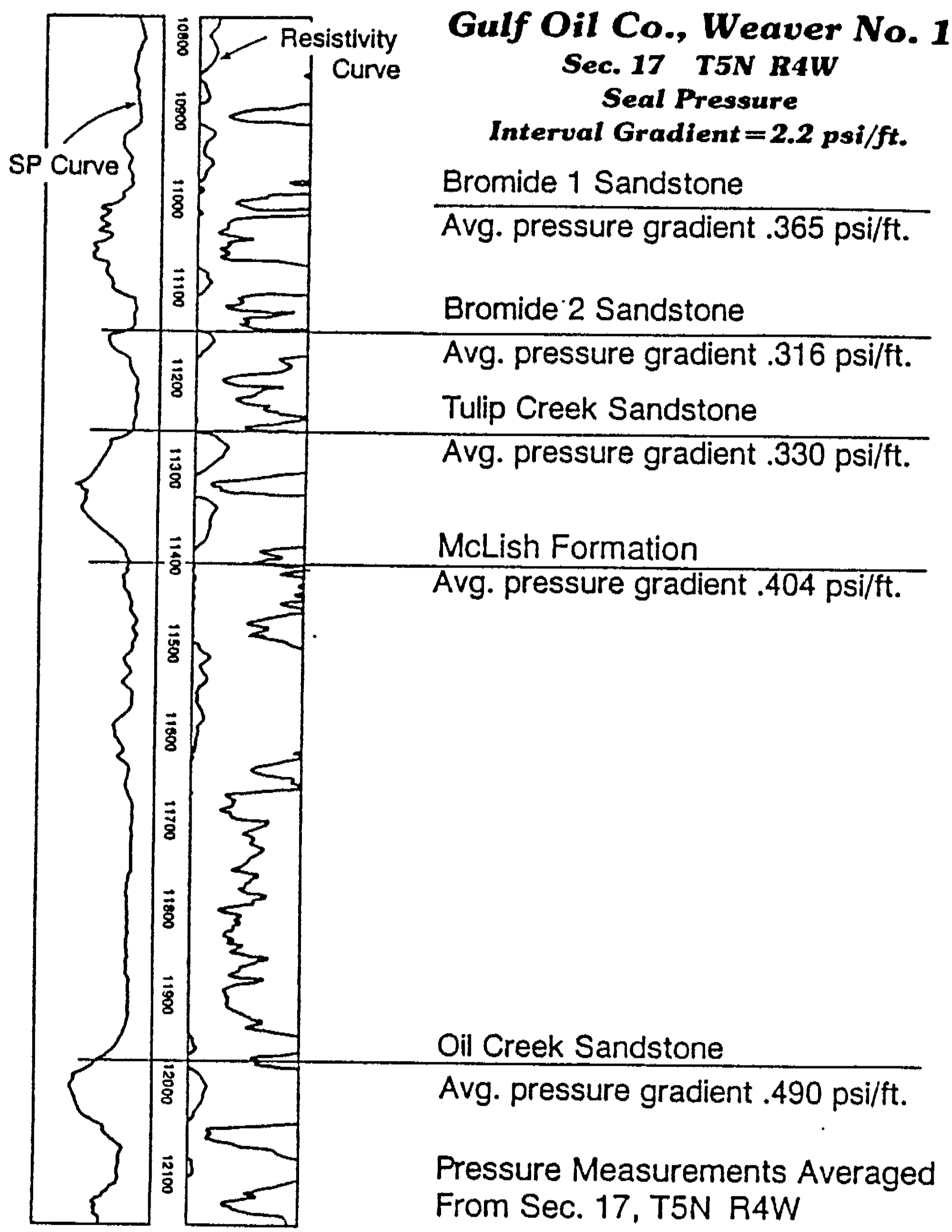

Figure 3. Simpson Group formations with average pressure gradients in relation to resistivity and spontaneous potential well logs of the Weaver Unit No. 1 (from Tigert, 1989).

pressured compartment volumes are effectively isolated from their surroundings by an envelope of pressure seals with low permeability. Seals have such low permeabilities that measurable pressure differentials across them have been maintained over geologic time scales (Bradley, 1975; Powley, 1987; Hunt, 1990).

Three types of seals may be recognized in deep sedimentary basins (Fig. 4). Basal seals tend to follow stratigraphy and demark the lower extent of many compartments (Powley, 1987). Lateral seals are generally at high angles to bedding and may coincide with high angle faults in highly fractured and faulted zones, coincide with lithologic facies changes or be related to chemical deposition in restricted zones. Lateral seals may also be a combination of these factors (Powley, 1987; Logan, 1989). Many top seals are oriented horizontally or at low angles to bedding and can be independent of lithology and can cross cut time-stratigraphic boundaries and structures (Powley, 1987). Hunt (1990) states that top seals of overpressured compartments in currently sinking basins commonly have temperatures between 90 to 100 °C (194 to 212 °F). Clastic-hosted top seals commonly consist of multiple horizontal calcite mineralized bands formed along a thermocline. Thickness of these seals range from 150 to 3000 ft. (45.7 to 914.4 m) thick with a majority approximately 600 ft. (182.8 m) thick. Carbonate-evaporate seals are generally somewhat

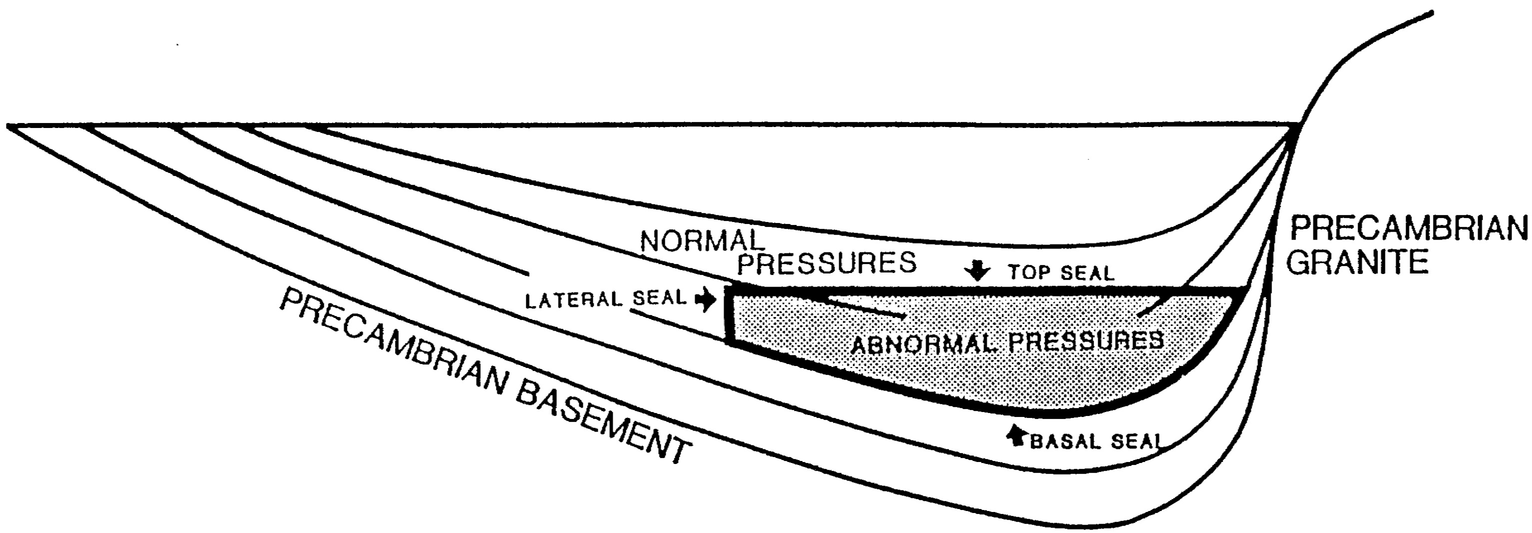

Figure 4. Top, lateral and basal pressure seals enclosing an abnormal pressure compartment (modified after Powley, 1987).

thinner (Powley, 1987).

Hunt (1990) notes that cores from seal zones frequently contain calcite filled fractures, as opposed to cores from within overpressured compartments that are barren of fracture mineralization. Seals may have variable internal permeability aside from fracturing. In a seal, Tigert (1989) noted alternation of impermeable and cemented verses permeable and porous intervals that are unrelated to depositional facies. Permeable and impermeable strata were originally the same material, but cementation patterns were further oppositionally enhanced by secondary porosity development.

Some seals contain interlayers of hydrocarbon-producing permeable zones or specifically permeable sandstones (Hunt, 1990; Tigert, 1989). Jansa and Urrea (1990) report condensate-gas accumulations in overpressured zones at temperatures of 125 to 150 °C (257 to 302 °F) and a vitrinite reflectance R_o value of 0.8 to 1.0 %. Meshri and Comer (1990) present a case of a proposed diagenetically sealed hydrocarbon reservoir in the Alberta Basin Glauconite Sandstone. The reservoir has water overlying and updip from gas in correlative beds.

Episodic expulsion of fluid phases from sealed pressure compartments in conjunction with fracturing and resealing may explain the common occurrence of fractured top seals (Powley, 1980; Bradley, 1975). U. S. Gulf Coast studies have shown that after a seal has ruptured, compartment fluid pressure decreases to approximately 13.5 kPa/m (0.6 psi/ft.), but doesn't decrease fully to hydrostatic pressure (Hunt, 1990). Ramboz and Charef (1988) examined fissure and late stage barite that contained fluid and hydrocarbon inclusions in a small compartment bounded by Jurassic normal faulting in a dome. They propose that the compartment overpressures were decreased to hydrostatic values of less than 100 bars when seals hydraulically fractured. Subsequently, H_2O-CO_2-NaCl fluids at temperatures greater than 150 °C (302 °F) were diluted by water and cooled to less than 135 °C (275 °F). Gas-pool pressure measurements indicate that fracture openings appear to reseal while a compartment still maintains moderate overpressures (Federal Power Commission data, 1973; from Hunt, 1990).

Oscillatory fluid release from overpressured compartment top seals on a geologic time scale has been modeled by Ghaith et al., 1989. This phenomenon may be promoted by rapid burial, high geothermal gradients and large volume compartments. Some aspects of basin compartmentalization may involve amplification of textural nonuniformity, or self-organization as discussed by Dewers and Ortoleva (1988). Current debate of the compartmentaliztion theory is presented by Waples (1991), Toth et al. (1991) and by Hunt (1991a, 1991b).

Geologic Background

The Simpson Group sediments are Middle Ordovician (approximately 465 to 488 Ma, Chazy and Mohawk Stages) in the southeastern region of the Anadarko Basin, Oklahoma. They were deposited by northward transgressive-regressive cycles of a shallow sea. Average thickness of the Simpson Group in McClain County is approximately 1250 ft. (381 m), and the Simpson Group reflects deformation that was contemporaneous with relatively rapid sedimentation in an actively subsiding basin (Tigert, 1989). Progressive burial of the Simpson Group in conjunction with subsidence was continual through the Pennsylvanian (Donovan, et al., 1983), and for the Weaver may have reached a maximum burial of approximately 14,000 ft. (4267.2 m) (Al-Shaieb, per. comm., 1990; Pitman and Burruss, 1989). Stratigraphic reconstruction and vitrinite reflectance studies indicate that late in the burial history erosion may have removed between 2,000 to 5,000 ft. (609.6 to 1524 m) of sediment depending on location in the basin (Schmoker, 1986).

The Weaver Simpson Group interval examined in this study occurs at a depth of 11,014 to 12,067 ft. (3357 to 3678 m), and consists of five formations; Joins, Oil Creek, McLish, Tulip Creek and Bromide (Fig. 5). The Joins Formation was deposited during a marine transgression. Four

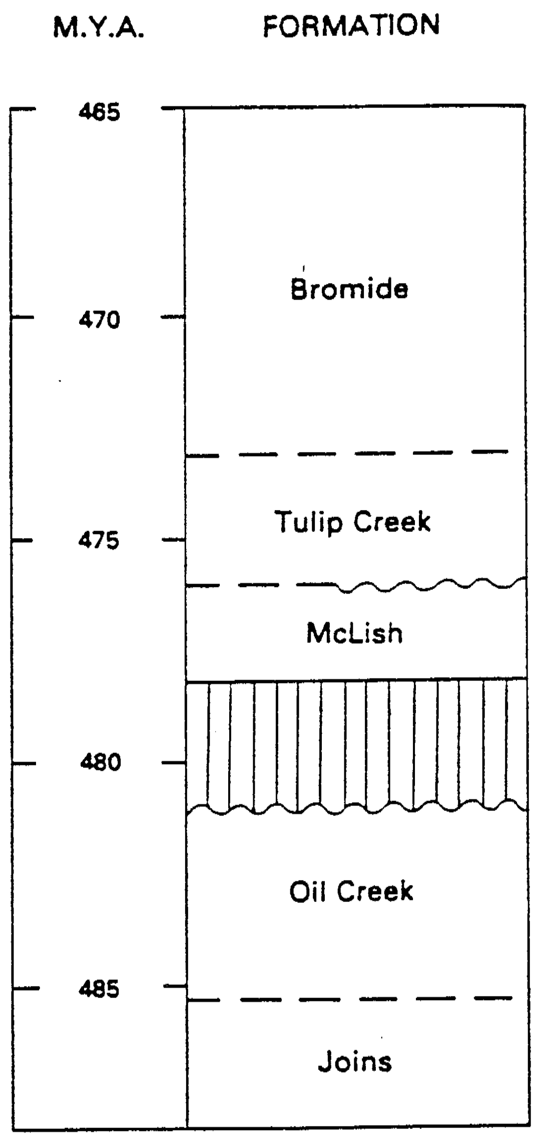

Figure 5. Stratigraphic column for Middle Ordovician Simpson Group formations (after Ross, 1982).

further subsidence pulses occurred with deposition of the Middle Ordovician Simpson Group on a low relief carbonate platform. The cyclic stratigraphy of the Oil Creek, McLish and Tulip Creek Formations corresponds with three transgressive-regressive related pulses. An unconformity bounds the upper extent of the Oil Creek Formation, and a disconformity to paraconformity is between the McLish and the Tulip Creek. The fourth pulse produced the Bromide Formation in conformable contact with the underlying Tulip Creek. Later the Bromide was subjected to regressive erosion of the upper surface. The Bromide is subdivided into an upper and lower unit, the First and Second Bromide Sandstones, respectively. Note that the Tulip Creek may be reported as the Third Bromide Sandstone on some scout tickets (Longman, 1981; Weber, 1978; Tigert and Al-Shaieb, 1989). Cyclicity of the Simpson Group in Oklahoma and West Texas is probably related to localized tectonic events proximal to the basin region (Weber, 1978).

Tigert (1989) presents a detailed description of the lithologic and diagenetic banding patterns of the Weaver core formations (Fig. 6). These descriptions were used as a groundwork for this study. Diagenetic processes observed are cementation, intergranular pressure-solution and mechanical brecciation. Differential cementation patterns have varying porosity and relative thickness, but the resulting permeable and impermeable variation collectively

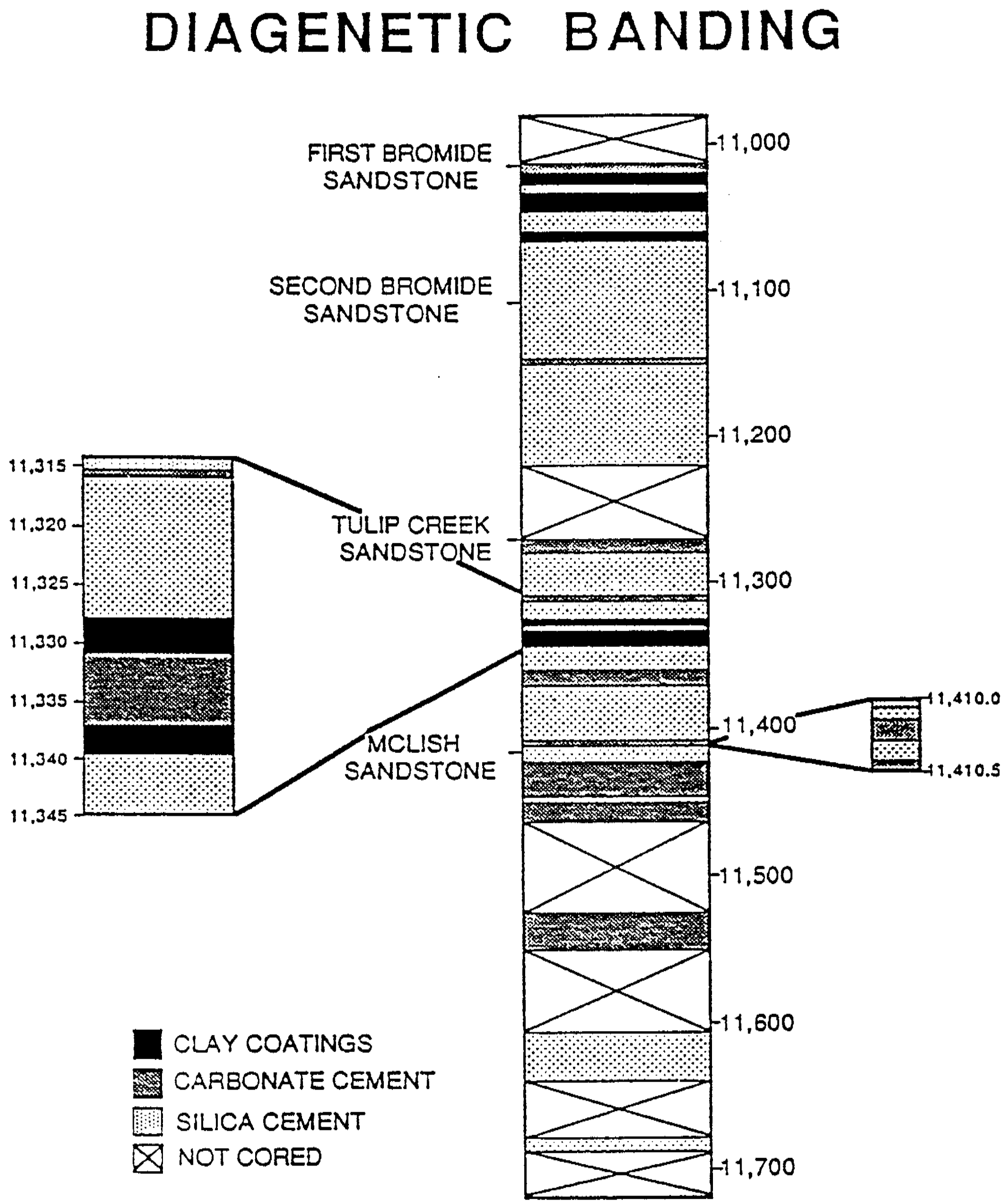

Figure 6. Schematic diagram of diagenetic banding of the pressure seal present in the Weaver Unit No. 1 (from Tigert, 1989)

acts as a pressure seal (Tigert, 1989). The cemented zones therefore invoke a similar role as more traditionally viewed shale and evaporite seals do. Tigert (1989) concluded that carbonate and/or silica cemented intervals alternating with porous and permeable zones resulted in uniquely banded "diagenetic lithologies" unrelated to depositional facies.

Fluid Inclusions

Prior Work

It has been demonstrated that temperature, composition of the cementing fluids, pressure, density and relative timing of precipitation may be determined for diagenetic features by careful analysis of fluid inclusions. Lundegard (1989) states that inclusion temperatures of homogenization are the most direct method of inferring diagenetic cementation temperatures. However, diagenetic mineralization is not a continuous process and cementing occurs only when fluid chemistry is favorable, and inclusions may only be trapped under certain crystal growth parameters (Burruss et al., 1985). Analysis of low temperature inclusions from diagenetic environments presents specific problems that must be considered. Clearly identifying primary (P) and pseudo-secondary (PS) as opposed to secondary (S) inclusions (as defined by Roedder, 1984) is critical and difficult to be absolutely certain of. But, a number of papers have demonstrated that fluid inclusions (and in some cases hydrocarbon inclusions) can be used to constrain and elucidate diagenetic temperatures and other factors in deep, subsurface sedimentary-environments (Aulstead et al., 1988; Aulstead and Spencer, 1985; Burley et al., 1989; Burruss et al., 1985; Cercone and Lomann, 1987; Ehrenberg, 1990; Haszeldine et al., 1984; Kaufman et al., 1990; McLimans and Videtich, 1989; Moore and Druckman, 1981; Pratt and Burruss, 1988; Tilley et al., 1989; Videtich et al., 1988; Visser, 1982; Walderhaug, 1990). McLimans (1987) has summarized some fluid inclusion studies applied to hydrocarbon maturation and migration and diagenesis in petroleum reservoirs. Th values from inclusions in sedimentary rocks usually represent the minimum trapping temperature and must have a pressure correction applied to ascertain the true trapping temperature (Tt), depending on the nature of the inclusion and the exact environment of formation at depth. Pressures at the time of mineralization may be determined using inclusions with particular chemical compositions or certain populations of inclusions formed under cogenetic pressure conditions with one another (Burruss, 1980; Burruss, 1985, summary).

Norman (unpubl. data interpretation) used fluid and hydrocarbon inclusion microthermometry and inclusion gas analysis (bulk crushing) by quadrupole mass spectrometry to determine the pressure and temperature gradients for MWX wells in the Piceance Basin, Colorado. Fracture and vug inclusions in quartz and two generations of calcite (one cogenetic with quartz) mineralization were analyzed. Fracture mineralization occurred with aqueous liquids present at temperatures of 90 to 190 °C (194 to 374 °F) and salinities of 0.35 to 11 eq. wt. % NaCl. An aqueous brine, hydrocarbon (blue fluorescence in UV) liquid and vapor phase of predominately methane were contemporaneous with fracture mineralization at overpressures ranging from 6000 to 8000 psi (413.6 to 551.5 bars) (Norman, 1987). The resultant fluid inclusion pressure gradient data shows an overpressure offset conforming to pressure seal documentation presented by Powley (1990).

Methods of Inclusion Analysis

Low-temperature, doubly-polished wafers for inclusion analysis were produced following methods and considerations detailed in Barker and Reynolds (1984). Wafers have a final polish of 0.5 microns done with diamond-paste. Unpolished cleavage-fragments were used whenever possible as a check that inclusions were not affected by heat induced by the polishing. Comparison of inclusion measurements from both cleavage and doubly polished wafer chips indicated that no detectable stretching or reequilibration of inclusions had occurred as a result of the preparation procedure. This was done to reduce possible experimental error as outlined by Meunier (1989). The number of inclusions analyzed by heating and freezing was limited to a maximum of five per chip to reduce the possibility of errors induced by stretching.

Inclusion microthermometric measurements were made with a Linkam TH600 heating and freezing stage (range -195 to 600 °C) (Shepherd, 1981). Calibration was done using melting point standards and USGS synthetic inclusions (Appendix A). In most cases temperature of melting (Tm) measurements were performed prior to temperature of homogenization (Th). But, for every inclusion population some Th values were done prior to freezing in consideration of possible low salinity aqueous (L-V) inclusion deformation with freezing (Lawler and Crawford, 1983; Roedder and Bodnar, 1980; Meunier, 1989; McLimans, 1987). According to McLimans (1987), stretching of inclusions as a result of freezing is unpredictable with respect to the fluid composition and inclusion size or shape.

To enhance the accuracy of Tm measurements cycling was commonly employed. Vapor bubble reappearance between eutectic and final melting temperatures commonly occurred on warming. A precision of -/+ 0.2 °C was maintained with slow cycling rates. Tm values were used to calculate salinity in equivalent weight percent (eq. wt. %) NaCl based on the data of Potter and Clynne (1978). Positive Tm values may represent either the presence of clathrates or inclusion metastability (Roedder, 1984). Therefore, all positive melting temperatures were assumed to represent clathritic melting and salinities were estimated based on the data of Collins (1979).

Cautious microthermometry was used in order to minimize errors in Th measurements resulting from stretching of inclusions as a consequence of heating. Chips used in heating runs may have inclusions with different Th values, hence it is possible to exceed the Th of some inclusions during measurements. To minimize stretching, no chip was heated to more than 5 °C above the lowest Th measurement. Experimental results for calcite-hosted inclusions indicate that stretching may occur if inclusions are heated in excess of Th by 5 °C (Prezbindowski and Larese, 1987). Heating runs were of as short a duration as possible, and cycling was employed to reduce the possibility of exceeding Th. Nearing phase homogenization a heating rate of 0.5 °C/min. was stopped and step heating was then employed. After step heating to what was considered the homogenization point, the temperature was reduced a minimum of 10 °C. If a vapor bubble reappeared within this 10 °C cooling range it was assumed that the inclusion did not homogenize. Stepped cycling was then resumed until inclusion homogenization had occurred. Estimated precision of Th measurements is +/- 1.0

°C. Th represents the minimum trapping temperature (Tt). Both Th and Tm measurements were obtained on the same inclusion as long as they appeared to maintain their competency during heating and freezing. Fluid densities were calculated using Th and salinities with data from Potter and Brown (1977) for individual inclusions.

Inclusions containing hydrocarbons were identified by their fluorescence using a blue-violet (400 to 440 nm, with a main wavelength of 436 nm) excitation light source. Levine et al. (1991) noted that the most intense fluorescence for hydrocarbon inclusions they examined occurred with blue light excitation of about 445 nm, whereas other authors commonly recommend a wavelength of 365 nm for identification of hydrocarbons.

Doubly polished sections were stained to distinguish among calcite, dolomite, ferroan calcite and ankerite. KCN and Alizarin red S in a weak HCl solution was used for staining in a modified method from Dickson (1965, 1966).

Fluid Inclusion Results

For all of the Weaver Simpson Group formations between 11014 and 12067 ft. (3357 to 3657 m) doubly polished wafers were made. Wafers were prepared from fifty three specific depths. Inclusions were microthermometrically analyzed in wafers from 23 of these depths in addition to cleavage chips and individual crystals from these and two more depths. Some 300 individual inclusions were analyzed from all formations except the Oil Creek Sandstone. In this study only P or PS inclusions were analyzed; these were from intergranular diagenetic cements, void-fill, fractures and stylolitic-associated mineralization. Most inclusions analyzed had a maximum dimension less than 15 microns, and the smallest analyzed were 3 microns. The exceptions were a few inclusions in void-fill mineralization with dimensions over 100 microns.

In the quartz grains of sandstones numerous inclusions are present. No microthermometric analysis or systematic observation of these inclusions was conducted, but some general observations are reported here. In many sections quartz grains displayed heavy internal fracturing and a variety of proposed pressure solution features as discussed by McBride (1989) and specifically by Tigert (1989). Within heavily fractured quartz grains relatively fewer inclusions were observed when compared to non-fractured grains. Fluid inclusions observed in quartz grains were single phase vapor (V), single phase liquid (L), V-L, L-V, L-V with varying numbers of daughter minerals, three phase CO_2-rich, and miscellaneous opaque (possibly some hydrocarbon), and solid melt inclusions. These inclusions were mainly P and PS with respect to the grains, with some S inclusions in planes, etc. that were unrelated to adjacent diagenetic features.

The quartz grain inclusions were consistently far more numerous and of far larger volume than inclusions analyzed in diagenetic mineralization.

Inclusions in Quartz

From the Bromide and McLish Formations aqueous (L-V) inclusions were analyzed in quartz cementing overgrowths of quartz grains. Inclusions in quartz overgrowths are few in number and very difficult to see because they are generally less than 5 microns. Aqueous inclusions (L-V) and two types of hydrocarbon inclusions (two phase (L-V) and multiphase (L or L-V) at room temperature) are present in void and vug filling quartz in the McLish Formation.

In vug and void-filling quartz mineralization, aqueous and hydrocarbon inclusions appear to be cogenetic. In void-fill quartz the aqueous (L-V) and hydrocarbon inclusions (at 25 °C, 77 °F) were frequently indistinguishable with respect to size, color (colorless liquid and vapor), distance between inclusions and liquid/vapor volume ratio. Only with microthermometry and fluorescence in blue-violet light could a distinction be made (Plates 5 and 6).

In the two phase (L-V) hydrocarbon inclusions the liquid fluoresced blue-white, separated into three phases with cooling, and homogenized to a vapor phase upon heating (Fig. 7 and Plates 1 through 4). Phase "homogenizations"

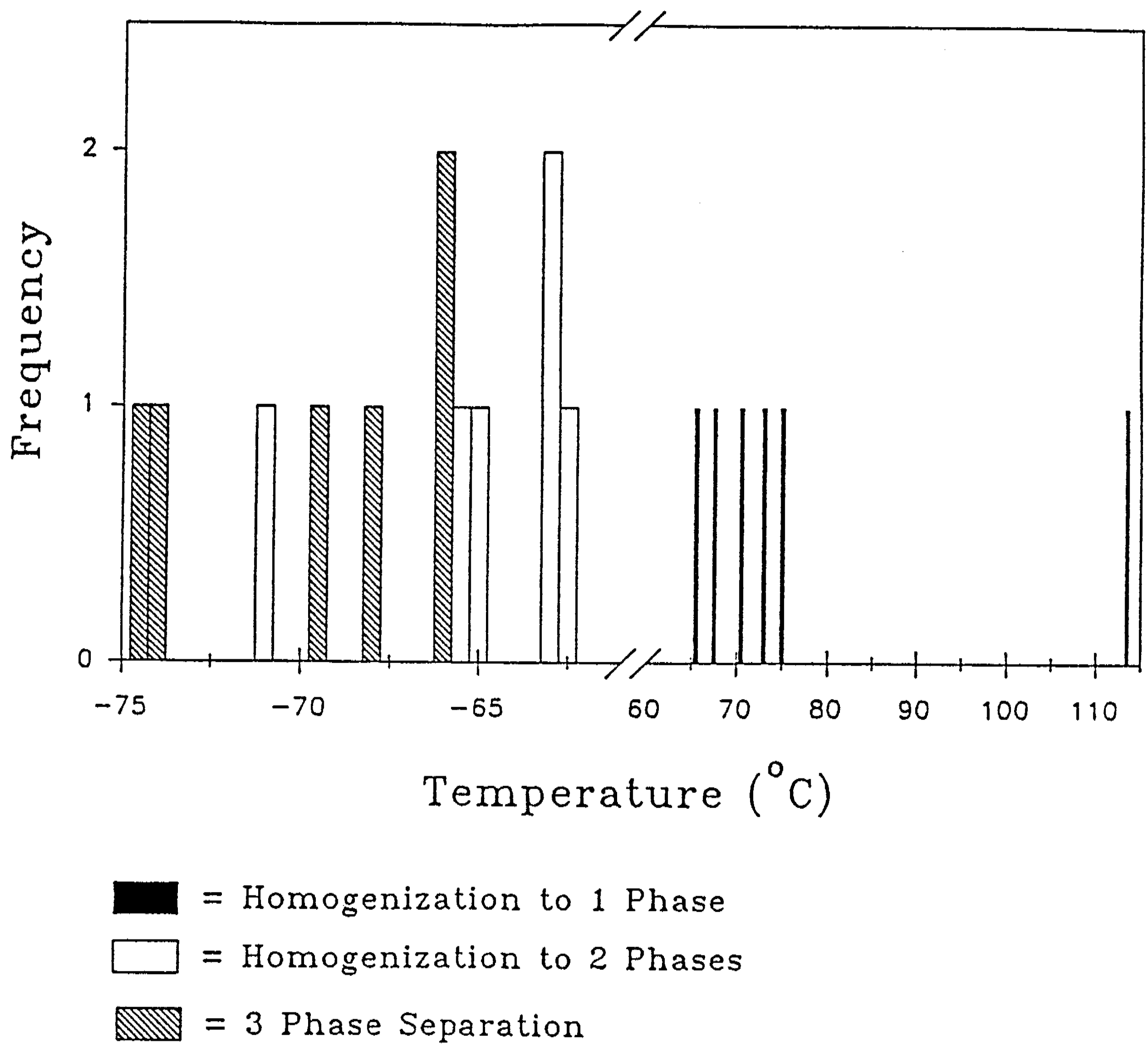

Figure 7. Histogram of hydrocarbon inclusion phase behavior upon heating and freezing.

Plate 1. First in the series of Plates showing heating and freezing of the same hydrocarbon inclusion, which is 75 microns across with respect to the long axis. The inclusion is in a quartz crystal, with two faces of it's termination creating the dark band in the Plate. At -91.9 °C the inclusion has separated into three phases which appear to be two immiscible liquids and a vapor.

Plate 2. At -70.7 °C the inclusion has almost completely coalesced into a vapor and liquid phase.

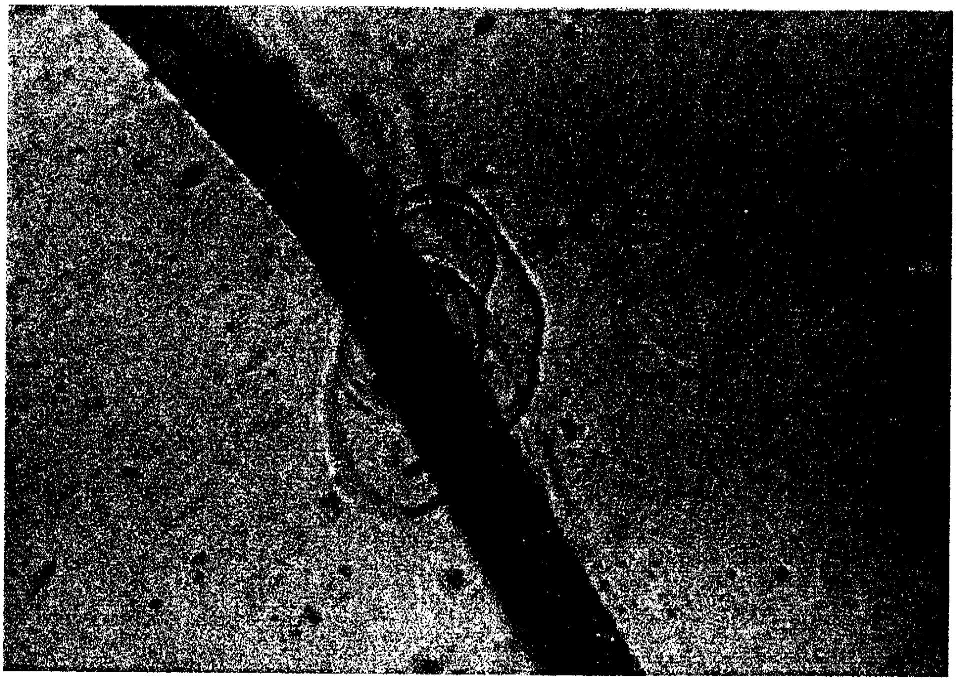

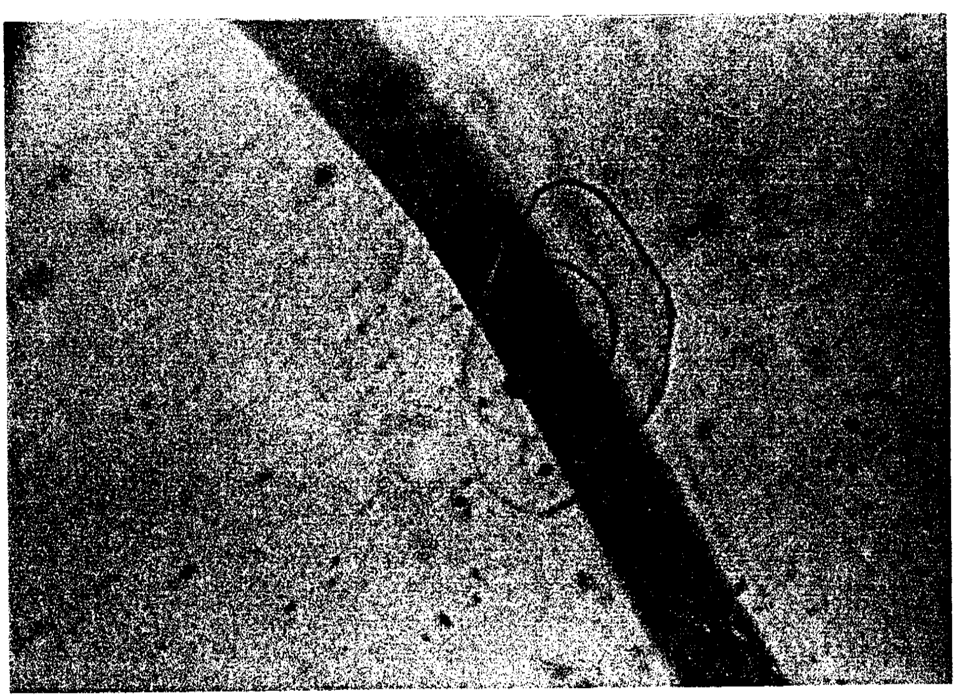

Plate 3. At 24.6 °C the inclusion has a liquid and vapor phase.

Plate 4. At 77.0 °C the inclusion has nearly homogenized to a single vapor phase.

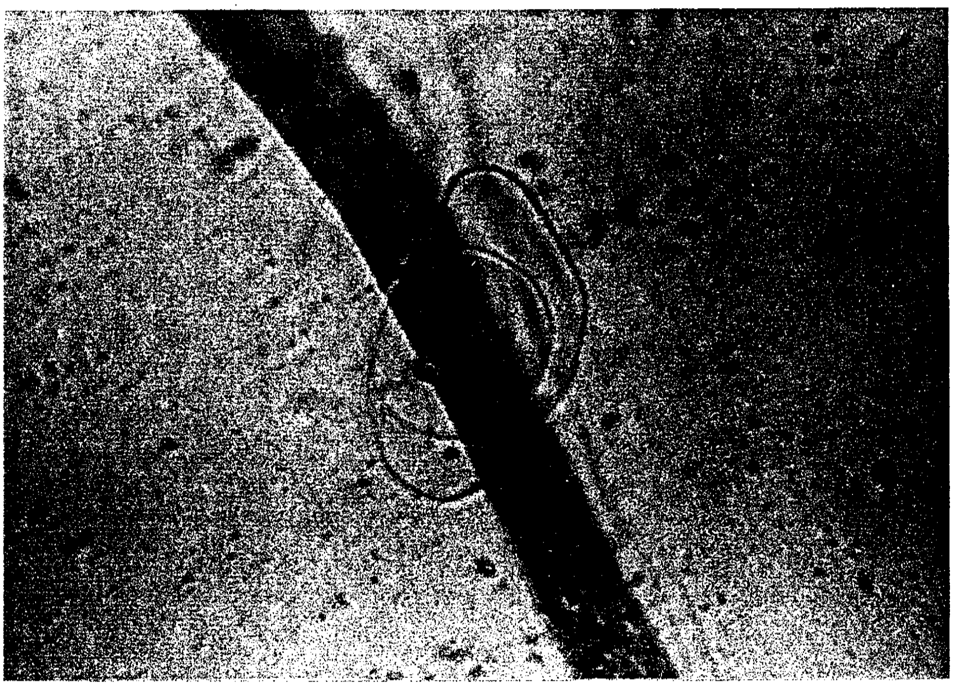

Plate 5. Transmitted light view of the same inclusion with a larger field of view of the quartz crystal termination at 25 °C.

Plate 6. Blue-violet light view of the same inclusion with the liquid phase fluorescing blue-white and the vapor phase that is non-fluorescing (note additional fluorescing inclusions).

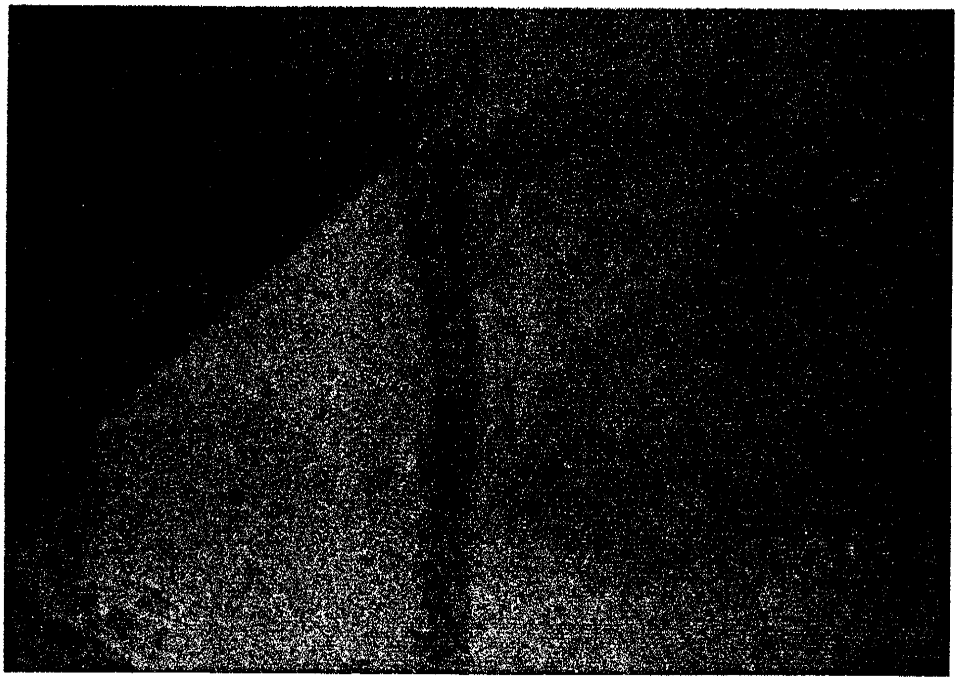

appeared to be part of a continuum of volumetric expansion to coalescence to two phases, and a gradual meniscus "fading" with homogenization to a single phase. Levine (1991) has observed similar types of behavior and temperature ranges of phases homogenizations with heating and freezing of hydrocarbon inclusions. These inclusions were almost always rounded, ellipsoid in shape. In some euhedral vug crystals these had exceptional 100 micron diameters.

Present in both void-fill and vug quartz were a variety of multiphase hydrocarbon inclusions which in transmitted light had separate phases ranging from clear through shades of tan/brown to dark brown/black with an occasional vapor bubble. When present, vapor bubbles were always located within the liquid hydrocarbon phase. Clear liquids fluoresced blue-white, and with progressive coloration (tan to brown), fluorescence was more blue-yellow to blue-green. The essentially opaque phases showed no detectable fluorescence. These hydrocarbon filled inclusions have from two to six separate, immiscible phases. The relative amount of each phase is highly variable within each individual inclusion at 25 °C. These inclusions frequently had an angular, chaotic morphology. Microthermometry of multiphase inclusions from -195 to 300 °C (-319 to 572 °F) produced no systematic results, in part due to the limited number of similar multiphase inclusions. Some inclusions contained liquids that fluoresced blue-white and showed meniscus fading with heating (as previously described), while other phases present in the same inclusion showed no change. Colored phases (in transmitted light) rarely displayed any change with heating and freezing. A few inclusions may have contained a minute water/brine portion squeezed between colored phases against the inclusion wall, based on non-fluorescence and apparent ice formation on freezing. Water is commonly invisible in hydrocarbon inclusions due to its tendency to coat inclusion walls (Roedder, 1984).

For all types of quartz mineralization the aqueous inclusion Tm values range from -15 to 6 °C, and are divided into two populations (Fig. 8). The lower Tm group represent void mineralization values and one cement value. The higher Tm group are overlapped values of void and cement mineralization. There is a slight mean shift toward a decrease of Tm with depth (Fig. 10). Calculated salinity values are from 0.5 to 19 eq. wt. % NaCl (Fig. 11). The salinities tend to cluster together based on the mineralization source, but there is no apparent data trend with depth (Fig. 12). The Th values have a range from 65 to 135 °C (Fig. 9). All values below 80 °C are aqueous inclusions associated with hydrocarbon inclusions in vug mineralization. Again there is a trend of decreasing Th values with depth (Fig. 10). The inclusion fluid density values show a related decrease with depth (Fig. 13). The

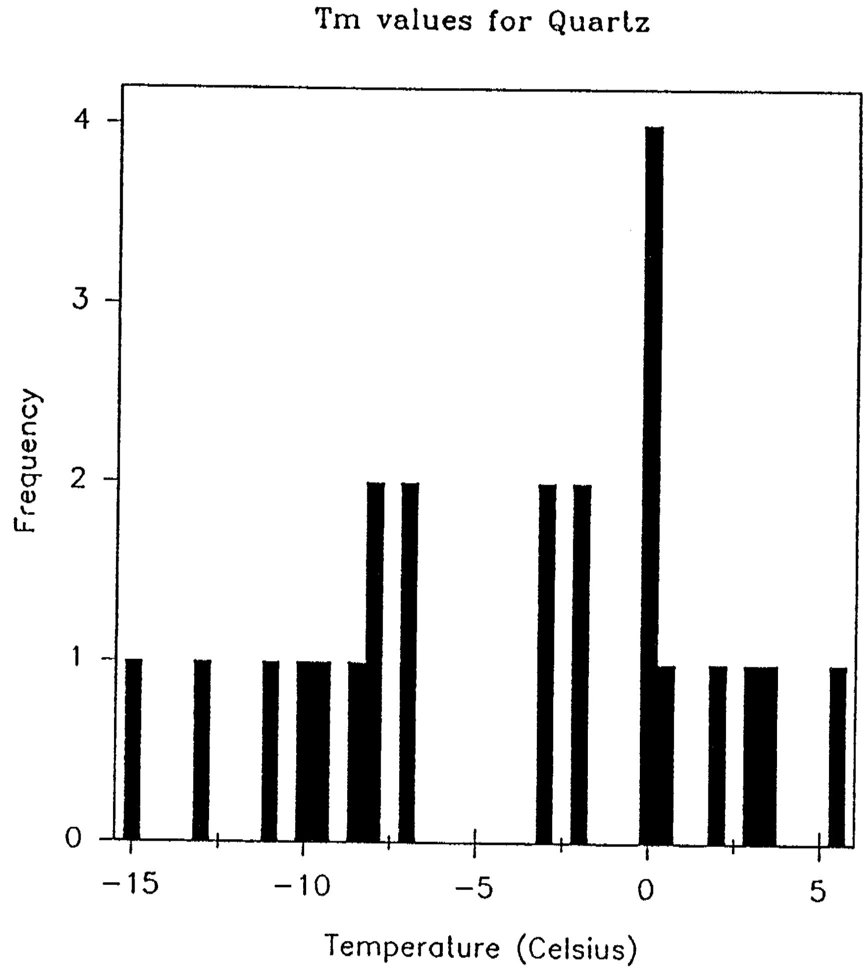

Figure 8. Histogram of temperatures of melting for aqueous (L-V) inclusions hosted in quartz mineralization.

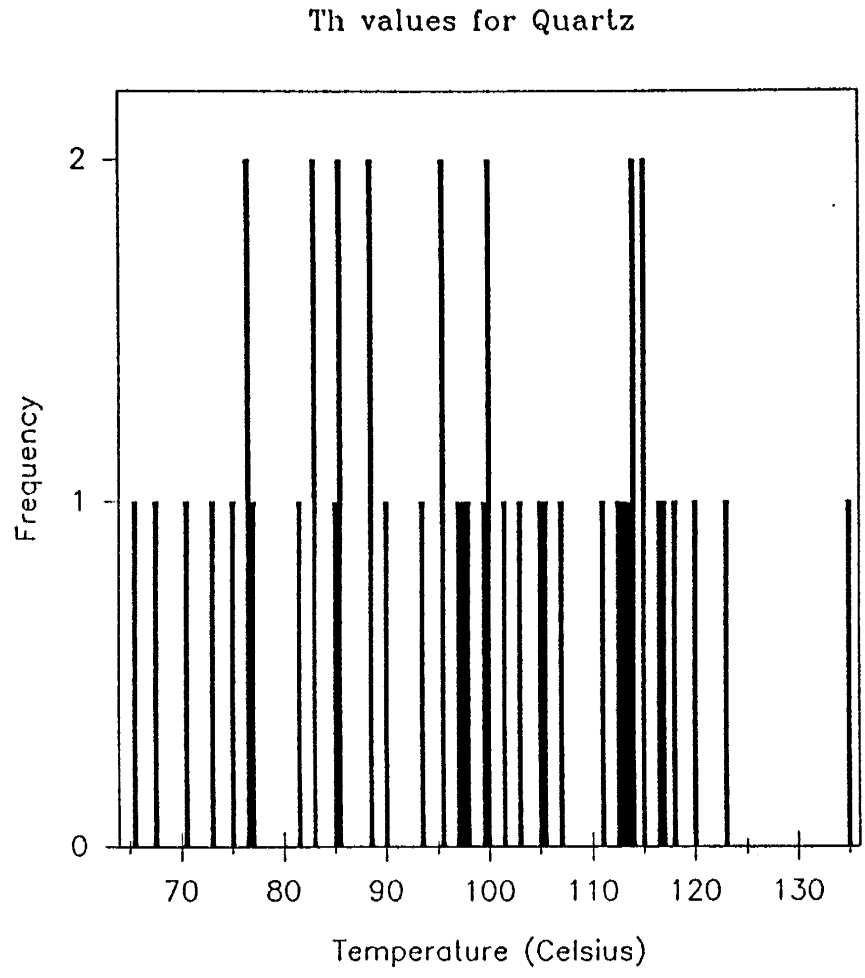

Figure 9. Histogram of temperatures of homogenization for aqueous (L-V) inclusions hosted in quartz mineralization.

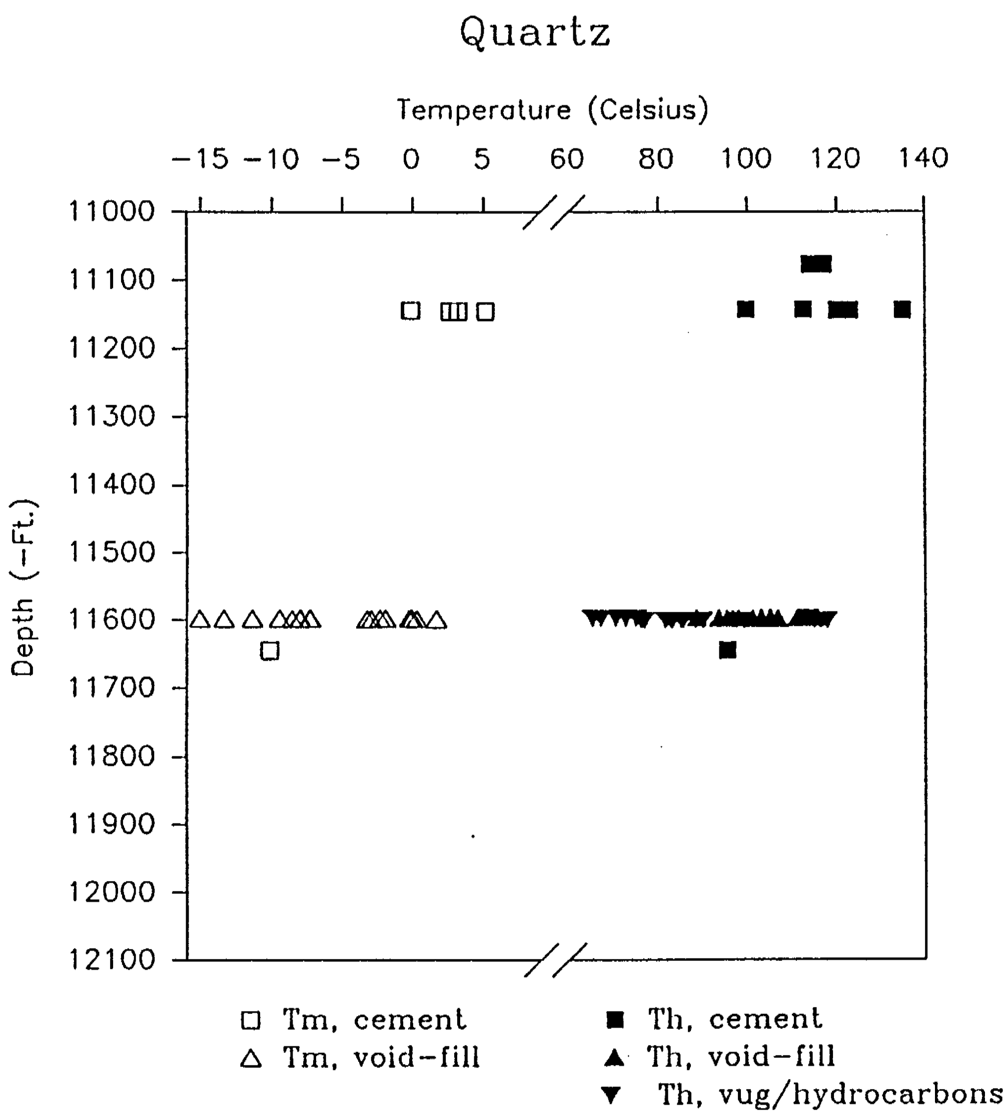

Figure 10. Temperatures of melting and homogenization for aqueous (L-V) inclusions verses sample depth for specific quartz mineralization features.

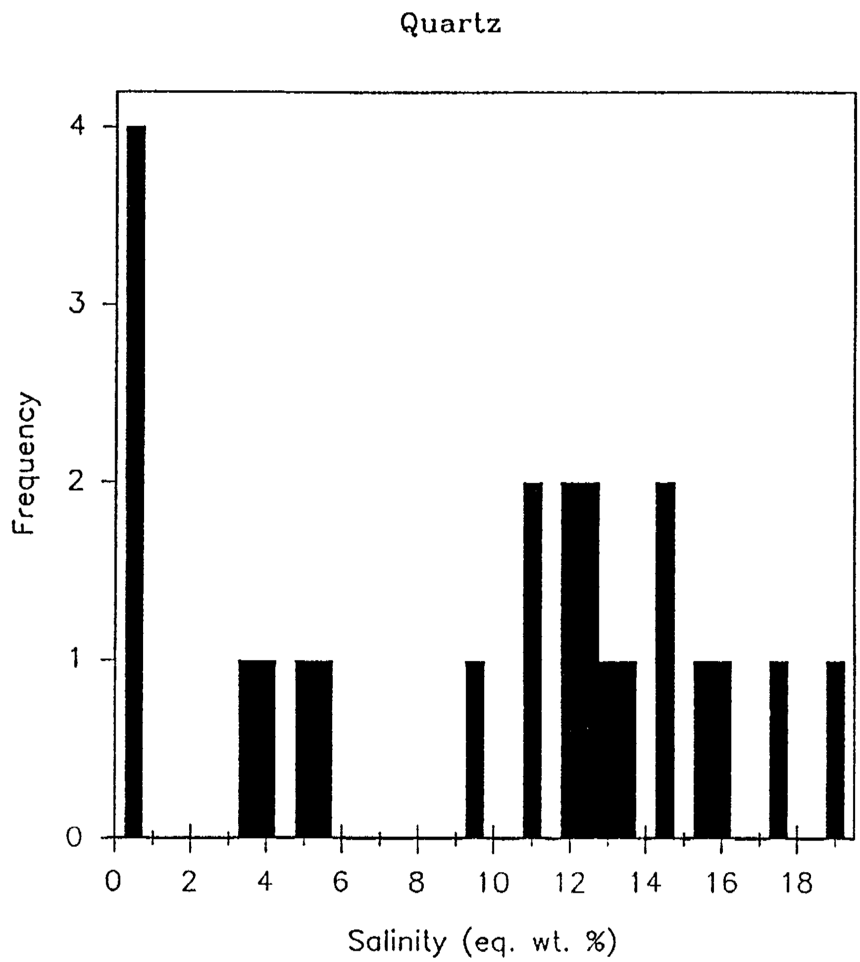

Figure 11. Histogram of salinities for aqueous (L-V) inclusions hosted in quartz mineralization.

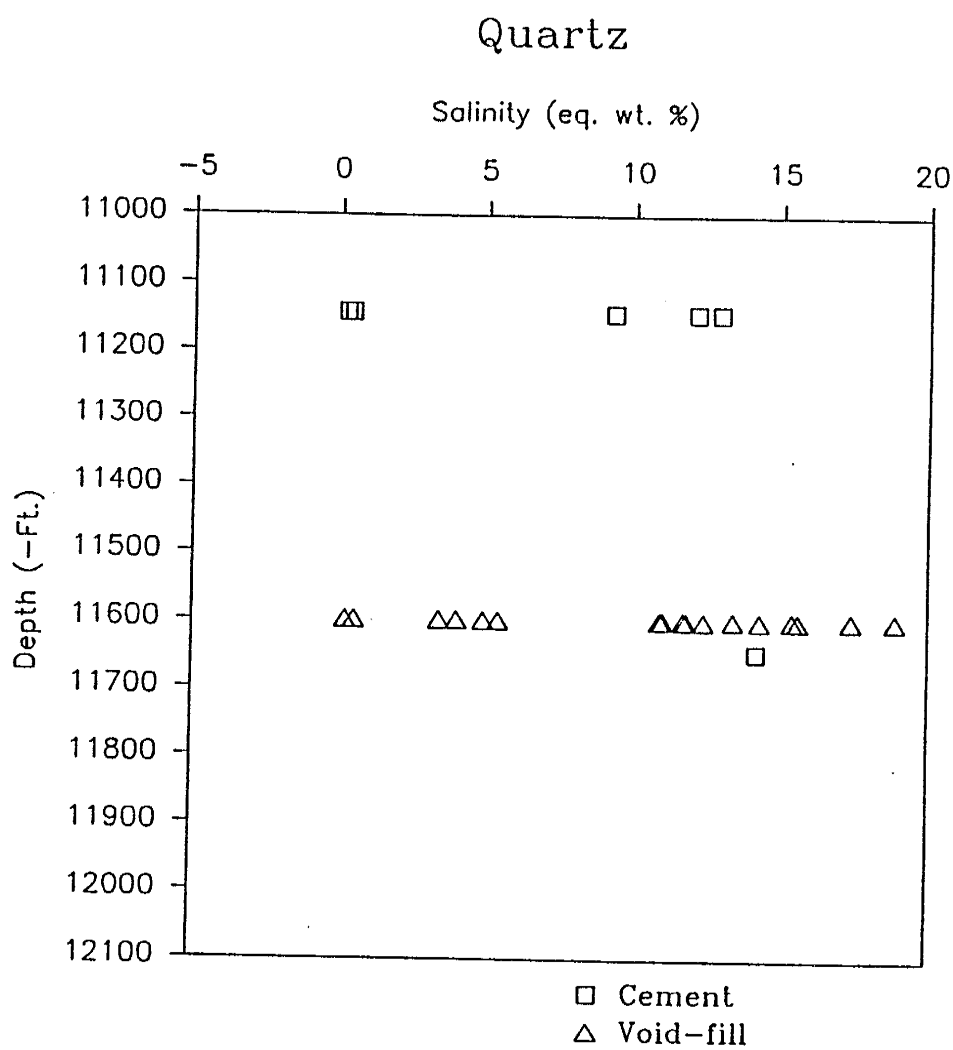

Figure 12. Salinities of aqueous (L-V) inclusions verses sample depth for specific quartz mineralization features.

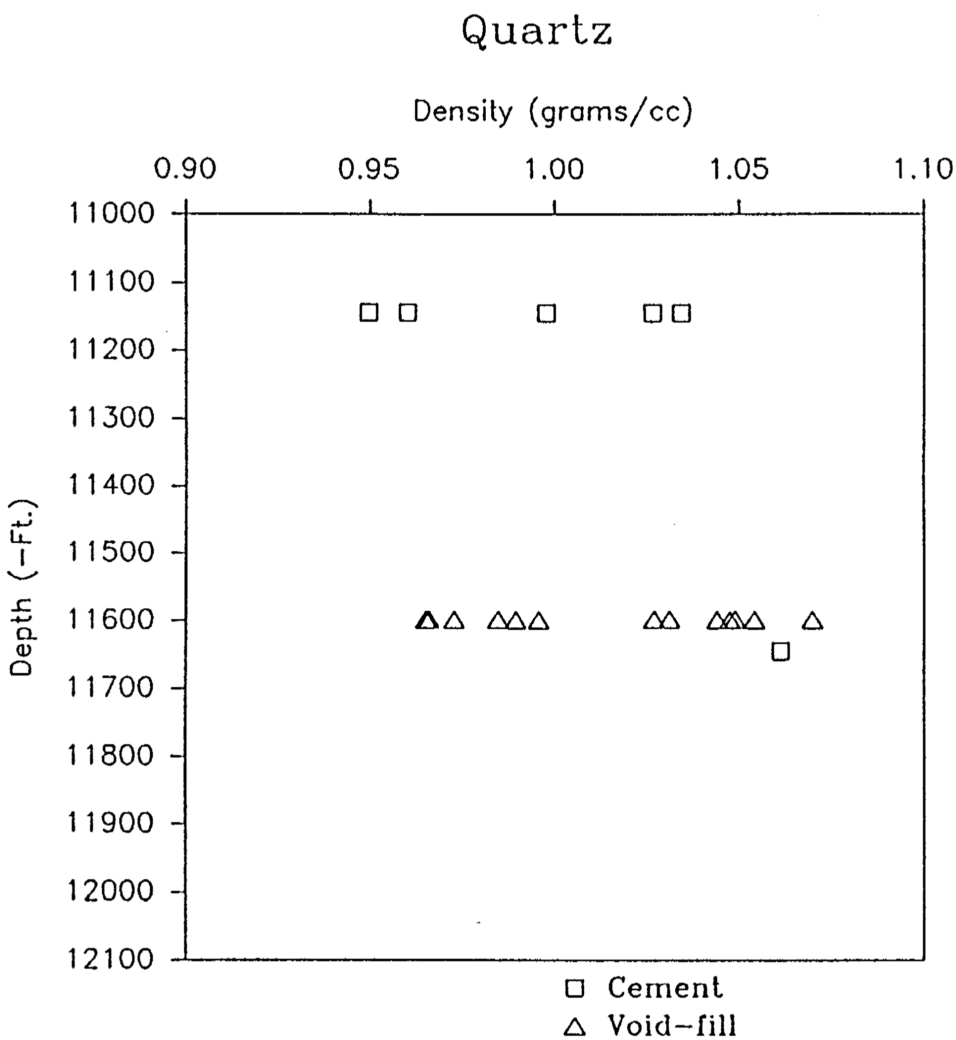

Figure 13. Densities of aqueous (L-V) inclusions verses sample depth for specific quartz mineralization features.

densities have a wide range from 0.95 to 1.07 grams/cc.

Inclusions in Calcite

Inclusions in calcite were analyzed from the Tulip Creek, McLish and Joins Formations. Cements, fractures, void-fill and stylolitic-associated calcite contained inclusions that were analyzed. This was done to see if fluids and other factors varied in conjunction with the relative timing of these diagenetic features. Fractures are no more than 3 mm in width. Stylolitic associated calcite is usually vertical with respect to the core and oriented perpendicular to jagged, dark suturing. Void-fill consists of blebs of calcite that are distinct from the host rock (from staining), and are not related to fossil replacement.

Two phase (L-V) hydrocarbon inclusions, as described for quartz mineralization, are present in a few calcite-mineralized fractures. These and multiphase hydrocarbon inclusions are present in clear and brown colored calcite crystals. The scalenohedral crystals were in a very small vug at 11360 ft. (3462.53 m). This vug appears to be a recrystallized fossil shell and is filled with black, solid residue. This material may be impsonite, which is a high-rank solid petroleum residue (Levine et al., 1991).

Primarily aqueous (L-V) inclusions were analyzed in calcite. Aqueous inclusion Tm values range from -25.5 to 6

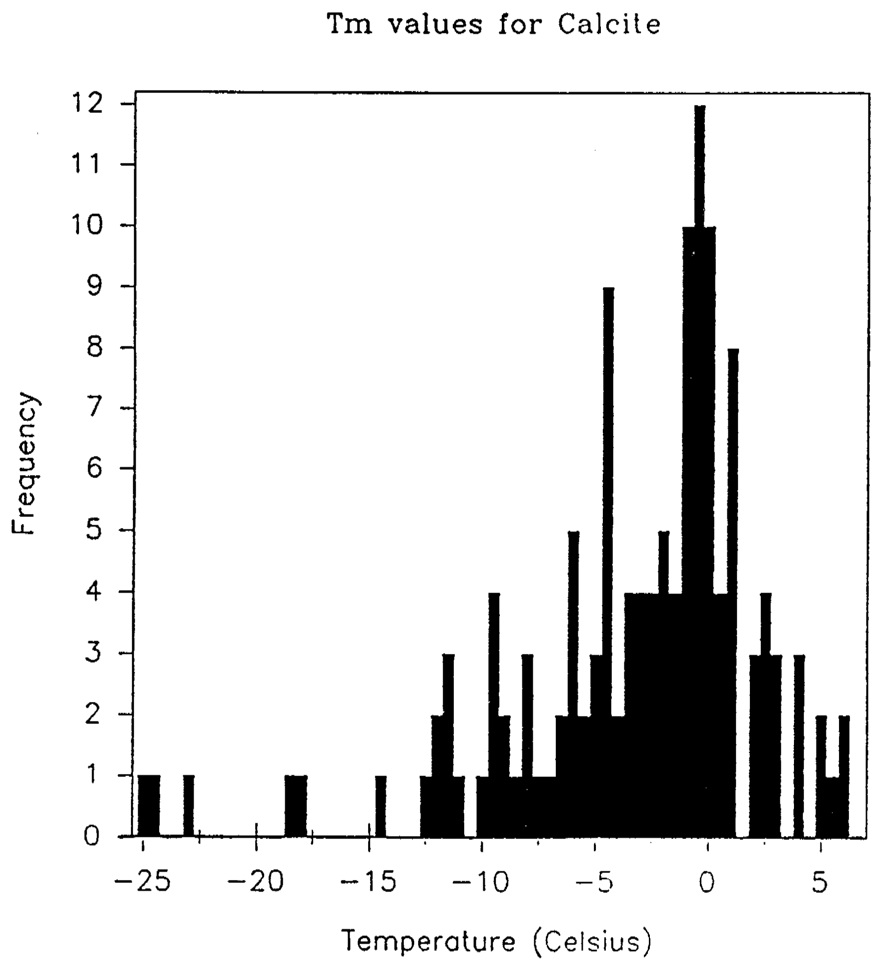

Figure 14. Histogram of temperatures of melting for aqueous (L-V) inclusions hosted in calcite mineralization.

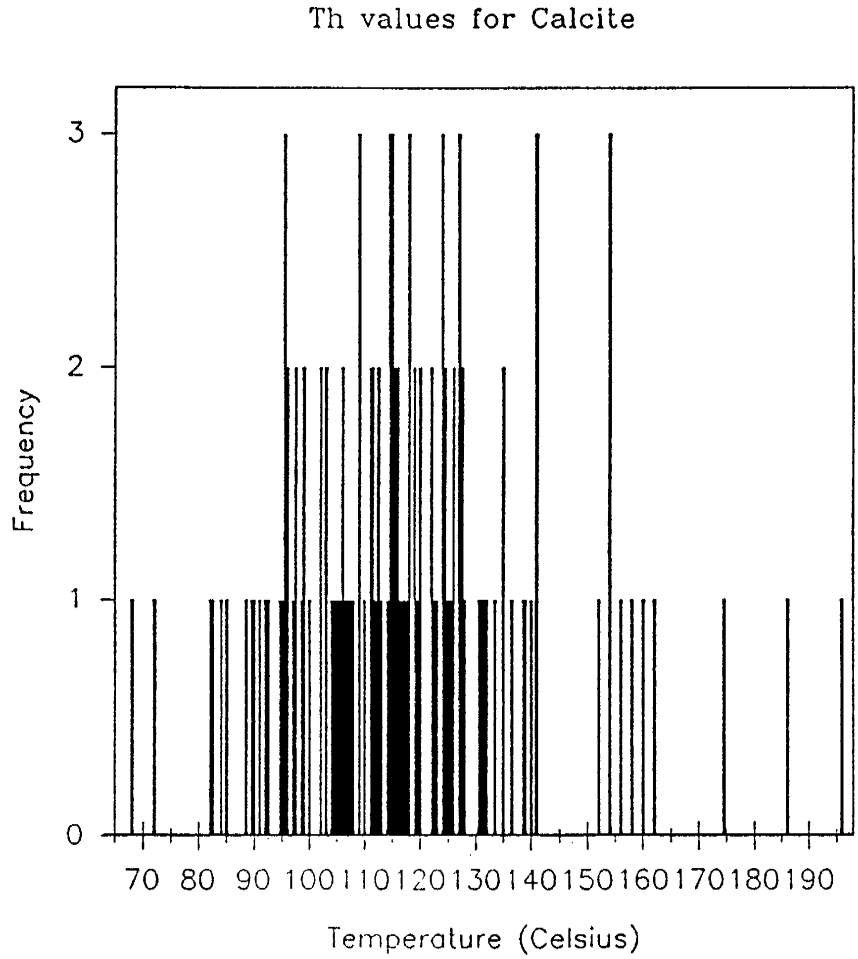

Figure 15. Histogram of temperatures of homogenization for aqueous (L-V) inclusions hosted in calcite mineralization.

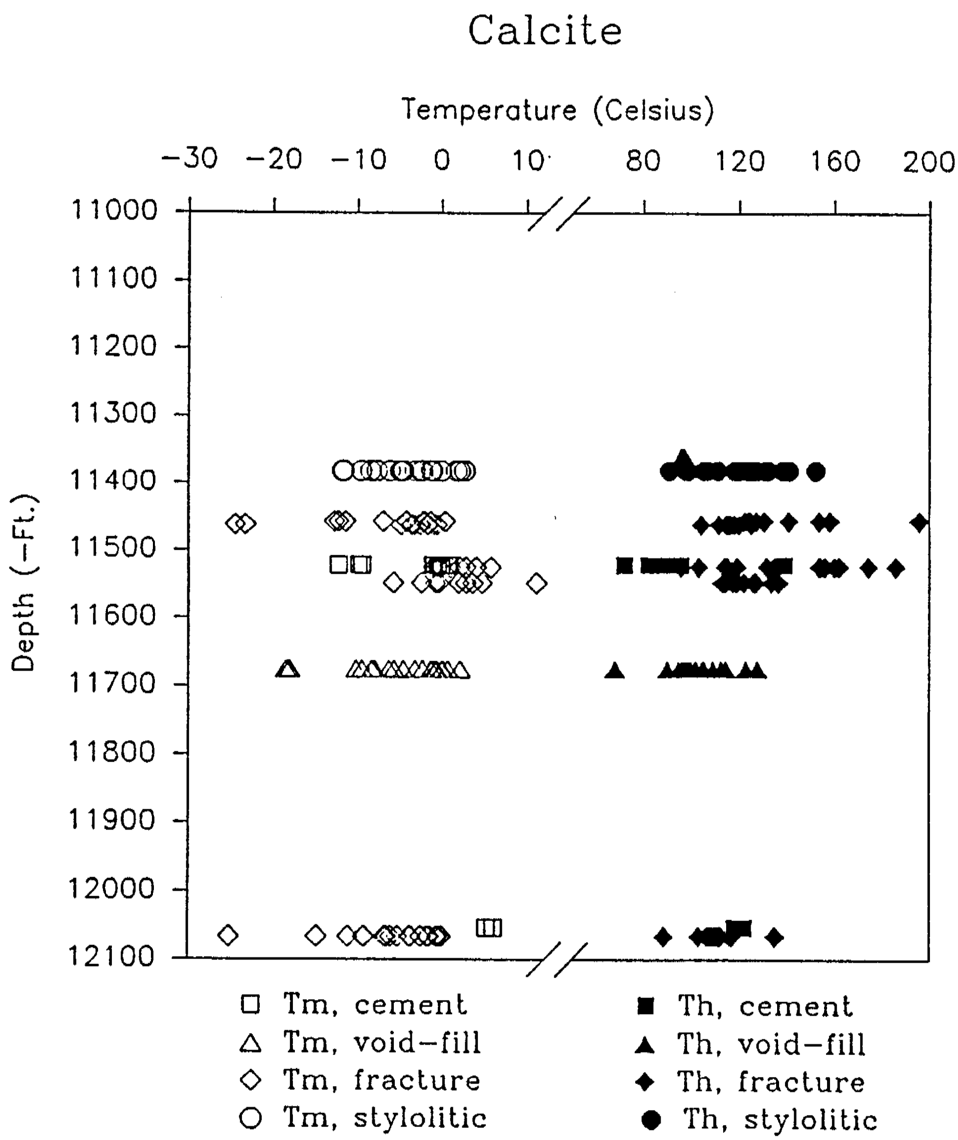

Figure 16. Temperatures of melting and homogenization for aqueous (L-V) inclusions verses sample depth for specific calcite mineralization features.

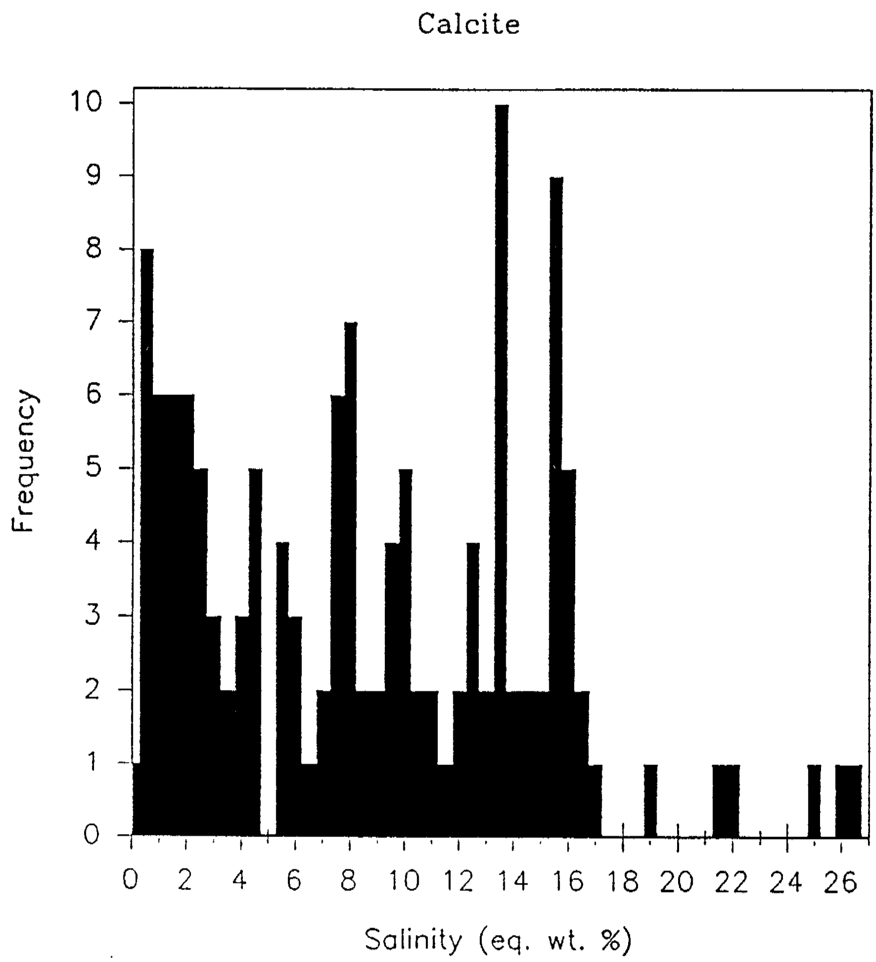

Figure 17. Histogram of salinities for aqueous (L-V) inclusions hosted in calcite mineralization.

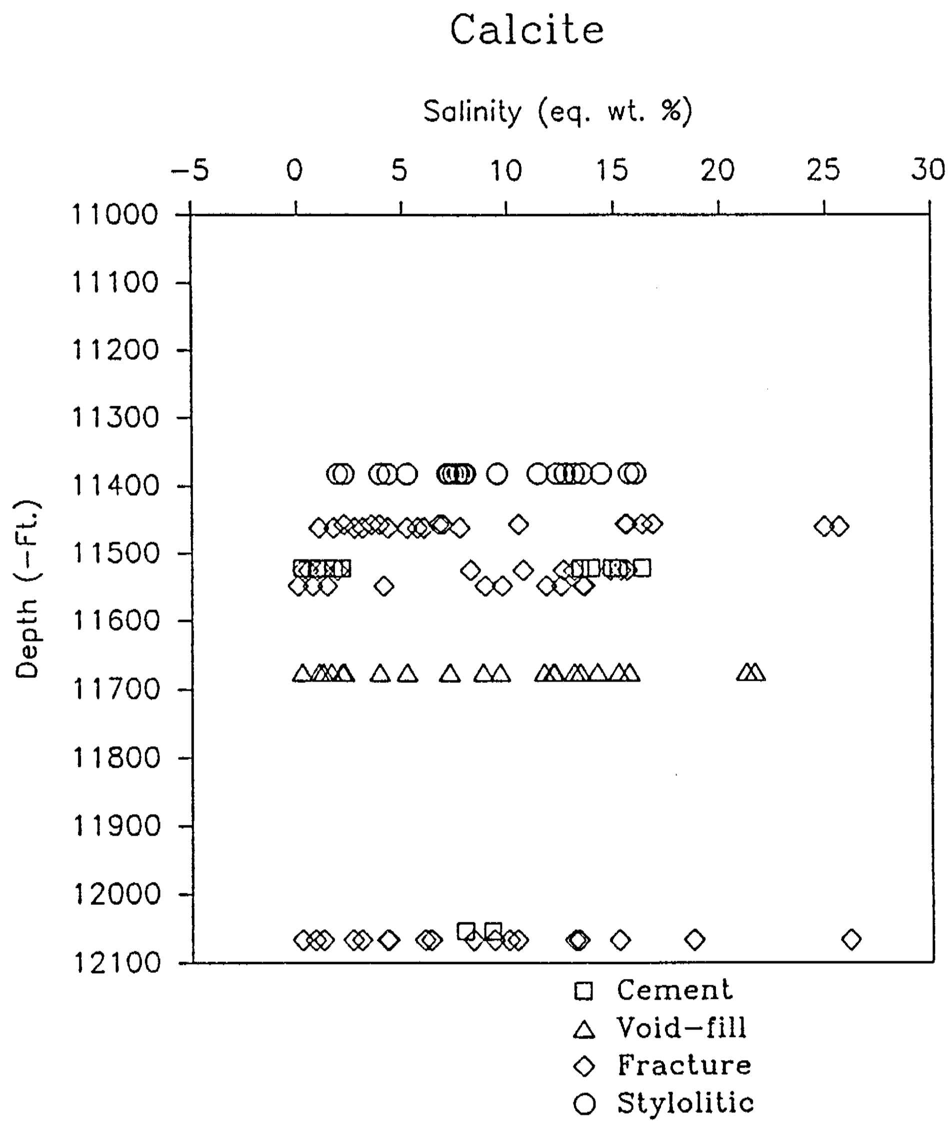

Figure 18. Salinities of aqueous (L-V) inclusions verses sample depth for specific calcite mineralization features.

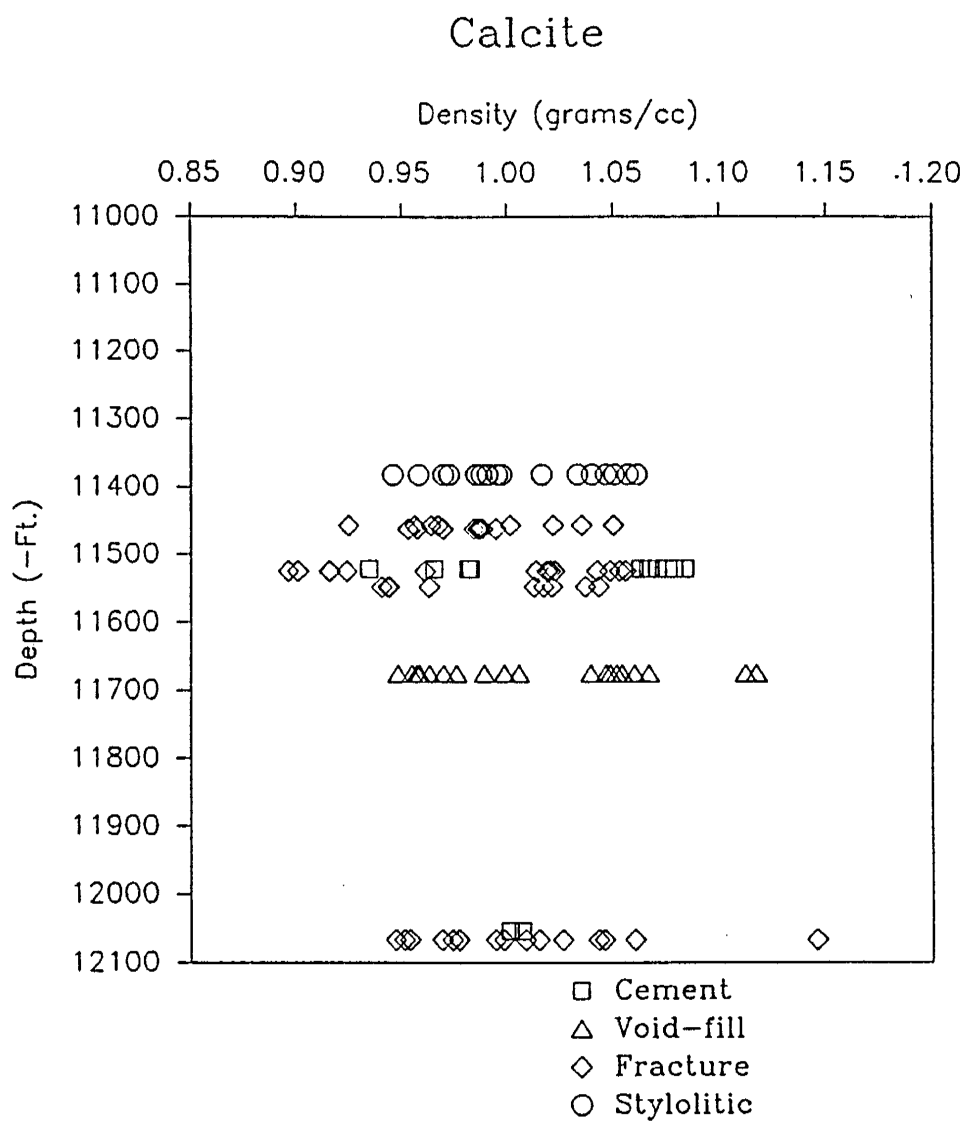

Figure 19. Densities of aqueous (L-V) inclusions verses sample depth for specific calcite mineralization features.

°C, with values concentrated between -10 to 1 °C (Fig. 14 and 16). Tm values below -20 °C represent fracture values, where as values between -20 to -15 °C are from void calcite. Calculated salinity values are mainly between 0 to 17 eq. wt. % NaCl. All values over 24 eq. wt. % NaCl are from fracture mineralization and likely represent the effect of excess ions present in inclusions (Shepherd et al., 1985). Some data peaks represent specific groups of fracture hosted inclusions, but there is no clear overall trend in the data (Fig. 17 and 18). Th values have a range of 66 to 196 °C with most between 90 to 140 °C. Values over 150 °C mainly represent inclusions from fracture mineralization (Fig. 15 and 16). Density values have a wide distribution from 0.87 to 1.15 grams/cc (Fig. 19).

Inclusions in Dolomite

Inclusions in dolomite were analyzed from the Second Bromide, Tulip Creek and McLish Formations in cements, fractures, stylolitic-associated mineralization and saddle dolomite. Fracture size and stylolitic mineralization were similar to that of calcite. Saddle dolomite occurs as void infill or as last stage vug crystallization on quartz in one case. Most analyses were of aqueous (L-V) inclusions. In saddle dolomite there are some colorless two phase (L-V) inclusions that exhibit behavior similar to that described

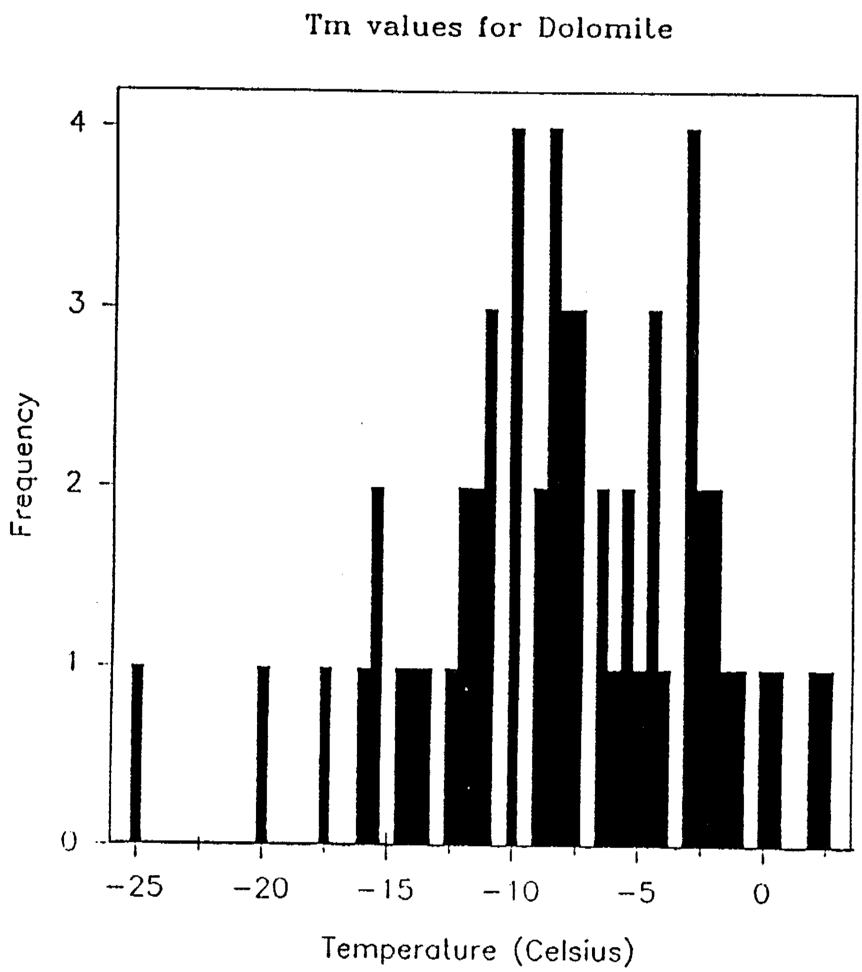

Figure 20. Histogram of temperatures of melting for aqueous (L-V) inclusions hosted in dolomite mineralization.

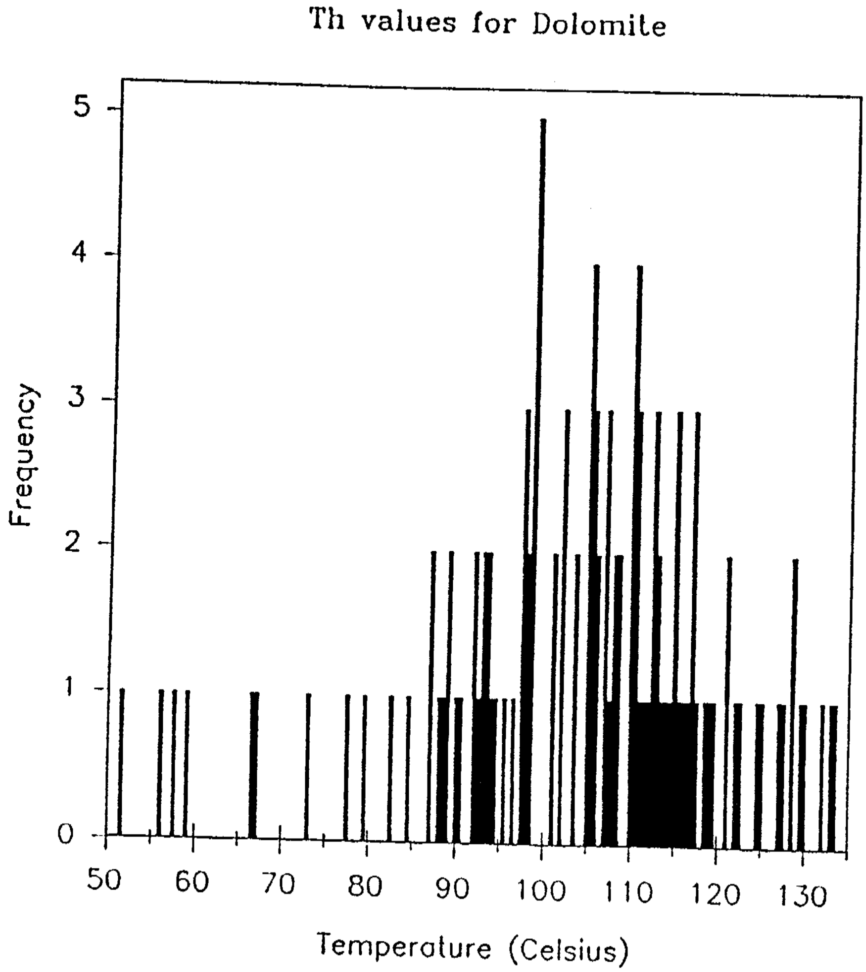

Figure 21. Histogram of temperatures of homogenization for aqueous (L-V) inclusions hosted in dolomite mineralization.

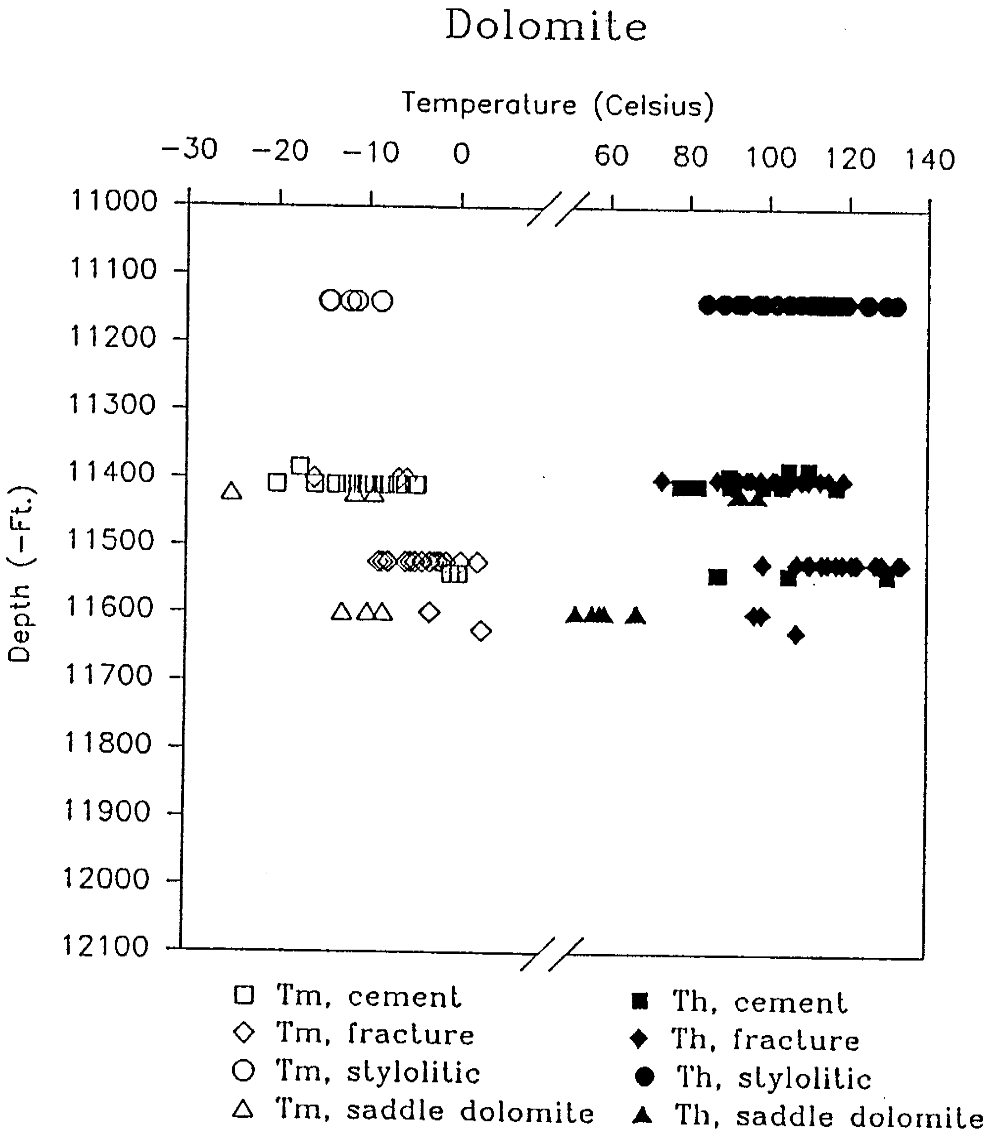

Figure 22. Temperatures of melting and homogenization for aqueous (L-V) inclusions verses sample depth for specific dolomite mineralization features.

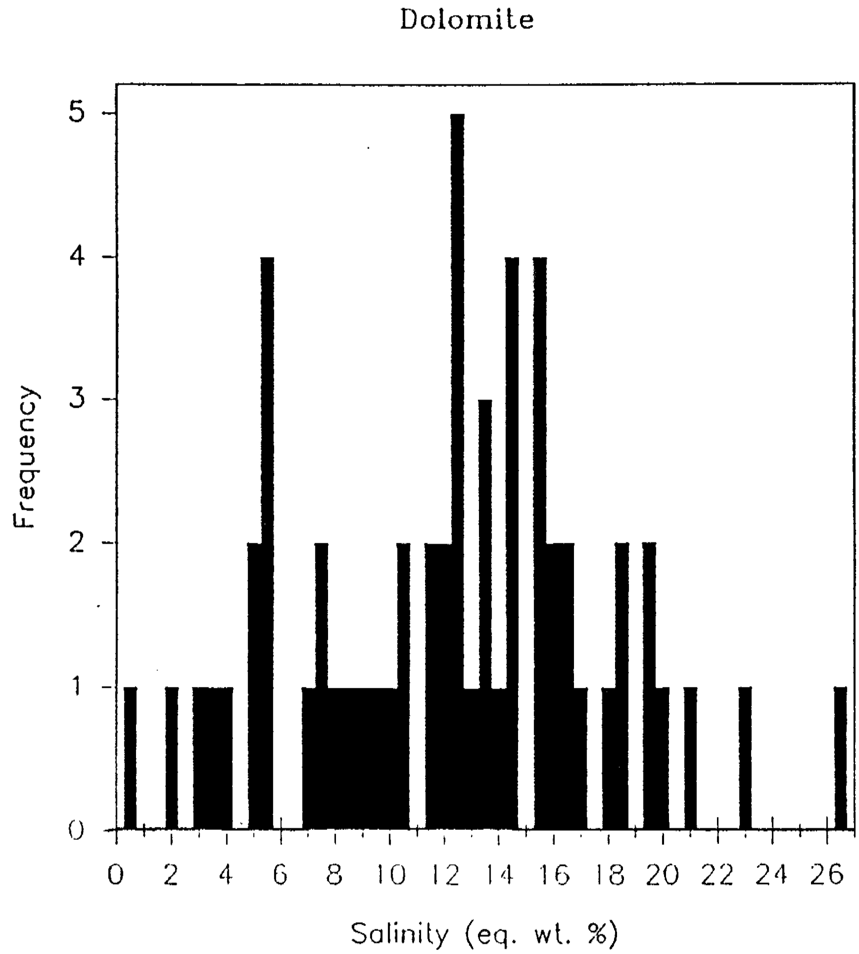

Figure 23. Histogram of salinities for aqueous (L-V) inclusions hosted in dolomite mineralization.

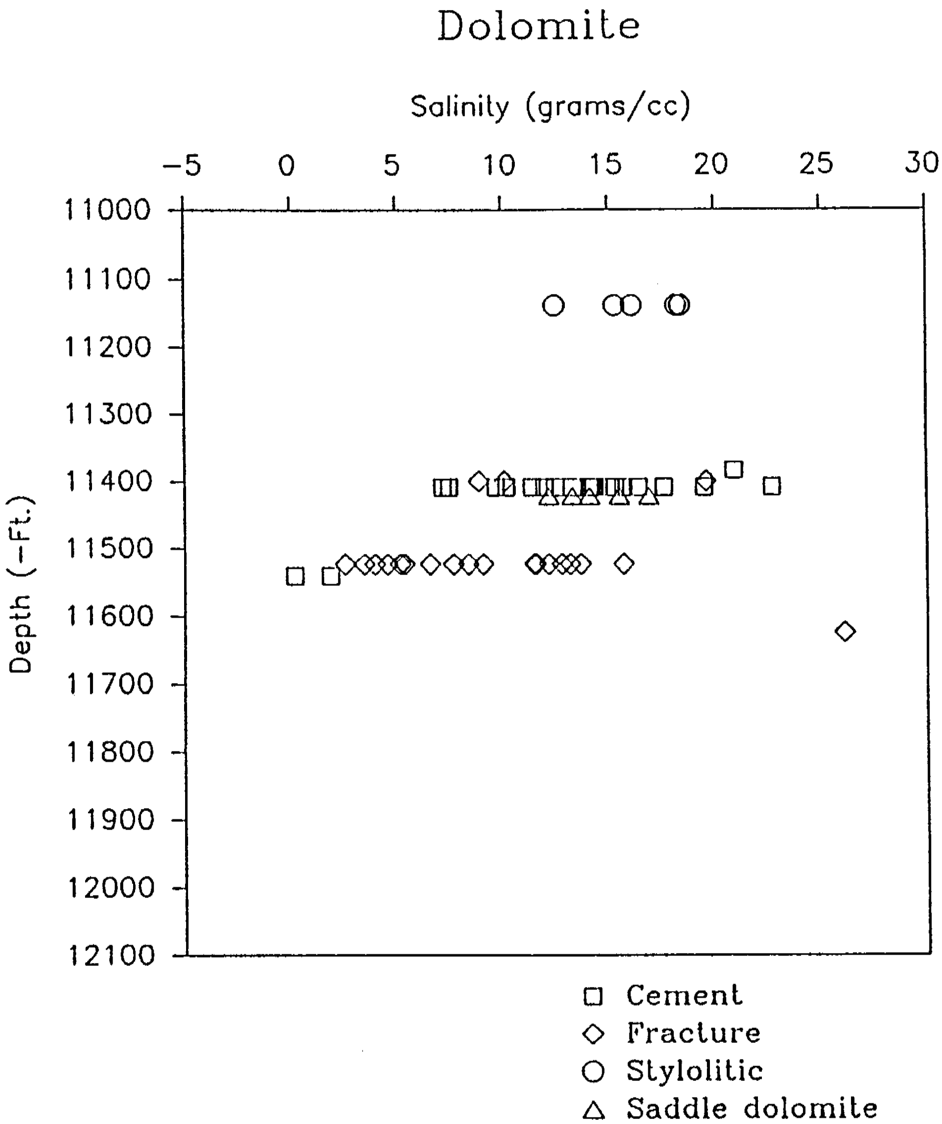

Figure 24. Salinities of aqueous (L-V) inclusions verses sample depth for specific dolomite mineralization features.

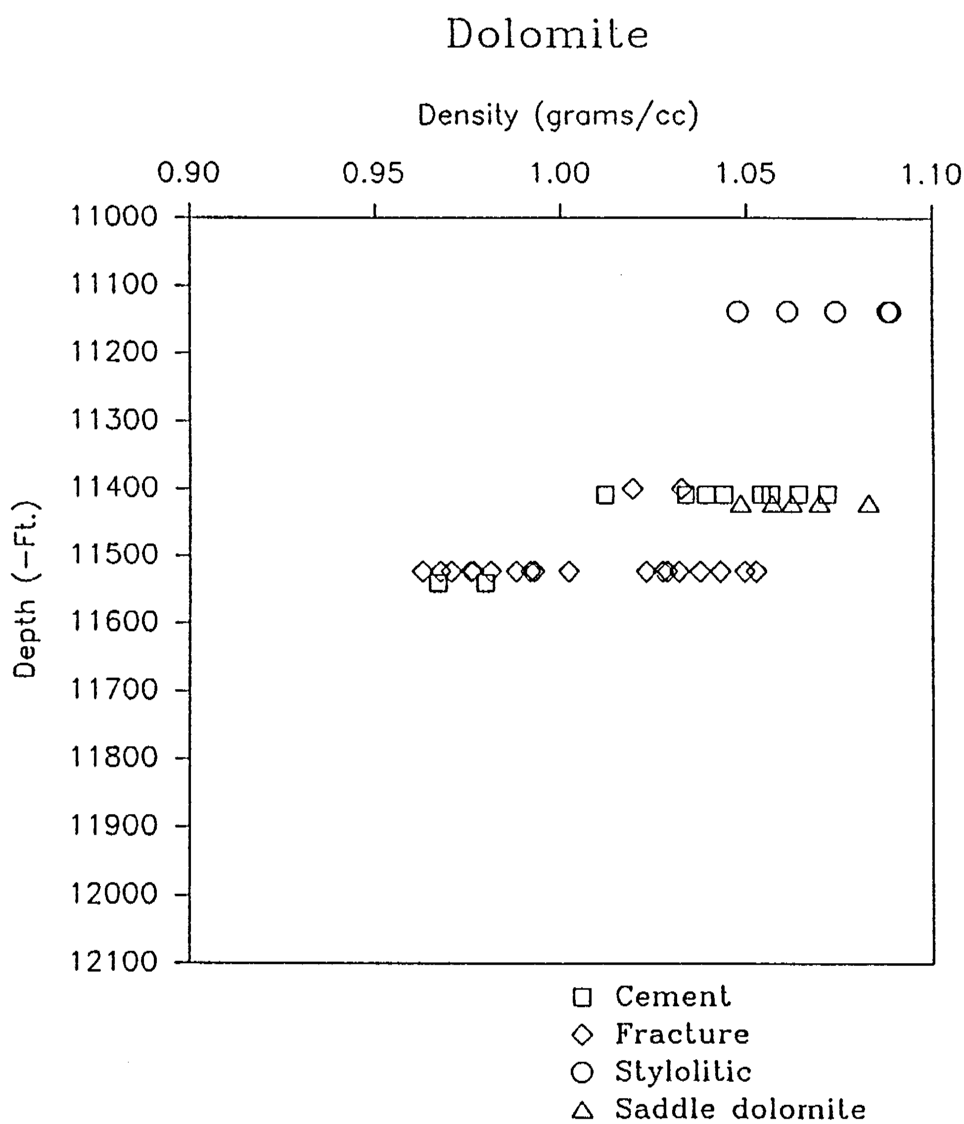

Figure 25. Densities of aqueous (L-V) inclusions verses sample depth for specific dolomite mineralization features.

for two phase (L-V) hydrocarbon inclusions, but lack fluorescence under blue-violet light.

Aqueous inclusion Tm values range from -25 to 2.5 °C, with the majority between -1.5 to -16 °C (Fig. 20 and 22). Calculated salinities have values from 0.5 to 26.5 eq. wt. % NaCl, and principally are between 5 and 20 eq. wt. % NaCl (Fig. 23 and 24). Th values range from 51.5 to 133.5 °C, and most are between 87 and 122.5 °C (Fig. 21 and 22). Temperatures under 70 °C are from saddle dolomite. This is in general agreement with the proposed temperature range (60 to 150 °C) given by Radke and Mathis (1980) for the formation of saddle dolomite. Th values greater than the mean tend to represent inclusions from fractures and stylolitic mineralization. Fluid densities again show a wide distribution, 0.95 to 1.09 grams/cc, with a trend of decreasing values with depth (Fig. 25).

Inclusion Discussion

The fact that Th values from inclusions in quartz overlap those of inclusions from calcite and dolomite is important when considering the validity of the data set. Quartz hosted inclusions generally require approximately 100 °C of heating beyond Th to induce stretching (or decrepitation). This overheating will result in a resetting of actual Th values to higher measured temperatures (Ulrich and Bodnar, 1988). According to experimental work (Bodnar et al., 1988), inclusions in quartz are the least susceptible to microthermometric stretching and geologic thermogradient resetting of temperatures (Ulrich and Bodnar, 1988). Hydrocarbon inclusions in quartz are likely the most resistant to these effects due to the relative uncompressibility of trapped liquid hydrocarbons when compared to aqueous inclusions (Burruss, 1985 and 1987). Further, McLimans (1987) states that thermal "cracking" of inclusion hydrocarbons could create very high internal pressures, sufficient to result in hydrocarbon inclusion decrepitation (using overheating beyond Th by 100 °C (180 °F) in the statement).

Calcite and dolomite can withstand far smaller amounts of heating beyond Th (as little as 5 °C, Prezbindowski and Larese, 1987) to result in resetting of inclusions to a wide distribution of Th values. The Th values of hydrocarbon inclusions in quartz are overlapped by the Th values from carbonates in this study. In vugs the saddle dolomite crystals clearly postdate the quartz crystals. Aqueous inclusions in this saddle dolomite have lower Th values than aqueous inclusions in the adjacent quartz. If the saddle dolomite had experienced the higher Th of the inclusions in quartz, then the inclusions in saddle dolomite would have been reset to temperatures equal to that of the inclusions in quartz, or more likely be stretched and/or decrepitated.

Different generations of diagenetic features from the carbonates have different Th values. If resetting of Th values in carbonates had occurred, then it would result in uniformity of Th measurements and eliminate different Th values for different diagenetic features. These facts indicate that the carbonate Th values are valid, and have not experienced sufficient overheating to be appreciably reset relative to Th values from inclusions in quartz.

If diagenetic banding that formed a pressure seal occurred at depth (Tigert, 1989), then a caveat is that the fluid inclusion Th values in sediments represent at least the minimum temperature of formation if the values are valid. The Th values are reported with no pressure correction here since the pressure at the time of trapping may be uncertain (see final discussion). Aqueous (L-V) inclusions represent a trapping pressure (assuming hydrostatic in this argument) that was greater than that of the particular solution's vapor pressure at that temperature. Otherwise the fluid would have been boiling, i.e. two phase, which is rather unlikely in this particular case. Further, there is the unanswered question of what happens to inclusions at depth that have experienced unloading (as may be the case of the Simpson Group) over a significant time period. What amount of change, if any, has occurred in the inclusions during slow reduction of pressure and temperature from possibly maximum values (Roedder and

Bodnar, 1980)?

Large volume hydrocarbon inclusions relative to quartz crystal size, as in the vug mineralization, have also been reported by Levine et al. (1991) and Murray (1957). Murray (1957) analyzed these inclusions which contained a blue fluorescing liquid and non-fluorescing vapor bubble, Th of 100 +/- 5.0 °C (212 +/- 9.0 °F), by mass spectrometry and found methane (64.9 mole %), ethane (10.7), CO_2 (7.53), propane (4.66) along with various other hydrocarbon molecules and nitrogen (but no water).

In this study the composition of hydrocarbon inclusions is not clear from the observed data and the presence of water is speculative. An important question is whether hydrocarbons and water/brine are coexisting in hydrocarbon inclusions and the relation of this evidence to petroleum maturation and migration.

Pagel et al. (1986) used laser mass microspectrometry (LAMMA) destructive microanalysis to prove the presence of water in hydrocarbon inclusions. And Horsfield and McLimans (1984) found aqueous inclusions to contain light paraffins, benzene, toluene and alkenes with thermal-decrepitation GC analysis. Pagel et al. (1986) also noted that hydrocarbon inclusion Th values about 40 °C (72 °F) lower than cogenetic aqueous inclusions, and Narr and Burruss (1984) and Haszedline (1984) present data with a Th difference of less than 20 °C (36 °F). Interestingly, Videtich et al. (1988)

present a data set of cogenetic, P hydrocarbon and aqueous inclusion Th measurements with respective means of 83 °C (181.4 °F) and 85 °C (185 °F) for calcite spar cements. The presence of aqueous and hydrocarbon inclusions in the same mineralization in reservoirs is interpreted as "unmixing" or immiscibility of coexisting fluids in a water-hydrocarbon system in accordance with PVT properties. The difference in Th values increases with hydrocarbon maturity. Since lighter hydrocarbons have the lowest critical point their Th is usually lower (Pagel et al., 1986; Neumann et al., 1981). Horsfield and McLimans (1984) and Videtich et al. (1988) have noted inclusions containing vapor and liquid hydrocarbons with the presence of water in diagenetic material.

Peter et al. (1990) have shown simultaneous trapping of aqueous and hydrocarbon inclusions during mineral growth in active hydrothermal mineralization (silica) of chimneys and mounds in the Guaymas Basin. Inclusions are L-V hydrocarbon (Th 75-190 °C), L-V aqueous (Th 101-211 °C) and L-V hydrocarbon with aqueous L (hydrocarbon Th 130-135 °C). Peter et al. (1990) conclude that the aqueous and hydrocarbon liquids were never a homogeneous solution, but instead the hydrocarbons were immiscible and possibly solvated during transport.

Pitman and Burruss (1989) report hydrocarbon inclusions from the Simpson Group interval from two wells. The Gulf

Costello No. 1 (11,000 to 12,000 ft.; 3352.8 to 3657.6 m) and the Sunray-DX Parker No. 1 Mazur (15,000 to 17,000 ft.; 4572 to 5181.6 m) are proximal to the Weaver (Fig. 1), and from subsurface pressure gradient mapping they are located in an overpressured environment observed below 10,000 ft. (3048 m) (Tigert, 1989, Fig. 4; Al Shaieb, per. comm., 1990). Pitman and Burruss (1989) report Th values of 98.8 to 121.1 °C (210 to 250 °F) for hydrocarbon inclusions from Simpson Group microfractures. This Th range is slightly higher than the average Th for hydrocarbon inclusions in the Weaver Simpson Group, but further supports the validity of the quartz and carbonate inclusion analysis from this study.

Pitman and Burruss (1989) examined inclusions in authigenic cements and in healed microfractures that cross cut detrital mineral grains and authigenic cements. Inclusions were trapped along dust rims of quartz overgrowths of detrital quartz and feldspar, or within syntaxial quartz overgrowths. Microfractures are commonly oriented perpendicular to stylolites, but occasionally are horizontally related to stylolites.

In the Costello core the most abundant inclusions are two phase (L-V) hydrocarbon, with a white-blue fluorescing liquid phase (Burruss, per. comm., 1990). These inclusions are present in microfractures along with less common aqueous (L-V) inclusions and very rarely three phase inclusions composed of hydrocarbon and aqueous liquid and a vapor phase. These 3 types of inclusions are also present along dust rims of detrital quartz grains in the Costello and Mazur Simpson Group. In the Costello the hydrocarbon inclusions on dust rims and in secondary quartz overgrowths on rare occasion contained a dark brown phase. Pitman and Burruss (1989) state that this phase is similar to bitumen or an "oil stain" and speculate that it is a precipitate from the hydrocarbon liquid after entrapment.

Pitman and Burruss (1989) note no fluorescence other than from hydrocarbon inclusions in cements from the Costello and Mazur Simpson Group interval. This was also the case for diagenetic mineralization in wafers from the Weaver core. Interestingly the 1955 well logs and core evaluation report fluorescence visible for all of the Simpson Group formations.

The limited number of inclusions observed in quartz overgrowths in this study may be related to pressure solution features observed in the First and Second Bromide and Tulip Creek Formations by Tigert (1989). Ernst and Blatt (1964) present experimental and Pittman (1972) and James et al. (1986) present observational results which indicate that inclusion formation may be retarded and reduced in overgrowths formed in pressured environments.

Stable Isotopes

Methods for Stable Isotope Analysis

Carbonate material for carbon and oxygen stable isotope analysis was obtained in this study by micro-drilling or slicing out portions of doubly polished wafers. Calcite and dolomite were reacted with 100% phosphoric acid at 25 °C for a minimum of 8 hours to liberate CO_2 gas (technique modified after McCrea, 1950). Isotope ratios for the CO_2 gas were determined on a Finnigan Mat delta E mass spectrometer. The fractionation factor for the phosphoric acid/carbonate reactions was based on NBS carbonate standards 18, 19 and 20. A regression equation (Appendix C) for these standards was used to calculate the true $\delta^{18}O$ values (Appendix D). Isotope measurement error is +/- 0.2 per mil for this study based on standard determination. All carbon and oxygen values for carbonate minerals are reported as per mil variations relative to PDB (Peedee belenmite calcite; Craig, 1957). All calculated water $\delta^{18}O$ values are reported in per mil relative to SMOW (Standard mean ocean water; Craig, 1961a). Water $\delta^{18}O$ values and curves were calculated using the program Mastercarb 1.0 (by Dr. P. Mozley, July 1990 version). The program uses the oxygen isotope mineral-water fractionation equation of Friedman and O'Neil (1977) after O'Neil et al. (1969) for calcite (0 to 500 °C), and the equation of Land (1983) after Fritz and Smith (1970) for dolomite (based on experimental protodolomite, 25 to 75 °C).

Stable Isotope Results

Isotope values are from two sets of analyses done on this core. Samples analyzed by the author have been designated (NMT) and are of calcite and dolomite mineralization from cement and fractures, and stylolitic and saddle dolomite. Additional isotope values for calcite and dolomite cements have been provided by Dr. Al-Shaieb (1990) (designated OSU, for Oklahoma State University).

All of the $\delta^{18}O$ and $\delta^{13}C$ values for the Weaver calcite and dolomite are presented in Fig. 26. Calcite $\delta^{18}O$ values range from -7.89 to -11.67 per mil and dolomite values from -3.27 to -10.63 per mil. Calcite $\delta^{13}C$ values range from -2.93 to -9.23 per mil and for dolomite from -0.73 to -3.70 per mil.

In order to compare dolomite and calcite values error bars have been attached to dolomite values. These represent a possible 3.0 per mil $\delta^{18}O$ correction for dolomite that is necessary if it is assumed that both calcite and dolomite are cogenetic. This correction is based on low temperature protodolomite, although extrapolation of high temperature experimental data to 25 °C suggests dolomite may be 5 to 7 per mil heavier than coexisting calcite (Northrop and Clayton, 1966; O'Neil and Epstein, 1966; Degens and Epstein, 1964; Fritz and Smith, 1970; Irwin et al., 1977). This has

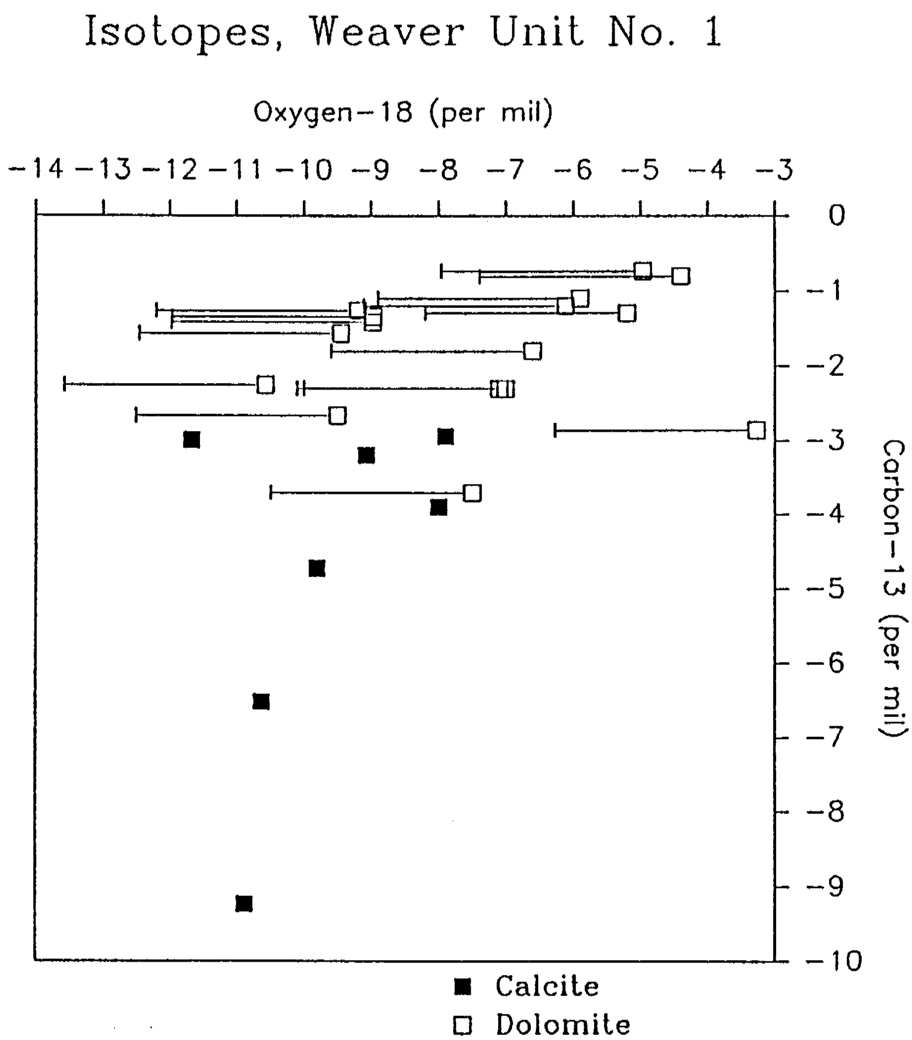

Figure 26. Oxygen-18 verses carbon-13 mineral values (per mil, PDB) for calcite and dolomite from the Weaver Unit No. 1 Simpson Group.

not yet been fully worked out, hence the open ended graphical approach.

Within the possible range of dolomite $\delta^{18}O$ values there is an overlap with the calcite $\delta^{18}O$ values. Conversely, $\delta^{13}C$ values of calcite and dolomite show a separation (Fig. 26).

Calcite and dolomite $\delta^{18}O$ and $\delta^{13}C$ values from the Weaver are plotted against depth in Fig. 27 and 28. There is no clear trend in isotope values with depth. However, diagenetic features that post date the cementation have lighter (more negative) $\delta^{18}O$ values than those of the cements With sample depths 11400 and 12067 this is clearly the relationship between cements and fractures.

Ten carbonate samples (calcite and dolomite) have both $\delta^{18}O$ isotope values and fluid inclusion Th measurements. These $\delta^{18}O$ mineral values were then plotted as curves of temperature verses $\delta^{18}O$ for the water (Fig. 29, note that the $\delta^{18}O$ is in per mil with respect to SMOW) using Mastercarb 1.0. Fluid inclusion Th values (range and average) were then plotted on the curves in Fig. 29 to constrain $\delta^{18}O$ water values. The $\delta^{18}O$ water values had a range from approximately -4.5 to 8.5 per mil (SMOW). Finally, water $\delta^{18}O$ values with averaged Th and salinity from inclusions are presented against depth in Fig. 30.

Stable Isotope Discussion

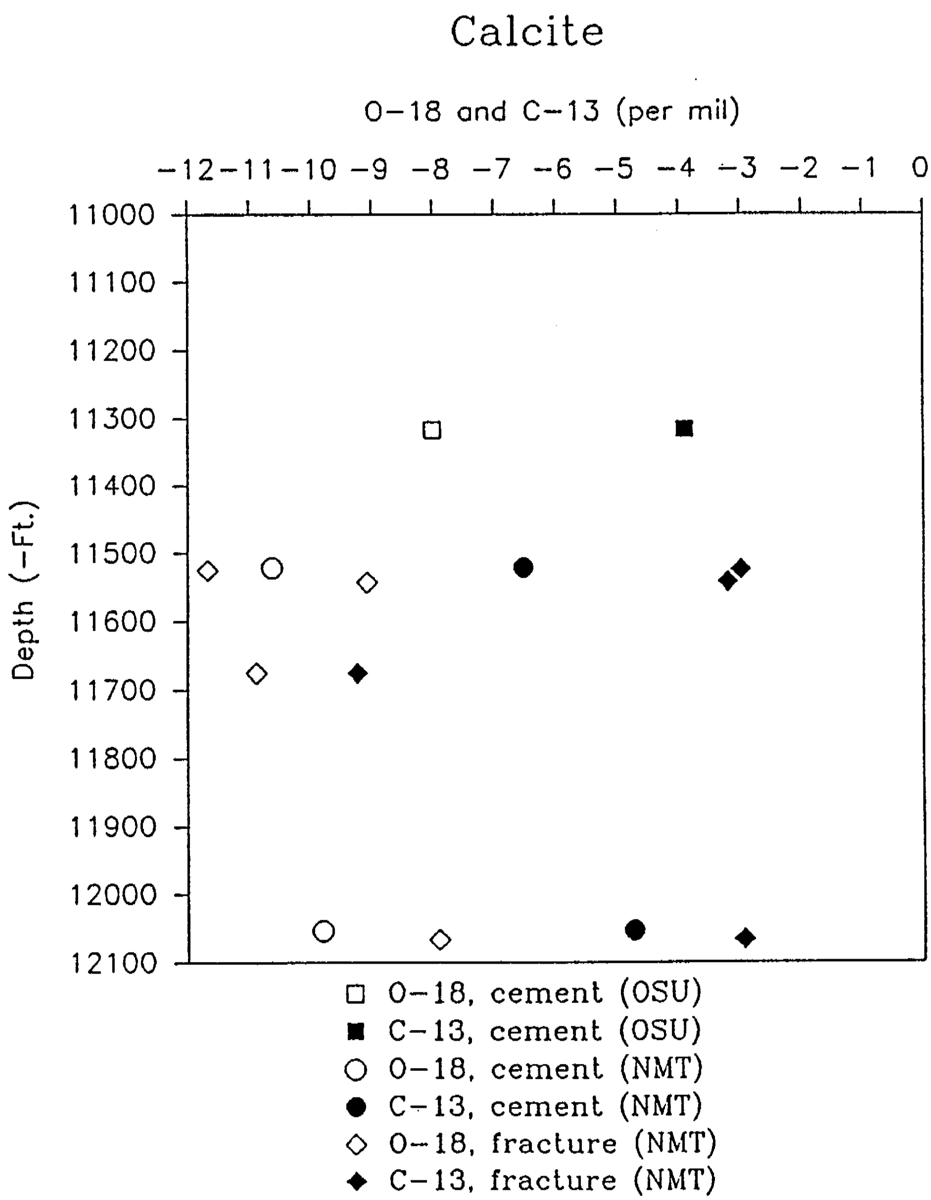

Figure 27. Oxygen-18 and carbon-13 mineral values (per mil, PDB) verses sample depth for specific calcite mineralization features.

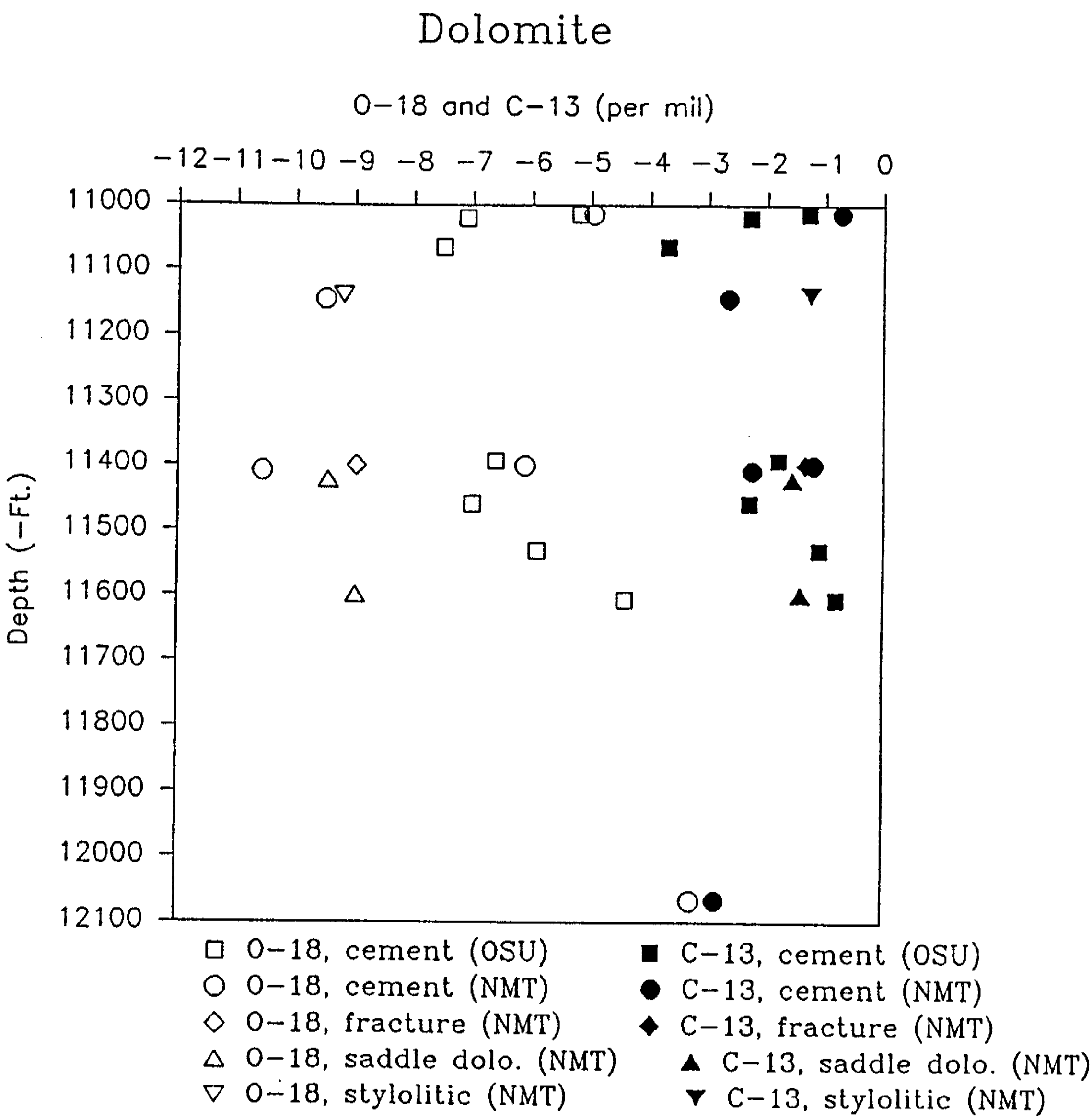

Figure 28. Oxygen-18 and carbon-13 mineral values (per mil, PDB) verses sample depth for specific dolomite mineralization features.

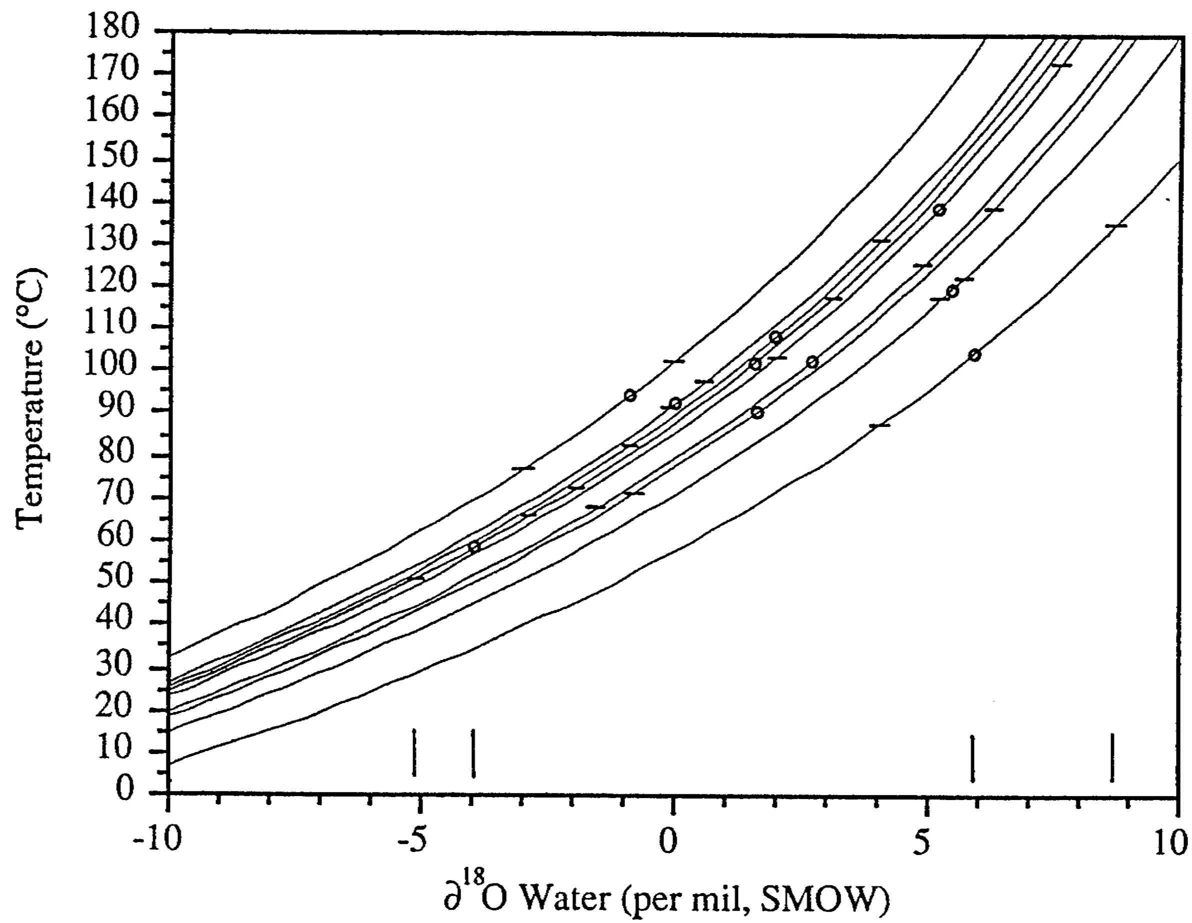

Figure 29. Oxygen-18 water (per mil, SMOW) verses temperature, with curves derived from oxygen values (converted from PDB) for calcite and dolomite mineralization. Fluid inclusion temperatures of homogenization are used to constrain the range of water oxygen-18 values for respective sample curves.

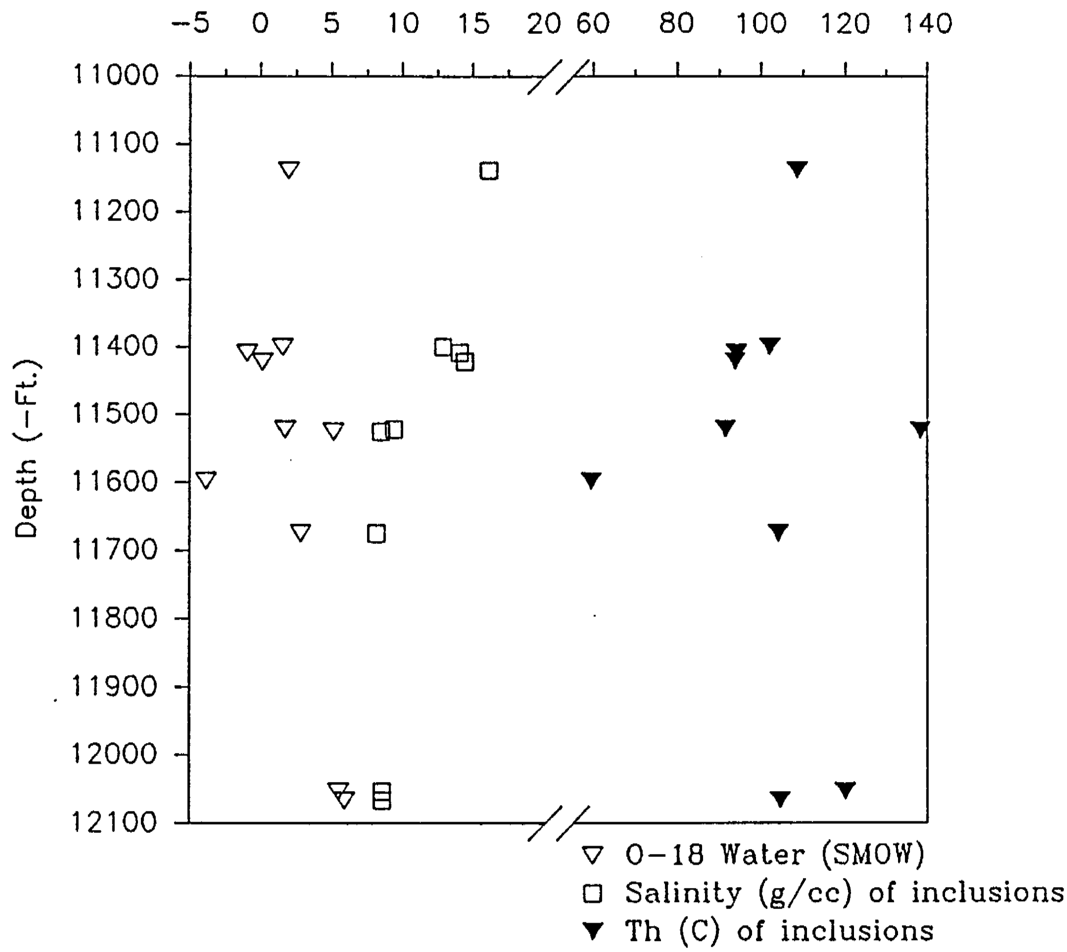

Figure 30. Inclusion salinities and temperatures of homogenization with oxygen-18 water values for the individual samples verses the depth.

To verify reproduction of cement isotope values from the OSU data set a duplicate analysis was done on a sample from 11014 ft. (3357 m) for this study. Respective $\delta^{18}O$ and $\delta^{13}C$ values of -4.97 and -0.73 for (NMT) and -5.2 and -1.3 for (OSU) show a reasonable precision between the studies. OSU cements were also obtained by microdrilling.

Fig. 31 compares the Weaver isotope values with other Simpson Group carbonate values from the Mazur and Costello cores (Pitman and Burruss, 1989). Specifically, these values are from the Oil Creek and Bromide Sandstones from the Mazur and mainly the Costello core (Pitman and Burruss, per. comm., 1990). The isotope values are of calcite and dolomite/ankerite cements and are called "end-member carbonate" by Pitman and Burruss (1989).

The $\delta^{13}C$ and $\delta^{18}O$ values from Pitman and Burruss (1989) are respectively about 0 to -5 per mil and -3 to -9 per mil. They interpret the carbon values as representing marine carbonates that have had no apparent organic carbon influence. Their $\delta^{18}O$ values have no trend with respect to depth and are interpreted as reflecting the combined effects of temperature during diagenesis and isotopically and chemically evolved porewater.

Oxygen isotope values for sedimentary basins deviate from meteoric values with water/rock interaction and exchange between formation water and sedimentary minerals.

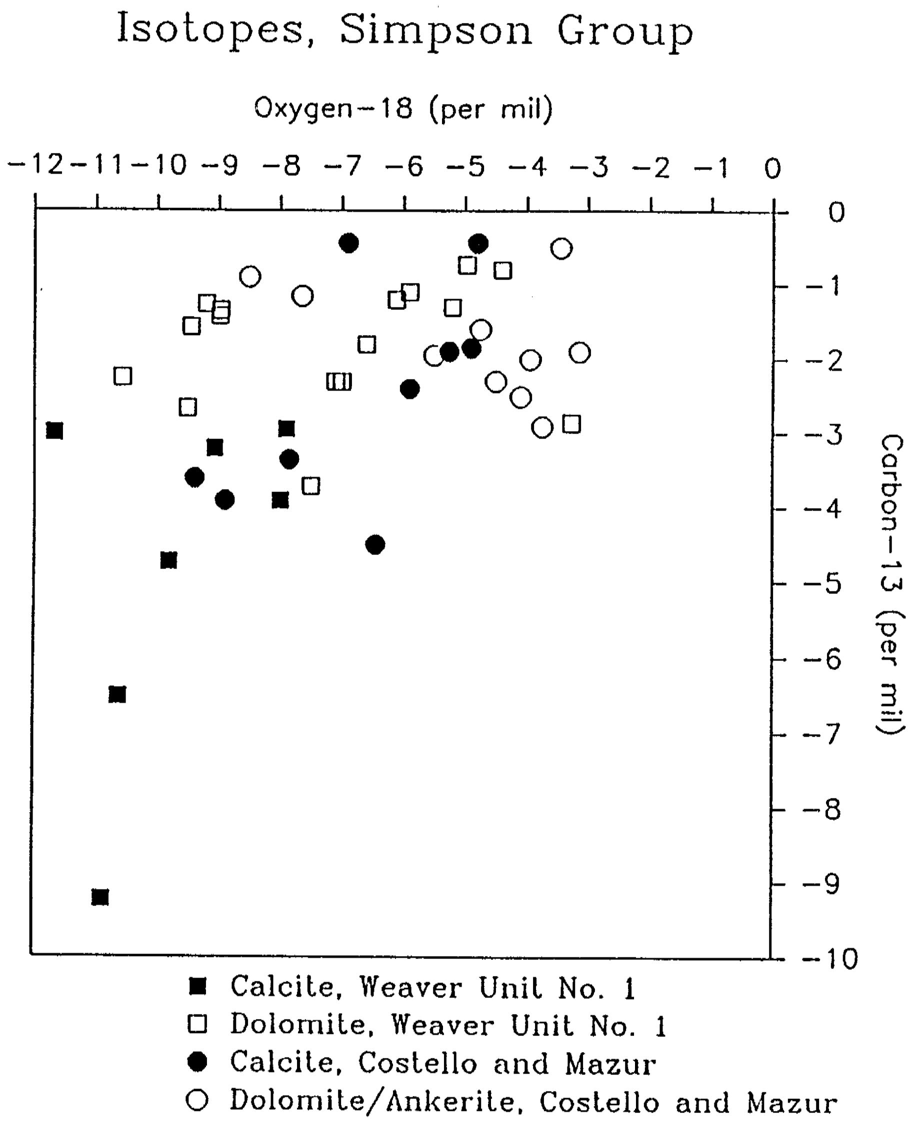

Figure 31. Comparison of oxygen-18 verses carbon-13 mineral values (per mil, PDB) from the Weaver Unit No. 1 (this study), Costello No. 1 and the Mazur No. 1 (from Pitman and Burruss, 1989).

The extent of isotopic enrichment is dependant on the isotopic composition of the exchanging solid phase, the effective water/mineral ratio and temperature of the system (Longstaffe, 1989).

For diagenetic mineralization the fluid isotopic composition present during crystallization is of prime importance. Other possible factors are the degree to which isotopic equilibrium was attained during crystallization, the mass balance of oxygen between the mineral and porewater during crystallization, the mode of diagenetic mineral formation and extent of isotopic exchange between mineral and fluids following crystallization. But if equilibrium isotope fractionation is assumed, then the temperature of crystallization is the most important parameter determining the isotopic fractionation between the diagenetic mineral and the water (Longstaffe, 1989; O'Neil et al., 1969).

Carbon in sedimentary and diagenetic environments can exist in oxidized, native or reduced forms. In each state the carbon isotope composition is dependant on temperature, pH, oxygen fugacity, the relative concentration of different carbon bearing species in the system and most importantly the mechanisms by which carbon isotopes fractionated. This results in wide variation of observed carbon isotope values. Two main carbon reservoirs are identified, the organic and inorganic (the carbonate system). The organic reservoir is ^{12}C rich, and the carbonate system reservoir is ^{13}C rich.

The organic carbon reservoir $\delta^{13}C$ values are determined by kinetic effects, as opposed to carbonate system values that are generally controlled by equilibrium carbon isotope fractionation. As a result of these factors and competing processes a wide variation in $\delta^{13}C$ values is observed. The range of $\delta^{13}C$ characterizes the origin of the CO_2. In relation to carbonate cements and deep burial diagenesis a qualitative assessment of $\delta^{13}C$ variations can be explained by mineral-organic matter-porewater reactions (Longstaffe, 1989; Irwin et al., 1977).

The conclusion of Pitman and Burruss (1989) is that much of the carbonate must have precipitated at relatively shallow depths and the original isotopic composition of fluids buried with the sediments likely approximated that of sea water (implying 0 per mil SMOW). This may not be the case if the $\delta^{18}O$ values reflect the diagenetic temperature and isotopically and chemically evolved porewater as they claim.

If the $\delta^{18}O$ water value was 0 per mil (SMOW) and diagenetic mineral precipitation occurred in a near surface environment, then the calculated temperatures (Mastercarb 1.0) should be essentially surface temperatures. Schmoker (1986) uses an estimated surface temperature of 27 °C for the early Paleozoic, with a temperature decrease to a present day mean surface temperature of 16 °C for Lopatin method TTI calculations for the Anadarko Basin. The heaviest (most positive) values for dolomite (-3.15 per mil) and calcite (-4.8 per mil) given by Pitman and Burruss (1989) have calculated temperatures that are 30 and 39 °C respectively. On the other hand the lightest (most negative) values for dolomite (-8.5 per mil) and calcite (-9.4 per mil) yield respective temperatures of 62 and 68 °C. The lower temperatures could support near surface diagenesis, but the higher temperatures would seem to refute a purely sea water isotopic source. Also if the porewaters have isotopically and chemically evolved as stated by Pitman and Burruss (1989) then the mineral isotopic values would be expected to have become heavier (more positive).

The dolomite/ankerite $\delta^{18}O$ and $\delta^{13}C$ values reported by Pitman and Burruss (1989) essentially plot within the dolomite values of the Weaver (Fig. 31). On the other hand the Costello and Mazur calcite isotope values are heavier (more positive) than those of the Weaver. Thus laterally in the Simpson Group similar cement isotope conditions may have been present.

For Weaver calcite and dolomite the calculated range of $\delta^{18}O$ water values (SMOW) is about -5 to 9 per mil. The data suggests that the $\delta^{18}O$ value of porewaters became lighter (more negative) through time based on the relation of the values in Fig. 29 and fracture/cement relations. The last stage saddle dolomite $\delta^{18}O$ water values are the lightest in Fig. 29.

A number of ideas have been presented for changes in oxygen isotope values of pore fluid at depth. The lighter (more negative) value trend in later mineralization may be explained by a meteoric water mixing with another heavier fluid to produce a lighter signature with time. Another possibility is that in a closed system the fluid $\delta^{18}O$ values should evolve toward lighter (more negative) values with mineral precipitation. Saigal and Bjorlykke (1987) noted that recrystallization of sparry calcite to poikilotopic calcite was accompanied by a shift toward lighter (more negative) $\delta^{18}O$ mineral values. If in fact the fluids became lighter through time, it is contrary to what is commonly expected for formation waters.

Discussion of Data and Compartmentalization Theory

The inclusion Th data indicates no temperature gradient with depth, but the samples analyzed are from a vertical interval of only 1000 ft. (304.8 m). Present Weaver temperature gradients are calculated using the 1955 well log data and an approximate present day mean surface temperature of 16 °C (60 °F) (Schmoker, 1986). The two gradients are plotted for the Weaver in Fig. 32. The lower gradient of 0.775 °F/100 ft. (0.5789 °C/100 ft.) is calculated with no bottom hole temperature (BHT) correction, and is comparable to a granite thermal gradient of 0.78 °F/100 ft. (Bradley, 1975). The higher temperature gradient of 1.11 °F/100 ft. (0.76 °C/100 ft.) is obtained if a BHT correction is applied. The BHT of 155 °F (68.3 °C) recorded on the well logs was corrected to 196 °F (91.1 °C) based on temperature curves from deep wells derived by Castano and Sparks (1974). The higher gradient is comparable to a sandstone gradient of 1.2 °F/100 ft. (Bradley, 1975). A subsurface temperature measurement from 1955 production testing records indicates that the corrected gradient is a better estimate of actual temperatures. At a depth of 11956 ft. (3644 m) a temperature of 184 °F (84 °C) was obtained, as indicated in Fig. 32.

The main body of fluid inclusion Th values (90 to 140 °C) plots between the paleothermal gradient calculated from vitrinite reflectance of Pusey (1973) (Fig. 32) and that of present thermal gradients for the Anadarko Basin. The paleothermal gradient should represent the maximum attained temperatures. Fig. 32 has the current depth range and the possible 2000 ft. of additional subsidence that Weaver units may have experienced indicated (box), along with an R_o based depth from Schmocker (1986) for comparison. Note that Jones and Philp (1990) use an estimated R_o of approximately 0.75 (based on Cardot and Lambert, 1985) for the Ordovician Viola Group which directly overlies the First Bromide, since the Ordovician rocks contain no vitrinite.

Pollastro (1988) examined clay mineral content to

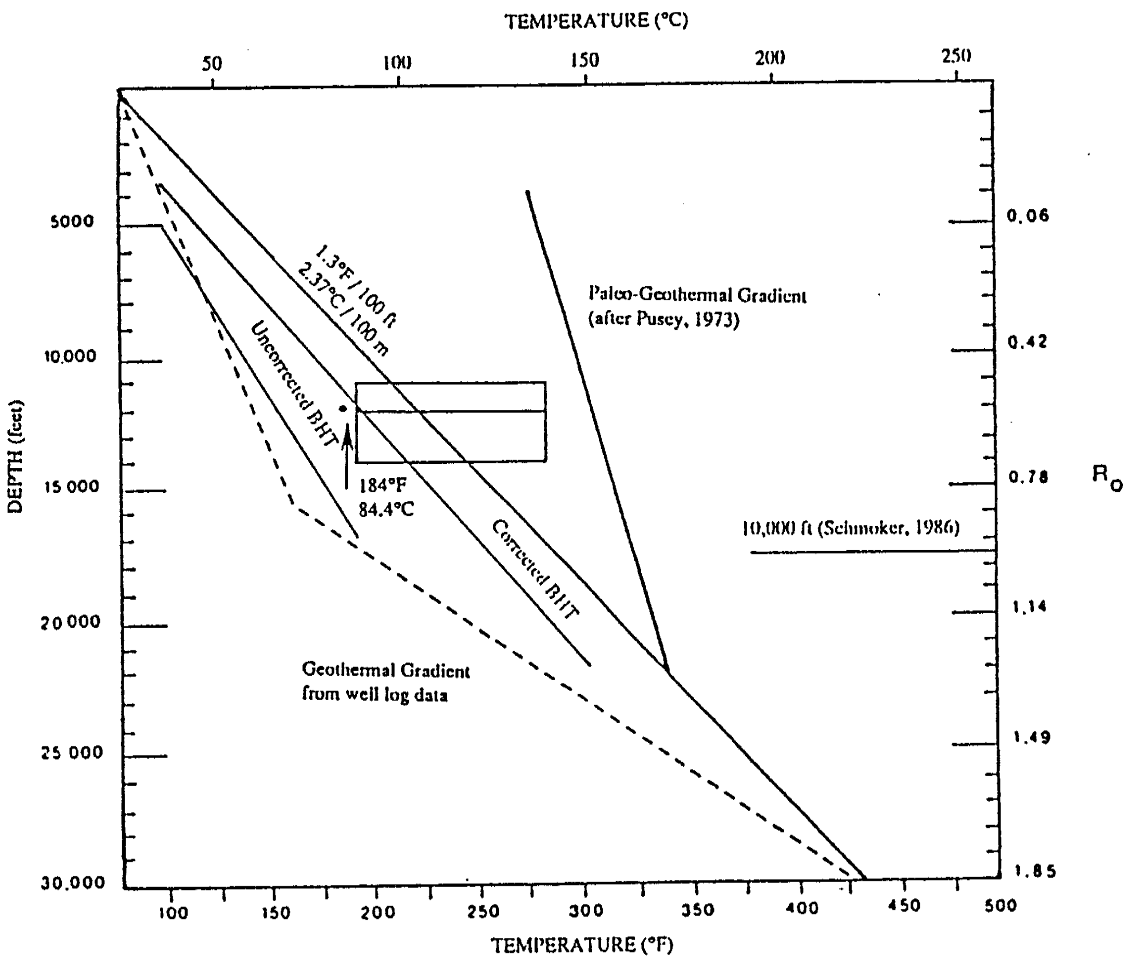

Figure 32. Anadarko Basin temperature and depth plot. Dashed line represents bottom hole temperatures measured in wells, and the thermal gradient of 1.3 F/100 ft. (2.37 C/100 m) is the accepted basin gradient (after Borak and Friedman, 1981). The paleothermal gradient is from Pusey, 1973, with additional Ro values and their estimated depths from Schmoker, 1986 to the right. Two gradients are shown for the Weaver Unit No. 1 using corrected and uncorrected bottom hole temperatures with fluid inclusion Th values superimposed.

arrive at subsurface temperatures in Simpson Group core from present depths of 15,900 to 17,200 ft. in the Anadarko Basin. Textural relationships suggested that at depth conversion of smectite to illite contributed in part to formation of dolomite and ankerite cements, with dolomite replacing detrital clay. Chlorite is authigenic and occurs as pore-lining cement and as replacement after kaolinite. Pollastro (1988) concluded that such an assemblage is consistent with burial conditions of greater than 150 °C, which would be close to the paleothermal gradient of Pusey (1973) (Fig. 32).

The fluid inclusion Th data shows that the diagenetic mineralization of the seal formed at a higher thermal gradient than that present today. Additionally the mineralization occurred at a lower temperature than the paleothermal gradient.

For the Weaver Simpson Group, the question of depth of diagenesis and pressure conditions (hydrostatic verses lithostatic or some intermediate pressure) when combined with possible error in an assumed fluid composition can cause relatively large uncertainties in a pressure correction of Th for fluid inclusions (Roedder and Bodnar, 1980). A 1955 pressure build-up test at 11956 ft. in the Weaver produced an overpressured reading of 5572 psi. (confirming Fig. 2 overpressured drill stem tests in the Weaver section). But the current of overpressuring may not have been present at the time of mineralization. Simpson Group diagenesis may have occurred under hydrostatic conditions as have been estimated at the depths of 9.16 and 9.58 km for the Lone Star Baden and Lone Star Bertha Rodgers 1 wells respectively, in the central portion of the Anadarko Basin (Borak and Friedman, 1981). Or, diagenesis may have occurred at intermediate to higher pressures at or near lithostatic, as the formation of fractures may or may not imply. Narr and Burruss (1984) have shown that subsurface fracturing can occur at about hydrostatic pressure. They used fluid inclusions in fracture mineralization (last stage diagenetic) in the Mission Canyon Formation, Little Knife Field, N. D. to show that the pore-fluid pressure gradient was normal hydrostatic (as it is presently) immediately after if not during development of the fracture system. Fracturing occurred at approximately the current depth of 9,800 ft. (2987 m) with fluid inclusion and present fluid salinities about the same. The hydrocarbon inclusions have a Th range of 90 to 106 °C and aqueous inclusions 102 to 120 °C, with hydrocarbon migration coming in the reservoir before fracture formation and the methane concentration possibly decreasing post-fracturing.

Despite not knowing the pressures at the time of fluid inclusion formation, an estimation of a possible pressure correction can be made. Using the current normal pressure gradient of 0.465 psi/ft. (Tigert, 1989) for the Anadarko

Basin and a depth of 11,500 ft. (3505 m), a pressure of 5347.5 psi or 36.86 MPa is obtained. This pressure and the fluid inclusion salinity and Th ranges can then be compared to pressure correction graphs of Potter (1977). For inclusion salinities between 1 to 15 percent NaCl and over the inclusion Th range of this study a maximum pressure correction of about 40 to 55 °C is obtained. For inclusions from diagenetic mineralization this seems to be an excessive correction, pushing Th values to over the paleothermal gradient of Pusey (1973) for the depth range of the Weaver Simpson Group. Therefore no pressure correction has been imposed on the fluid inclusion Th data, although some correction may be required.

The top seal temperature range of 90 to 100 °C given by Hunt (1990) is overlapped by the inclusion Th range of 50 to 175 °C (mean range of about 90 to 140 °C). If Hunt's subsurface range is for current seal temperatures, considered post seal formation, then the range of inclusion Th values indicates seal formation at a higher thermal gradient at some prior time. The higher Th range is problematic in relation to linkage of "cooler" seal formation, trapping and compartmentally containing hydrocarbons that may be generated at temperatures over 95 °C "where most oil and gas generation occurs from deeper sourced rocks in the pressure compartments" (Hanor and Sassen 1988 in Hunt, 1990).

Fluid inclusion salinities range from about 0 to 17 eq. wt. % NaCl. Compared to salinity in TDS (mg/liter) given by Tigert (1989) for the seal zone (Fig. 33), the inclusion fluids apparently had a lower salinity than fluids currently present in McClain County Simpson Group formations (realizing that unit comparisons are not exact by definition). This indicates that the salinity has increased since the time of fluid inclusion entrapment to the present formation water salinity levels.

Densities calculated for the fluid inclusions have a very wide range. This could reflect fluid density stratification, or the presence of more than one fluid. Another possibility is that fluids are separate and unable to equilibrate with each other.

The Bromide, Tulip Creek and Oil Creek Sandstone Formations from the Weaver are hydrocarbon producing zones, as is the Simpson Group throughout the basin. Hydrocarbon influx or migration has occurred rather late in the diagenetic history, as evidenced by the occurrence of hydrocarbon inclusions. The occurrence of an early stage hydrocarbon migration (Pitman and Burruss, 1989) seems more tenuous, based on "dust rims" between clastic grains and overgrowths, which are small and display no detectable fluorescence. Tigert, Pitman and Burruss, in personal communication (1990), concur that the early stage hydrocarbon migration is rather speculative.

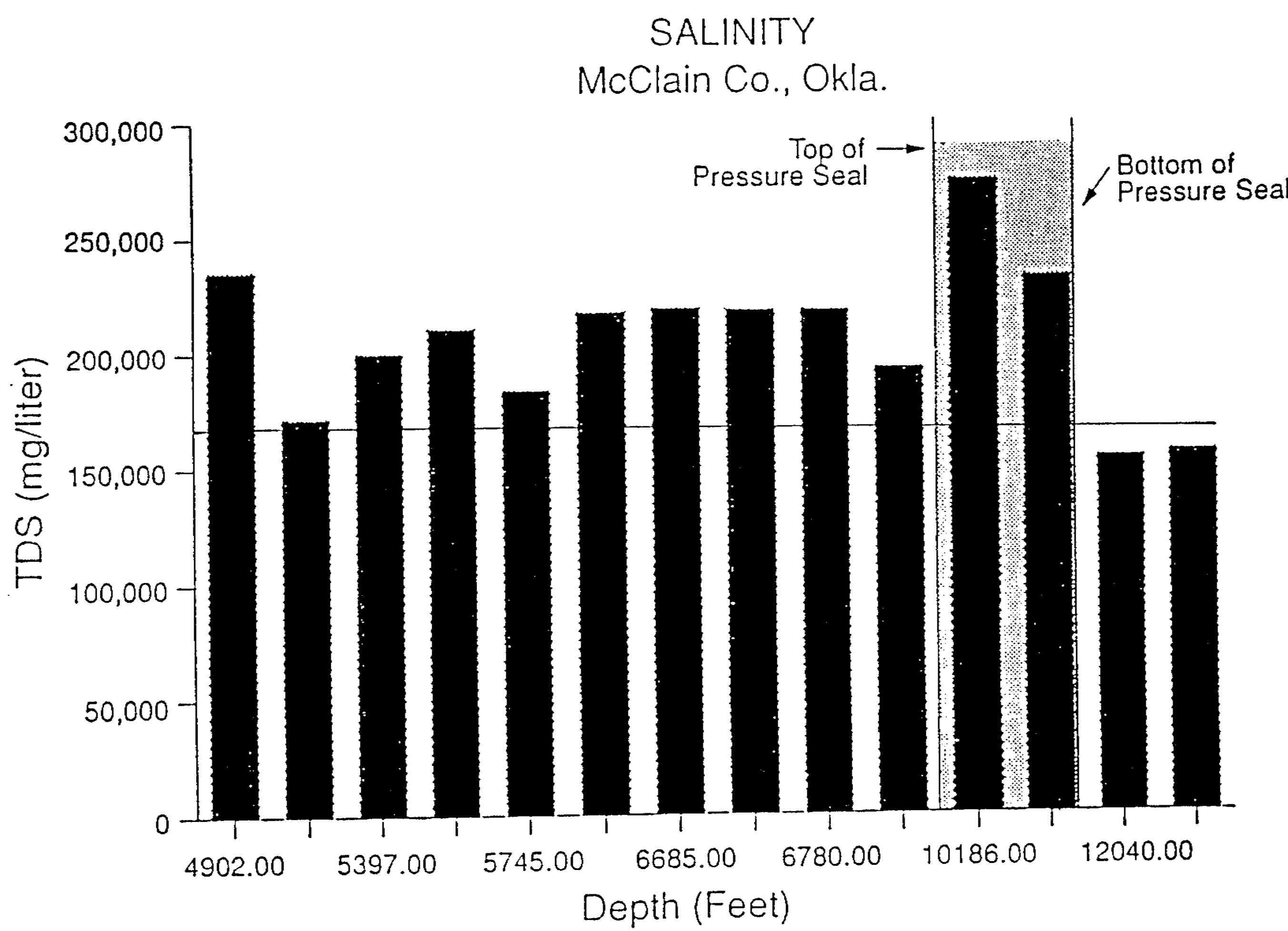

Figure 33. Comparison of fluid inclusion salinities to those of present formation water salinities from McClain Co., Okla. (modified after Tigert, 1989).

The diagenetic sequence in the Simpson Group has been complex, in light of the paragenetic sequence by Tigert (1989), and Weber (1978) for the McLish Formation, emphasizing the fact that diagenesis may not have been a continuous process throughout the length of the Weaver core, especially in respect to different formations. Hunt (1990) reports seal formation/mineralization has initiated in the lower pressure zone and proceeded downward for the Tuscaloosa Formation of the US Gulf Coast. Statement of an equivalent situation occurring for the Weaver seal formation can not be made based on the observed diagenetic mineralization.

According to McBride (1989), most quartz cement is introduced in sandstones post burial of 1 to 2 km, with the interval of one to two km presumed to be the most active zone of cementation. Pressure solution is cited as being an important source of silica, exhibited at grain contacts and by stylolitization in sandstones. McBride (1989) also note that a number of studies have observed quartz cementation at or near the top of overpressured zones. Eocene Gulf Coast sandstones have apparently been selectively cemented near the top of an overpressured zone at an interface where important differences in temperature, pressure and fluid may exist. In Gulf Coast and North Sea Basins most quartz cement is precipitated by rising, possibly convecting from deep within the basin, cooling formation water with temperatures of 60 to 100 °C. This is based on fluid inclusion and oxygen isotope data from quartz overgrowths. Most quartz cementation takes place in the silica mobility window that is basinally specific, with similar diagenetic sequences in sandstones resulting. McBride (1989) also states that quartz cementation can proceed from formation waters of variable composition, and can be interrupted or overlapped by calcite cementation. Ehrenberg (1990) and Walderhaug (1990) both conclude that quartz cementation in sandstones on the Norwegian shelf has not been prevented by hydrocarbon emplacement, and may have continued post it's influx. Quartz may have come from local pressure solution along stylolites or grain contacts with silica transported by diffusion through residual water saturation. Finally quartz cementation may presently be occurring, with the comparison of fluid inclusion Th and well temperatures (Walderhaug, 1990; Ehrenberg, 1990)

Organic components from the Weaver core have been analyzed by Pyrolysis-gas chromatography mass spectrometry and gas chromatography by Hennet et al. (1989). Hennet et al. (1989) interrupt the preliminary pyrolysis data as being characteristic of a higher proportion of asphaltic material. The asphaltic residue can be characteristic of either remaining polar, non-migrational residue in source rock in which expulsion has occurred, or a residue of migration conduits where asphaltine compounds are trapped as lighter/lower molecular weight compounds migrate through. Comparison of the ratios of odd to even carbon chain length alkanes within and out of the seal zone in conjunction with GC results show variation. Hennett et al. (1989) state that definite changes have occurred for organic matter in the seal, with data suggesting a higher thermal maturation within and just below rather than above the seal. Problematic is that the base of the seal zone in the Weaver has not been clearly delineated when comparing Tigert (1989) and Hennet et al. (1989). Hennet et al. (1989) show the seal base of about 11300 ft. as fitting their data and conclusions. On the other hand Tigert (1989) states that the lower seal boundary occurs between shales/limestones and underlying sandstones of the Oil Creek Formation or approx. 12000 ft. based on log interpretation, while at the same time the pressure data of Tigert (1989), Fig. 2, for the Weaver map section would seem to indicate a basal depth of approx. 11700 ft.

Fig. 26 shows a separation of calcite and dolomite in respect to $\delta^{13}C$. Additionally, there is a trend of lighter (more negative) $\delta^{18}O$ mineral values with later diagenetic features. This is observed with cements verses later fractures and other diagenetic features (Fig. 27 and 28). The $\delta^{18}O$ water value curves indicate that the isotopes have evolved lighter (more negative) in terms of SMOW, considering that the lowest temperature is of the very last stage saddle dolomite material (avoiding complex diagenetic histories that may vary at each depth, as discussed previously). The saddle dolomite Th values are below those expected using gradients given for the Weaver. Fractures frequently have the higher end Th values, yet overall can be considered as late diagenetic events with lighter $\delta^{18}O$ values. This would seem to lessen the likelihood of $\delta^{18}O$ variation being primarily temperature dependant, and instead may be the result of host carbonate recrystallization or continued precipitation in a closed system.

But evidence for isotopic changes due solely to temperature variation in the subsurface has been reported by Barker and Halley (1986). They examined a reservoir limestone with calcite cemented fractures. The early calcite cement contained dull-blue fluorescent hydrocarbon inclusions with Th values mainly between 55 to 90 °C (131 to 194 °F) which were precipitated from fluids with a $\delta^{18}O$ water value of about 9 per mil (SMOW). Late calcite cements contain sparse hydrocarbon inclusions, and have P aqueous inclusion Th values between 90 to 135 °C (194 to 275 °F), with a $\delta^{18}O$ water of about 7.5 per mil. Barker and Halley (1986) conclude that both calcite generations may have been precipitated from the same fluid, with isotopic differences due solely to temperature changes.

Bjorkum and Walderhaug (1990) report diagenetic cementation data indicating at depth formation paralleling that discussed for the Weaver core. They examined calcite cementation of sandstones on the Norwegian shelf at a depth of 1 to 2 km (3280.8 to 6561.67 ft.). Cement fluid inclusion values are 50 to 70 °C (rarely up to 105 °C), and isotope values are -14 to 10 per mil (PDB) for $\delta^{18}O$. They conclude that the calcite cementation took place outside the influence of any groundwater flow. Relatedly, Connolly et al. (1990) recognize isolation of two hydrologic regimes in the Alberta Basin. They used O, D, Sr isotopes of formation waters in addition to chemical compositional trends to recognize this. The upper regime is dominated by flushing of modern meteoric waters through the upper sedimentary rock portion. The lower regime became isolated during the Pliocene and contains original connate and meteoric water associated with Laramide tectonism. The lower formations have become more saline as a result of upward diffusional flow and density stratification. One interesting point is that Jurassic and Mississippian diagenetic calcite cements show a pronounced discrepancy of as much as 5 per mil lighter than the whole rock $\delta^{18}O$ values. This is a greater separation than noted for most cements and later fracturing in this study.

Miles (1990) used subsurface pressure data and oil residue patterns to unravel a complex of isolated pressure compartments in the East Shetland Basin/Viking Graben.

Evidence of sustained pressure differences here indicates that fluids have been unable to move to equalize the differences, in agreement with Bradley's (1975) statement that without a seal pressure, pressures would equalize to hydrostatic. Pressure differences in this case are hypothesized by Miles (1990) to be a constantly changing product of overpressure build-up from shales. And release of overpressure occurs by natural hydrofracturing and slow leakage of fluids between compartments and out of the system at the graben edges. In two of the fields the pressure gradient approaches that of lithostatic, with the one believed to exceed the pressure gradient threshold for natural hydrofracturing and gas release. Miles (1990) further states that disturbed seismic reflector above the field may indicate gas release by hydrofracturing, which may explain why some shallow fields do not have a gas cap.

Finally, Jansa and Urrea (1990) report that overpressuring, seals and secondary reservoirs have all been diagenetically driven by a series of diagenetic events that overlapped through time in a sedimentary environment similar to that of the Weaver core. In the Venture Gas Field, the sandstone reservoirs are overpressured 1.9 times the normal hydrostatic pressure gradient (10.518 KPa/m). They cite stacking of slightly permeable and impermeable lithologies (thick non-porous limestone, silica/carbonate cemented sandstones and shales) as producing a multi-layered seal in which the sealing effect, porosity loss, has been achieved by progressive diagenetic changes. The diagenesis is an accumulation of dissolution and precipitation processes which frequently overlap and fluctuate according to changes in the physical and chemical parameters of the diagenetic system. The overpressures cut across stratigraphic and formation boundaries leading Jansa and Urrea (1990) to conclude that overpressuring onset is neither directly related to lithology nor to facies or formation boundaries. Overpressure may be the result of hydrocarbon maturation from kerogen, with the onset of overpressures correlating approximately with wet gas generation. R_o at the top of the seal is about 0.8 in their study, and the current temperature gradient of 2.8 °C/100 m remains constant despite the onset of overpressures (note the current accepted gradient for the Anadarko is 2.37 °C/100 m and R_o values in Fig. 32) . The temperature of the onset of overpressure is about 125 °C and linearly increases to a maximum of 155 °C at 5700 m. Within the overpressured strata salinities of the pore waters are 155,000 to 270,000 mg/L (Cl, Na and Ca compose 99% of TDS), and interestingly are reported to be lower than comparable normal pressured strata. This is the opposite of what is observed for the Weaver. Jansa and Urrea (1990) give eleven $\delta^{18}O/\delta^{13}C$ values for samples above the seal zone from 2000 to 5000 m depth. These fit within the range of values given for the Weaver.

They also see a trend toward lighter $\delta^{18}O$ values with later carbonate cements. Their interpretation is that the carbon has been derived in part from thermal decarboxylation of organic compounds, and $\delta^{18}O$ values are in the range of an early diagenetic sulfate reduction condition. The combination of light carbon and oxygen is taken to suggest that crystallization has occurred under high temperature. This and other facts are evoked to conclude that ferroan dolomite cement appeared at a depth of 3600 m (11811 ft.) and at a temperature of about 90 °C (194 °F). Finally Jansa and Urrea (1990) propose that carbonate dissolution and precipitation occurred within the seal zone, and that the diagenetic sealing is dynamic and likely a periodic process. Carbonate enriched solutions wouldn't need to migrate much distance before bicarbonate reprecipitation. Also concluded is that porosity enhancement is almost simultaneous with overpressure development. This parallels Tigert's conclusion that permeable and impermeable strata were originally the same material and were oppositionally enhanced with secondary porosity development.

Conclusions

The results of this study indicate the following conclusions:

-The thermal gradient indicated by diagenetic-mineralization fluid inclusion Th values was at or greater then that currently present, and likely was less than the maximum paleo-thermal gradient for the Anadarko Basin based on vitrinite reflectance from Pusey (1973).

-Diagenetic mineralization occurred at depth, over a broad temperature range, from fluids of highly variable density and lower salinity than that of current formation waters.

-Mineral oxygen and carbon isotope values (PDB) for carbonates are light, indicating higher temperatures of mineral precipitation than expected for a purely marine water source.

-$\delta^{18}O$ water values (SMOW) straddle that of standard mean ocean water with later diagenetic mineralization apparently becoming lighter (more negative).

-The occurrence of potentially mobile hydrocarbon phases (gas and condensates) was late in the diagenetic time frame for quartz, calcite and dolomite.

References

Aulstead K. L. and Spencer R. J. Jr. (1985) Diagenesis of the Keg River Formation, northwestern Alberta: Fluid inclusion evidence. Bull. Can. Petrol. Geol. 33, 167-183.

Aulstead K. L., Spencer R. J. Jr. and Krouse H. R. (1988) Fluid inclusion and isotopic evidence on dolomitization, Devonian of Western Canada. Geochem. et Cosmochemica Acta 52, 1027-1035.

Barker C. E. and Halley R. B. (1986) Fluid inclusion, stable isotope and vitrinite reflectance evidence for the thermal history of the Bone Spring Limestone, southern Guadalupe Mountains, Texas. in Gautier D. L. (1986) Roles of organic matter in sediment diagenesis: SEPM Spec. Publ. 38, 189-203.

Barker C. E. and Reynolds T. J. (1984) Preparing doubly polished sections of temperature sensitive sedimentary rocks. Jour. Sed. Pet. 54, 635-663.

Bjorkum P. A. and Walderhaug O. (1990) Geometrical arrangement of calcite cementation within shallow marine sandstones. Earth-Sci. Rev. 29, 145-161.

Bjorlykke K., Aagaard P., Dypvik H., Hastings D. S. and Harper A. S. (1986) Diagenesis and reservoir properties of Jurassic sandstones from the Haltenbanken area, offshore mid Norway. in Habitat of Hydrocarbons on the Norwegian Continental Shelf, Norwegian Petroleum Society, 275-286.

Bodnar R. J., Binns P. R. and Hall D. L. (1988) Synthetic fluid inclusions. VI. Quantitative evaluation of the decrepitation behavior of fluid inclusions in quartz at one atmosphere confining pressure. Jour. Metamorphic Geol. 7, 229-242.

Borak B. and Friedman G. M. (1981) Textures of sandstones and carbonate rocks in the world's deepest wells (in excess of 30,000 ft. or 9.1 km): Anadarko Basin, Oklahoma. Sed. Geol. 29, 133-151.

Bradley J. S. (1975) Abnormal formation pressure. AAPG Bull. 59, 957-973.

Burley S. D., Mullis J. and Matter A. (1989) Timing diagenesis in the Tartan Reservoir (UK North Sea): constraints from combined cathodoluminescence microscopy and fluid inclusion studies. Marine and Petrol. Geol. 6, 98-120.

Burruss R. C. (1980) Geologic pressure determinations from fluid inclusion studies. Ann. Rev. Earth Planet. Sci. 8, 263-301.

Burruss R. C. (1985) Paleotemperatures from fluid inclusions: Advances in theory and technique. in Thermal history of sedimentary basin, Methods and case histories, Chap. 7, Springer-Verlag NY Inc.

Burruss R. C. (1987) Diagenetic paleotemperatures from aqueous fluid inclusions: re-equilibration of inclusions in carbonate cements by burial heating. Min. Mag. 51, 477-481.

Burruss R. C., Cercone K. R. and Harris P. M. (1985) Timing of hydrocarbon migration: evidence from fluid inclusions in calcite cements, tectonics and burial history. in Carbonate Cements, SEPM Special Publ. 3, 277-289.

Cardott B. J. and Lambert M. W. (1985) Thermal maturity by vitrinite reflectance of Woodford Shale, Anadarko Basin, Oklahoma. AAPG Bull. 69, 1982-1998.

Castano J. R. and Sparks D. M. (1974) Interpretation of vitrinite reflectance measurements in sedimentary rocks and determination of burial history using vitrinite reflectance and authigenic minerals. in Dutcher R. R., Hacquebard P. A., Schopf J. M. and Simon J. A., eds., Carbonaceous Materials as Indicators of Metamorphism: GSA Special Paper 153, 31-52.

Cercone K. R. and Lohmann K. C. (1987) Late burial diagenesis of Niagaran (Middle Silurian) pinnacle reefs in Michigan Basin. AAPG Bull. 71, 156-166.

Collins P. F. (1979) Gas hydrates in CO_2-bearing fluid inclusions and the use of freezing data for estimation of salinity. Econ. Geol. 74, 1435-1444.

Connolly C. A., Walter L. M., Baadsgaard H. and Longstaffe F. J. (1990) Origin and evolution of formation waters, Alberta Basin, Western Canada Sedimentary Basin. II. Isotopic systematics and water mixing. Appl. Geochem. 5, 397-413.

Craig H. (1957) Isotopic standards for carbon and oxygen and correction factors for mass-spectrometric analysis of carbon dioxide. Geochim. Cosmochim. Acta 12, 133-149.

Craig H. (1961a) Standards for reporting concentrations of deuterium and oxygen-18 in natural waters. Science 133, 1833-1834.

Degens E. T. and Epstein S. (1964) Oxygen and carbon isotope ratios in coexisting calcites and dolomites from recent and ancient sediments. Geochim. Cosmochim. Acta 28, 23.

Dewers T. and Ortoleva P. (1988) The role of geochemical self-organization in the migration and trapping of hydrocarbons. Appl. Geochem. 3, 287-316.

Dickson J. A. D. (1965) A modified staining technique for carbonates in thin section. Nature 205, 587.

Dickson J. A. D. (1966) Carbonate identification and genesis as revealed by staining. Jour. Sed. Pet. 36, 491-505.

Donovan R. N., Beauchamp W., Ferraro T., Lojek C., McConnell D., Munsil M., Ragland D., Sweet B. and Taylor D. (1983) Subsidence rates in Oklahoma during the Paleozoic. Oklahoma City Geological Society, Shale Shaker 33, 86-88.

Ehrenberg S. N. (1990) Relationship between diagenesis and reservoir quality in sandstones of the Garn Formation, Haltenbanken, Mid-Norwegian Continental Shelf. AAPG Bull. 74, 1538-1558.

Ernst W. G. and Blatt H. (1964) Experimental study of quartz overgrowths and synthetic quartzites. Jour. of Geol. 72, 461-469.

Federal Power Commission Report (1973) Report of the Technical Advisory Committee, data tape H.

Friedman I. and O'Neil J. R. (1977) Compilation of stable isotope fractionation factors of geochemical interest. in, Data of Geochemistry, sixth edition, M. Fleischer, ed., USGS Prof. Paper 440-KK.

Fritz P. and Smith D. G. W. (1970) The isotopic composition of secondary dolomites. Geochim. et Cosmochim. Acta 34, 1161-1173.

Ghaith A. Y., Bradley J. S., Powley D. E. and Ortoleva P. (1989) Oscillatory fluid release from overpressured compartments in Basin Compartments and Seals: A Characterization and Predictive Modeling Study (Okintex group), Progress Report IA, Chap.8.

Hanor J. S. and Sassen R. (1988) Deep basin hydrodynamics of the Louisiana Gulf Coast: implications of oil and gas migration. Ninth Annual Research Conf., Gulf Coast Section, SEPM Foundation, Prog. and Abstr., 15.

Haszedline R. S., Samson I. M., Cornford C. (1984) Dating diagenesis in a petroleum basin, a new fluid inclusion method. Nature 307, 354-357.

Hennet R., Hunt J., Whelan J. and Dickinson P. (1989)

Organic Geochemistry (Task 8) in A research program leading to the understanding of "pressure chambers"; GRI contract number 5088-260-1746; Third quarterly report, Geosciences Dept. the Pennsylvania State Univ., 91-105.

Horsfield B. and McLimans R. K. (1984) Geothermometry and geochemistry of aqueous and oil-bearing fluid inclusions from Fateh Field, Dubai. Org. Geochem. 6, 733-740.

Hunt J. M. (1990) Generation and migration of petroleum from abnormally pressured fluid compartments. AAPG Bull. 74, 1-12.

Hunt J. M. (1991) Generation and migration of petroleum from abnormally pressured fluid compartments: reply. AAPG Bull. 75, 328-330.

Hunt J. M. (1991) Generation and migration of petroleum from abnormally pressured fluid compartments: reply. AAPG Bull. 75, 336-338.

Irwin H., Curtis C. and Coleman M. (1977) Isotopic evidence for source of diagenetic carbonates formed during burial of organic-rich sediments. Nature 269, 209-213.

James W. C., Wilmar G. C. and Davidson B. G. (1986) Role of quartz type and grain size in silica diagenesis, Nugget Sandstone, south-central Wyoming. Jour. Sed. Pet. 56, 657-662.

Jansa L. F. and Urrea V. H. N. (1990) Geology and diagenetic history of overpressured sandstone reservoirs, Venture Gas Field, offshore Nova Scotia, Canada. AAPG Bull. 74, 1640-1658.

Jones P. J. and Philp R. P. (1990) Oils and source rocks from Pauls Valley, Anadarko Basin, Oklahoma, U.S.A. Applied Geochem. 5, 429-448.

Kaufman J., Meyers W. J. and Hanson G. N. (1990) Burial cementation in the Swan Hills Formation (Devonian), Rosevear Field, Alberta, Canada. Jour. of Sed. Pet. 60, 918-939.

Land L. S. (1983) The application of stable isotopes to the studies of the origin of dolomite and to problems of diagenesis of clastic sediments. in Stable Isotopes in Sedimentary Geology, SEPM Short Course 10, 4.1-4.22.

Lawler J. P. and Crawford M. L. (1983) Stretching of fluid inclusions resulting from a low-temperature microthermometeric technique. Econ. Geol. 678, 527-529.

Levine J. R., Samson I. M. and Hesse R. (1991) Occurrence of fracture-hosted impsonite and petroleum fluid inclusions, Quebec City Region, Canada. AAPG Bull. 75, 139-155.

Logan J. M. (1989) Vertical seals: Their occurrence, formation and importance to pressure chambers in Basin Compartments and Seals: A Characterization and Predictive Modeling Study (Okintex group), Progress Report IA, Chap. 3.

Longman M. W. (1981) Deposition of the Bromide Formation, Arbuckle Mountains, Oklahoma: Ontogeny of an ancient carbonate shelf. Oklahoma Geological Survey Bulletin 32, 1-18.

Longstaffe F. J. (1989) Stable isotopes as tracers in clastic diagenesis. in Mineralogical Association of Canada Short Course in Burial Diagenesis v. 15, Chap. 6.

Lundegard P. D. (1989) Temporal Reconstruction of Sandstone Diagenetic Histories. in Mineralogical Association of Canada Short Course in Burial Diagenesis v. 15, Chap. 5.

McBride E. F. (1989) Quartz cement in sandstones: A review. Earth-Sci. Rev. 26, 69-112.

McCrea J. M. (1950) On the isotopic chemistry of carbonates and a paleotemperature scale. J. Chem. Phys. 18, 849-857.

McLimans R. K. (1987) The application of fluid inclusions to migration of oil and diagenesis in petroleum reservoirs. Appl. Geochem. 2, 585-603.

McLimans R.K. and Videtich P. E. (1989) Diagenesis and burial history of Great Oolitic Limestone, Southern England. AAPG Bull. 73, 1195-1205.

Meshri I. D. and Comer J. B. (1990) A subtle diagenetic trap in the Cretaceous Glauconite Sandstone of Southwest Alberta. Earth-Sci. Rev. 29, 199-214.

Meunier J. D. (1989) Assessment of low-temperature fluid inclusions in calcite using microthermometry. Econ. Geo. 84, 167-170.

Miles J. A. (1990) Secondary migration routes in the Brent Sandstones of the Viking Graben and East Shetland Basin: Evidence from oil residues and subsurface pressure data. AAPG Bull. 74, 1718-1735.

Moore C. H. and Druckman Y. (1981) Burial diagenesis and porosity evolution, Upper Jurassic Smackover, Arkansas and

Louisiana. AAPG Bull. 65, 597-628.

Murray R. C. (1957) Hydrocarbon fluid inclusions in quartz. Bull. AAPG 41, 950-952.

Narr W. and Burruss R. C. (1984) Origin of reservoir fractures in Little Knife Field, North Dakota. AAPG Bull. 68, 1087-1100.

Neumann H. J., Paczynska-Lahme B. and Swerin D. (1981) Composition and Properties of Petroleum. N.Y. Holsted Press.

Norman, D. I. (1987) Report on fluid inclusion study of fracture mineralization from the Piceance Basin, Colorado. Sandia National Laboratory Contract 33-6617.

Norman, D. I. (1987) Report on inclusion volatile analyses on samples from the Piceance Creek Basin. Sandia National Laboratory Contract 33-6617.

Northrop D. A. and Clayton R. N. (1966) Oxygen isotope fractionations in systems containing dolomite. Jour. of Geology 74, 174-195.

O'Neil J. R. and Epstein S. (1966) Oxygen isotope fractionation in the system dolomite-calcite-carbon dioxide. Science 152, 198-201.

O'Neil J. R., Clayton R. N. and Mayeda T. K. (1969) Oxygen isotope fractionation in divalent metal carbonates. Chem. Phys. 51, 5547-5558.

Pagel M., Walgenwitz F. and Dubessy J. (1986) Fluid inclusions in oil and gas-bearing sedimentary formations. in Thermal modelling in sedimentary basins. First IFP exploration research conference, Carcans, France, 1985, Gulf Publishing Co.

Peter J. M., Simoneit B. R. T. and Kawka O. E. (1990) Liquid hydrocarbon-bearing inclusions in modern hydrothermal chimneys and mounds from the southern trough of Guaymas Basin, Gulf of California. Applied Geochem. 5, 51-63.

Pitman J. K. and Burruss R. C.(1989) Diagenesis of hydrocarbon-bearing rocks in the Middle Ordovician Simpson Group, southeastern Anadarko Basin, Oklahoma. Oklahoma Geological Survey Circ. 90, 134-142.

Pittman E. D. (1972) Diagenesis of quartz in sandstones as revealed by scanning electron microscopy. Jour. Sed. Pet. 42, 507-519.

Pollastro R. M. (1988) Clay mineralization and diagenetic cements of deeply buried rocks of the Simpson Group (Middle Ordovician), Anadarko basin, Oklahoma. Program and Abstr., Twenty fifth Annual Meeting, Clay Minerals Society, Grand Rapids, Mich., p. 54.

Potter R. W. II (1977) Pressure corrections for fluid-inclusion homogenization temperatures based on volumetric properties of the system $NaCl-H_2O$. Jour. Research USGS 5, 603-607.

Potter R. W. II and Brown D. L. (1977) The volumetric properties of aqueous sodium chloride solutions from 0-500 °C at pressures up to 2000 bars based on a regression of available data from the literature. USGS Bull. 1421-C.

Potter R. W. II and Clynne M. A. (1978) Solubility of highly soluble salts in aqueous media--part 1, NaCl, KCl, $CaCl_2$, Na_2SO_4, and K_2SO_4 solubilities to 100 °C. Jour. Research USGS 6, 701-705.

Powley D. E. (1987) Abnormal pressure seals: Gas Research Institute Gas Sands Workshop, Chicago, Unpublished.

Powley D. E. (1990) Pressures and hydrogeology in petroleum basins. Earth-Sci. Rev. 29, 215-226.

Pratt L. M. and Burruss R. C. (1988) Evidence for petroleum generation and migration in the Hartford and Newark Basins. in Studies of the Early Mesozoic Basins of the Eastern United States, USGS Bull. 1776, 74-79. Froelich A. J. and Robinson G. R. Jr. ed.

Prezbindowski D. R. and Larese R. E. (1987) Experimental stretching of fluid inclusions in calcite-Implications for diagenetic studies. Geology 15, 333-336.

Pusey W. C. (1973) The ESR method: A new technique of estimating the organic maturity of sedimentary rocks. Petroleum Times, Jan. 12, 21-24.

Radke B. M. and Mathis R. L. (1980) On the formation and occurrence of saddle dolomite. Jour. Sed. Pet. 50, 1149-1168.

Ramboz C. and Charef A. (1988) Temperature, pressure, burial history, and paleohydrology of the Les Malines Pb-Zn deposit: Reconstruction from aqueous inclusions in barite. Econ. Geo. 83, 784-800.

Roedder E. (1984) Fluid Inclusions in Reviews in Mineralogy, v. 12, Mineralogical Society of America.

Roedder E. and Bodnar R. J. (1980) Geologic pressure determination from fluid inclusion studies. Ann. Rev. Earth. Planet. Sci. 8, 263-301.

Ross R. J., et al. (1982) The Ordovician System in the United States: International Union of Geological Sciences, Publ. No. 12, Correlation Chart.

Saigal G. C. and Bjorlykke K. (1987) Carbonate cements in clastic reservoir rocks from offshore Norway-relationships between isotopic composition, textural developments and burial depth. in Diagenesis of Sedimentary Sequences (ed. J. D. Marshal) p. 313-324, Geol. Soc. Spec. Publ. 36.

Schmoker J. W. (1986) Oil generation in the Anadarko Basin, Oklahoma and Texas: Modeling using Lopatin's Method. Oklahoma Geological Survey, Special Publication 86-3.

Shepherd T. J. (1981) Temperature-programmable, heating-freezing stage for microthermometric analysis of fluid inclusions. Econ. Geol. 66, 1244-1247.

Shephard T. J., Rankin A. H. and Alderton D. H. M. (1985) A Practical Guide to Fluid Inclusion Studies. Blackie.

Tigert V. A. (1989) Identification and characterization of a pressure seal in south-central Oklahoma. MS thesis, Oklahoma State Univ.

Tigert V. A. and Al-Shaieb Z. (1990) Pressure seals: their diagenetic banding patterns. Earth-Sci. Rev. 29, 227-240.

Tilley B. J., Nesbitt B. E. and Longstaffe F. J. (1989) Thermal history of Alberta Deep Basin: Comparative study of fluid inclusion and vitrinite reflectance data. AAPG Bull. 73, 1206-1222.

Toth J., Maccagno M. D., Otto C. J. and Rostron B. J. (1991) Generation and migration of petroleum from abnormally pressured fluid compartments: discussion. AAPG Bull. 75, 331-335.

Ulrich M. R. and Bodnar R. J. (1988) Systematics of stretching of fluid inclusions II: Barite at 1 atmosphere confining pressure. Econ. Geol. 83, 1037-1046.

Videtich P. E., McLimans R. K., Watson H. K. S. and Nagy R. M. (1988) Depositional, diagenetic, thermal, and maturation histories of Cretaceous Mishriff Formation, Fateh Field, Dubai. AAPG Bull. 72, 1143-1159.

Visser W. (1982) Maximum diagenetic temperature in a petroleum source rock from Venezuela by fluid inclusion geothermometry. Chem. Geol. 37, 95-101.

Walderhaug O. (1990) A fluid inclusion study of quartz-cemented sandstones from offshore Mid-Norway-Possible evidence for continued quartz cementation during oil emplacement. Jour. Sed. Pet. 60, 203-210.

Waples D. W. (1991) Generation and migration of petroleum from abnormally pressured fluid compartments: discussion. AAPG Bull. 75, 326-327.

Weber S. J. (1978) Petrography and diagenesis of the McLish Formation, Simpson Group (Middle Ordovician), southeastern Anadarko Basin, Oklahoma. MS thesis, Oklahoma State Univ.

Appendix A

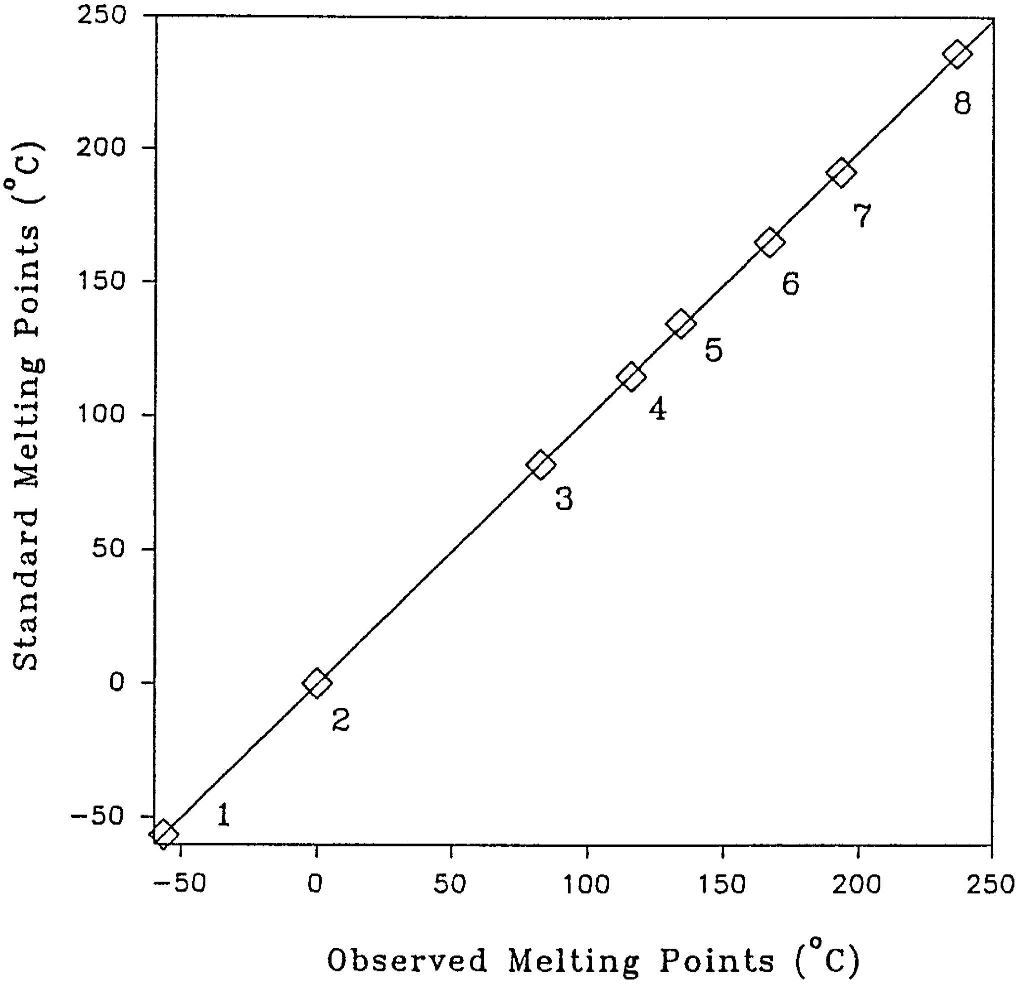

Standard	Melting point (°C)
1. CO_2-H_2O synthetic inclusion (USGS)	-56.6
2. H_2O synthetic inclusion (USGS)	0.0
3. Vanillin	81-83
4. Acetanilid	114-116
5. Acetophenetidin	134-136
6. Sulfanilamide	164.5-166.5
7. Sulfapyridine	190-193
8. Caffeine	235-237.5

Appendix B

Quartz Fluid Inclusion Data

DEPTH	CEMENT	TM	TH	SALINITY	DENSITY
11078.00	QTZ	--	117.00	--	--
11078.00	--	--	114.00	--	--
11144.00	--	--	99.70	--	--
11144.00	--	-0.20	99.70	0.40	0.96
11144.00	--	-0.10	112.50	0.20	0.95
11145.00	--	2.60	120.00	12.90	1.03
11145.00	--	5.10	135.00	9.30	1.00
11145.00	--	3.20	123.00	12.10	1.03
11645.00	--	-10.20	95.50	14.20	1.06
--	VUG/INFI	--	--	--	--
11598.00	--	-2.00	114.00	3.40	0.97
11598.00	--	-2.40	103.00	4.00	0.98
11598.00	--	-9.50	105.00	13.40	1.05
11598.00	--	-7.40	--	11.00	--
11598.00	--	-8.00	113.00	11.70	1.03
11598.00	--	-7.30	111.00	10.90	1.03
11598.00	--	--	115.00	--	--
11598.00	--	-11.40	--	15.40	--
11598.00	--	-13.40	--	17.40	--
11598.00	--	-0.10	88.50	0.20	0.97
11598.00	--	-15.10	--	18.90	--
11598.00	--	-0.30	93.50	0.50	0.97
11599.00	--	-3.30	101.10	5.40	1.00
11599.00	--	-3.00	105.20	4.90	0.99
11599.00	--	1.60	106.70	14.30	1.05
11599.00	--	-8.60	96.60	12.40	1.05
11599.00	--	-8.10	95.40	11.80	1.04
11599.00	--	0.20	98.00	15.60	1.07
--	VUG/HC	--	--	--	--
11598.00	--	--	72.60	--	--
11598.00	--	--	74.90	--	--
11598.00	--	--	67.10	--	--
11598.00	--	--	70.40	--	--
11598.00	--	--	65.20	--	--
11598.00	--	--	113.50	--	--
11601.00	--	--	89.90	--	--
11601.00	--	--	97.50	--	--
11601.00	--	--	117.80	--	--
11601.00	--	--	114.90	--	--
11601.00	--	--	116.25	--	--
11601.00	--	--	76.80	--	--
11601.00	--	--	81.40	--	--
11601.00	--	--	84.90	--	--
11601.00	--	--	83.00	--	--
11601.00	--	--	99.20	--	--
11601.00	--	--	88.20	--	--
11601.00	--	--	85.50	--	--
11601.00	--	--	85.50	--	--
11601.00	--	--	82.80	--	--
11601.00	--	--	76.10	--	--
11601.00	--	--	76.10	--	--

12067.00	--	-11.20	107.50	15.20	1.06
12067.00	--	-9.40	108.00	13.30	1.05
12067.00	--	-25.20	109.00	26.10	1.15
12067.00	--	-6.90	--	10.40	--
12067.00	--	-6.60	103.00	10.00	1.03
12067.00	--	-6.10	112.00	9.30	1.01
12067.00	--	-5.30	111.50	8.30	1.01
12067.00	--	-3.90	106.50	6.30	1.00
12067.00	--	-2.50	116.00	4.20	0.98
12067.00	--	-0.70	88.30	1.20	0.97
12067.00	--	-0.50	117.00	0.80	0.95
12067.00	--	-1.80	135.00	3.00	0.95
12067.00	--	-3.70	109.00	6.00	0.99
12067.00	--	-1.50	111.00	2.60	0.97
12067.00	--	-2.60	--	4.30	--
12067.00	--	-0.10	116.00	0.20	0.95
DEPTH	CEMENT	TM	TH	SALIN	DENSITY
11522.00	--	0.70	92.00	15.20	1.07
11522.00	--	-1.20	85.00	2.10	0.98
11522.00	--	0.70	72.00	15.20	1.08
11522.00	--	-0.10	89.50	0.20	0.97
11522.00	--	-9.50	84.00	13.40	1.06
11522.00	--	-9.90	82.30	13.90	1.07
11522.00	--	-12.30	92.50	16.30	1.08
11522.00	--	0.90	95.50	14.90	1.07
11522.00	--	-0.50	139.00	0.90	0.93
11522.00	--	-1.00	82.00	1.70	0.98
12054.00	--	6.00	118.00	7.90	1.00
12054.00	--	5.20	122.00	9.20	1.01
DEPTH	STYLO	TM	TH	SALIN	DENSITY
11382.00	--	-4.65	127.00	7.40	0.99
11382.00	--	-4.50	132.00	7.10	0.99
11382.00	--	-4.70	131.00	7.40	0.99
11382.00	--	-11.70	110.90	15.70	1.06
11382.00	--	-9.60	118.00	13.50	1.04
11382.00	--	-11.90	119.40	16.00	1.06
11382.00	--	-1.30	105.80	2.20	0.97
11382.00	--	-1.10	98.60	1.90	0.97
11382.00	--	-8.50	90.60	12.30	1.05
11382.00	--	1.70	97.40	14.40	1.06
11382.00	--	2.10	105.00	13.10	1.05
11382.00	--	-5.10	--	8.00	--
11382.00	--	-4.70	--	7.40	--
11382.00	--	-4.80	120.00	7.60	1.00
11382.00	--	-6.20	139.60	9.50	1.00
11382.00	--	-2.60	141.00	4.30	0.96
11382.00	--	-5.00	138.10	7.90	0.99
11382.00	--	--	125.40	--	--
11382.00	--	-2.30	152.00	3.90	0.95
11382.00	--	-0.10	123.90	8.00	1.00
11382.00	--	-4.50	125.60	7.20	0.99
11382.00	--	-7.70	106.60	11.40	1.03
11382.00	--	2.70	141.00	12.70	1.02
11382.00	--	-3.20	106.00	5.20	0.99
11382.00	--	-4.90	124.00	7.70	1.00
11382.00	--	--	126.60	--	--
DEPTH	VOID	TM	TH	SAL	DENSITY
11360.00	--	--	95.50	--	--

Calcite Fluid Inclusion Data

DEPTH	FRACTURE	TM	TH	SALIN	DENSITY
11457.00	--	-4.20	--	6.70	--
11457.00	--	0.30	124.20	15.60	1.05
11457.00	--	-12.30	--	16.30	--
11457.00	--	-4.30	195.80	6.90	0.92
11457.00	--	-12.80	153.55	16.80	1.04
11457.00	--	-2.30	130.50	3.90	0.96
11457.00	--	-2.05	122.33	3.50	0.97
11457.00	--	--	127.30	--	--
11457.00	--	-1.30	124.50	2.20	0.96
11457.00	--	0.40	123.70	15.50	1.05
11457.00	--	-7.00	140.65	10.50	1.00
11457.00	--	-11.50	158.00	15.50	1.02
11462.00	--	-1.60	--	2.70	--
11462.00	--	-23.30	--	24.90	--
11462.00	--	-2.60	104.00	4.30	0.99
11462.00	--	-1.80	115.50	3.10	0.97
11462.00	--	-1.00	118.00	1.70	0.96
11462.00	--	-3.20	111.50	5.20	0.99
11462.00	--	-0.60	116.50	1.00	0.95
11462.00	--	-3.20	115.50	5.20	0.98
11462.00	--	-4.90	125.00	7.70	0.99
11462.00	--	-3.70	120.00	6.00	0.99
11462.00	--	-3.50	114.70	5.70	0.99
11462.00	--	-24.50	--	25.60	--
11525.00	--	2.80	135.00	12.60	1.02
11525.00	--	-0.30	156.00	0.50	0.92
11525.00	--	5.70	103.00	8.20	1.01
11525.00	--	-0.50	174.30	0.90	0.90
11525.00	--	0.20	162.00	15.60	1.02
11525.00	--	-0.70	--	1.20	--
11525.00	--	4.00	115.00	10.70	1.02
11525.00	--	0.60	131.40	15.30	1.04
11525.00	--	4.00	--	10.70	--
11525.00	--	2.10	95.50	13.10	1.05
11525.00	--	0.60	160.00	15.30	1.02
11525.00	--	0.60	114.00	15.30	1.06
11525.00	--	1.00	119.00	14.80	1.05
11525.00	--	-1.10	186.00	1.90	0.90
11525.00	--	-0.10	154.00	0.20	0.92
11525.00	--	-0.70	153.60	1.20	0.92
11525.00	--	2.10	--	13.10	--
11525.00	--	-1.00	115.00	1.90	0.96
11548.00	--	3.60	127.00	11.80	1.02
11548.00	--	4.70	112.80	9.70	1.02
11548.00	--	4.70	119.00	9.70	1.01
11548.00	--	-5.80	--	8.90	--
11548.00	--	1.93	122.00	13.50	1.04
11548.00	--	-0.40	126.00	0.70	0.94
11548.00	--	-0.80	--	1.40	--
11548.00	--	-2.45	133.50	4.10	0.96
11548.00	--	2.80	--	12.50	--
11548.00	--	-0.80	136.50	1.40	0.94
11548.00	--	11.10	117.50	0.00	0.94
11548.00	--	2.00	114.50	13.60	1.04
12067.00	--	-9.20	110.00	13.10	1.04
12067.00	--	-14.90	--	18.70	--
12067.00	--	-6.10	112.30	9.30	1.01

11360.00	--	--	96.90	--	--
11360.00	--	--	95.80	--	--
11675.00	--	-18.50	96.00	21.60	1.12
11675.00	--	-18.10	98.90	21.20	1.11
11675.00	--	-0.10	105.20	0.20	0.95
11675.00	--	0.10	112.50	15.70	1.06
11675.00	--	--	114.50	--	--
11675.00	--	0.70	98.10	15.20	1.07
11675.00	--	-0.10	101.60	0.20	0.96
11675.00	--	-0.10	99.80	0.20	0.96
11675.00	--	-0.70	104.50	1.20	0.96
11675.00	--	-5.70	68.00	8.80	1.04
11675.00	--	-8.40	--	12.20	--
11675.00	--	-8.00	--	11.70	--
11675.00	--	-3.20	94.50	5.20	1.00
11675.00	--	-2.30	122.90	3.90	0.97
11675.00	--	-6.30	127.70	9.60	1.01
11675.00	--	-6.30	--	9.60	--
11675.00	--	-1.20	--	2.10	--
11675.00	--	-9.50	97.10	13.40	1.05
11675.00	--	-0.60	--	1.00	--
11675.00	--	-10.20	109.00	14.20	1.05
11675.00	--	-8.30	94.60	12.10	1.05
11675.00	--	-0.10	114.50	0.20	0.95
11675.00	--	-4.60	127.50	7.20	0.99
11675.00	--	2.10	101.90	13.10	1.05
11675.00	--	-1.30	--	2.20	--
11675.00	--	-0.90	89.90	1.60	0.98

Dolomite Fluid Inclusion Data

DEPTH	CEMENT	TM	TH	SAL	DENSITY
11384.00	--	-17.60	105.00	20.90	1.11
11384.00	--	--	110.00	--	--
11394.00	--	--	90.00	--	--
11409.00	--	-8.20	82.20	12.00	1.05
11409.00	--	-10.10	90.20	14.10	1.06
11409.00	--	-6.80	77.50	10.20	1.04
11409.00	--	-6.40	79.50	9.70	1.04
11409.00	--	-10.20	--	14.20	--
11409.00	--	-9.40	--	13.30	--
11409.00	--	-4.60	--	7.20	--
11409.00	--	-11.10	--	15.10	--
11409.00	--	-7.80	--	11.40	--
11409.00	--	-8.70	--	12.50	--
11409.00	--	-13.60	--	17.60	--
11409.00	--	-11.25	--	15.30	--
11409.00	--	-15.90	--	19.50	--
11409.00	--	-15.90	--	19.50	--
11409.00	--	-4.80	98.50	7.50	1.01
11409.00	--	-8.70	117.00	12.50	1.03
11409.00	--	-12.40	103.50	16.40	1.07
11409.00	--	-11.70	--	15.70	--
11409.00	--	-20.10	--	22.70	--
11409.00	--	-10.30	103.30	14.30	1.06
11540.00	--	--	105.10	--	--
11540.00	--	-1.00	87.60	1.90	0.98
11540.00	--	-0.10	87.00	0.20	0.97
11540.00	--	--	129.90	--	--
DEPTH	STYLO	TM	TH	SAL	DENSITY
11139.00	--	--	88.90	--	--
11139.00	--	-14.50	101.75	18.40	1.09
11139.00	--	-14.30	98.50	18.20	1.09
11139.00	--	-11.30	88.40	15.30	1.07
11139.00	--	--	107.90	--	--
11139.00	--	-8.70	97.30	12.50	1.05
11139.00	--	--	97.50	--	--
11139.00	--	-12.10	115.10	16.10	1.06
11139.00	--	--	110.40	--	--
11139.00	--	--	111.00	--	--
11139.00	--	--	111.20	--	--
11139.00	--	--	115.90	--	--
11139.00	--	--	114.00	--	--
11139.00	--	--	125.00	--	--
11139.00	--	--	124.50	--	--
11139.00	--	--	84.30	--	--
11139.00	--	--	104.90	--	--
11139.00	--	--	112.30	--	--
11139.00	--	--	116.10	--	--
11139.00	--	--	116.90	--	--
11139.00	--	--	129.40	--	--
11139.00	--	--	115.00	--	--
11139.00	--	--	112.00	--	--
11139.00	--	--	105.20	--	--
11139.00	--	--	112.50	--	--

11139.00	--	--	104.90	--	--
11139.00	--	--	119.50	--	--
11139.00	--	--	93.60	--	--
11139.00	--	--	112.60	--	--
11139.00	--	--	114.40	--	--
11139.00	--	--	112.50	--	--
11139.00	--	--	117.50	--	--
11139.00	--	--	110.50	--	--
11139.00	--	--	92.00	--	--
11139.00	--	--	105.00	--	--
11139.00	--	--	98.50	--	--
11139.00	--	--	93.00	--	--
11139.00	--	--	132.00	--	--
DEPTH	FRACTURE	TM	TH	SALIN	DEPTH
11400.00	--	--	110.00	--	--
11400.00	--	--	113.00	--	--
11400.00	--	--	108.00	--	--
11400.00	--	--	106.00	--	--
11400.00	--	--	110.00	--	--
11400.00	--	--	118.70	--	--
11400.00	--	--	108.50	--	--
11400.00	--	--	101.00	--	--
11400.00	--	--	105.50	--	--
11400.00	--	--	95.50	--	--
11400.00	--	--	115.00	--	--
11400.00	--	--	108.50	--	--
11400.00	--	--	102.00	--	--
11400.00	--	--	94.50	10.10	1.03
11400.00	--	--	102.00	8.90	1.02
11400.00	--	--	92.50	--	--
11400.00	--	--	106.00	--	--
11400.00	--	--	87.00	--	--
11400.00	--	--	73.00	19.60	1.12
11400.00	--	--	98.00	--	--
11400.00	--	--	89.00	--	--
11400.00	--	--	101.00	--	--
11400.00	--	--	98.00	--	--
11523.00	--	-2.80	128.50	4.60	0.97
11523.00	--	-2.40	126.80	4.00	0.97
11523.00	--	-3.20	127.40	5.20	0.98
11523.00	--	-5.40	133.50	8.40	0.99
11523.00	--	-2.10	128.40	3.50	0.96
11523.00	--	-4.10	132.80	6.60	0.98
11523.00	--	-2.80	120.80	4.60	0.98
11523.00	--	-7.90	116.90	11.60	1.03
11523.00	--	-8.40	120.90	12.20	1.03
11523.00	--	0.10	122.30	15.70	1.05
11523.00	--	-4.90	114.80	7.70	1.00
11523.00	--	-5.90	98.50	9.10	1.02
11523.00	--	-7.80	109.90	11.50	1.03
11523.00	--	-1.50	113.40	2.60	0.97
11523.00	--	-8.90	107.10	12.80	1.04

11523.00	--	-3.30	122.00	5.40	0.98
11523.00	--	1.95	107.00	13.70	1.05
11523.00	--	-3.30	107.00	5.40	0.99
11523.00	--	-3.20	110.50	5.20	0.99
11523.00	--	2.40	118.50	13.20	1.04
11598.00	--	--	96.50	--	--
11598.00	--	--	98.30	--	--
11624.00	--	-25.10	107.00	26.10	1.15
DEPTH	SD/VUG	TM	TH	SALIN	DENSITY
11422.00	--	-9.40	92.00	13.30	1.06
11422.00	--	-11.50	97.10	15.50	1.07
11422.00	--	-12.90	93.10	16.90	1.08
11422.00	--	-8.40	93.10	12.20	1.05
11422.00	--	-10.10	92.90	14.10	1.06
11598.00	--	--	66.90	--	--
11598.00	--	--	55.60	--	--
11598.00	--	--	66.50	--	--
11598.00	--	--	58.70	--	--
11598.00	--	--	51.50	--	--
11598.00	--	--	57.50	--	--

Hydrocarbon Inclusion Data

3 phase separation	2 phase homogenization	1 phase homogenization
-66 (°C)	-62.7	72.6
-66	-63	74.9
-74.5	-63.4	67.1
-74	-71	70.4
-68	-65.2	65.2
-69.8	-65.8	113.5

Explanation

DEPTH units is in feet
Tm is temperature of melting (°C)
Th is temperature of homogenization (°C)
SALINITY units is in eq. wt. % NaCl
DENSITY units is in grams/cm^3

VUG/INFI is vug or void mineralization
VUG/HC is vug mineralization with analyzed aqueous inclusions in the presence of cogenetic hydrocarbon inclusions
STYLO is stylolitic associated mineralization
CEMENT is cement mineralization
FRACTURE is fracture mineralization

Appendix C

Stable Isotope Standards

Sample Number	13/12 C (per mil) PDB	18/16 O (per mil) PDB	Converted 18/16 O (per mil) PDB	18/16 O (per mil) SMOW	Converted 18/16 O (per mil) SMOW
Zero enrich.					
CO2-2	-38.11	-30.51	-40.84	-0.59	-11.19
NBS 18	-4.67	-12.61	-23	17.85	7.2
NBS 19	2.2	8.26	-2.18	39.37	28.65
NBS 20	-0.8	6.3	-4.14	37.35	26.64

Regressions

X = NBS value
Y = SI Lab value

SMOW : Y = 0.997X - 10.603 R squared = 1
PBD : Y = 0.997X - 10.426 R squared = 1

Appendix D

Stable Isotope Data

Sample Number	13/12 C (per mil) PDB	18/16 O (per mil) PDB	Converted 18/16 O (per mil) PDB	18/16 O (per mil) SMOW	Converted 18/16 O (per mil) SMOW
11014 dolo/cemt	-0.73	5.47	-4.96	36.5	25.79
11139 dolo/stylol	-1.26	1.22	-9.2	32.12	21.42
11145 dolo/cemt	-2.65	0.92	-9.5	31.81	21.11
11400 dolo/fract	-1.34	1.46	-8.96	32.36	21.66
11400 dolo/cemt	-1.2	4.32	-6.11	35.31	24.6
11409 dolo/cemt	-2.24	-0.14	-10.57	30.7	20
11422 s. dolo/void	-1.56	0.97	-9.45	31.86	21.1
11522 calc/cemt	-6.51	-0.2	-10.63	30.64	19.95
11525 calc/fract	-2.98	-1.25	-11.67	29.56	18.87
11543 calc/fract	-3.19	1.35	-9.07	32.26	21.56
11598 s. dolo/void	-1.41	1.45	-8.97	32.3	21.65
11675 calc/fract	-9.23	-0.45	-10.88	30.38	19.69
12054 calc/cemt	-4.72	0.61	-9.81	31.49	20.79
12067 calc/fract	-2.93	2.53	-7.89	33.47	22.77
12067 dolo/cemt	-2.85	7.17	-3.27	38.25	27.53

This thesis is accepted on behalf of the faculty of the Institute by the following committee:

David I. Norman
____
Adviser

Andrew Campbell
____

David E. [illegible]
____

____

____

April 10, 1991
____
Date